Characterization of two *C. elegans* molecular chaperone families, CCT (chaperonin containing TCP-1) and the small heat shock proteins

by

Michel Rejean Leroux

B. Sc., McGill University, 1991

A THESIS SUBMITTED IN PARTIAL FULFILLMENT OF

THE REQUIREMENTS FOR THE DEGREE OF

Doctor of Philosophy

in

THE FACULTY OF GRADUATE STUDIES

Department of Biochemistry and Molecular Biology

We accept this thesis as conforming

to the required standard

THE UNIVERSITY OF BRITISH COLUMBIA

June 1997

In presenting this thesis in partial fulfilment of the requirements for an advanced degree at the University of British Columbia, I agree that the Library shall make it freely available for reference and study. I further agree that permission for extensive copying of this thesis for scholarly purposes may be granted by the head of my department or by his or her representatives. It is understood that copying or publication of this thesis for financial gain shall not be allowed without my written permission.

Department of Biochemistry & Molecular Biology

The University of British Columbia
Vancouver, Canada

Date June 4, 1997

DE-6 (2/88)

ABSTRACT

Molecular chaperones belong to a class of proteins whose function is to interact with and stabilize proteins that are partly or totally unfolded, as is the case when proteins are in the process of being synthesized, translocated into an organelle, or damaged by cellular stress. The work presented in this thesis describes the first studies aimed at characterizing some of the structural and functional properties of two molecular chaperone families of the nematode *Caenorhabditis elegans*, CCT (chaperonin containing TCP-1) and the small heat shock proteins (smHSPs).

CCT is involved in folding newly synthesized actin and tubulin, and may play a more general role in protein folding within the eukaryotic cytosol. *C. elegans* CCT is an ATP-binding complex of about 900 kDa. Sucrose gradient fractionation and ATP-agarose chromatography were used to purify the CCT complex from embryos. Over 7 subunits ranging between 52-65 kDa were detectable, of which two were shown to be CCT-1 and CCT-5 by immunoblotting. Native gel electrophoresis of the CCT revealed three distinct species: one contains CCT-1 and CCT-5 and hence represents the CCT complex, another contains HSP60, which has the highest affinity for chemically-denatured actin, and the last species remains unidentified. A 3.7 kb *Pst*I genomic fragment encoding the 59 kDa CCT-1 protein was cloned and sequenced. The *cct-1* transcript undergoes both *cis*-splicing of its four introns and *trans*-splicing to SL1. Three additional *cct* cDNAs were sequenced (*cct-2*, *cct-4*, and *cct-5*), and the sequence of a fifth *cct* gene (*cct-6*) was obtained from the *C. elegans* sequencing consortium. The *C. elegans cct* multigene family displays 23-35% sequence identity between members and about 65% identity to the corresponding murine *cct* homologues. Northern blot analyses show that the five *C. elegans cct* genes are expressed in all life stages. Transgenic lines carrying a *cct-1*-promoter-*lacZ* construct revealed that *cct-1* is expressed in various tissues, including muscles and the nervous system.

The smHSP and α-crystallin genes encode a family of proteins which assemble into large multimeric structures, function as chaperones by preventing protein aggregation, and contain a

conserved region termed the α-crystallin domain. Studies on wild-type HSP16-2 and five derivatives demonstrate that multimerization and chaperone activity depend on the full-length nonconserved N-terminal region and are not affected by removal of most of the C-terminal extension which follows the α-crystallin domain. The N-terminal region of HSP16-2 is buried within an oligomeric complex which can accomodate an additional 4 kDa of heterologous protein sequence. It was found that HSP16-2 has an equally high affinity for unfolded actin and tubulin intermediates which form early on the renaturation or aggregation pathway. The structure-function data on HSP16-2 are complemented by studies on HSP12.6, the smallest smHSP to be characterized. In contrast to other smHSPs, the stage-specific HSP12.6 does not multimerize and lacks chaperone activity.

TABLE OF CONTENTS

LIST OF FIGURES

LIST OF TABLES

LIST OF ABBREVIATIONS

aa	amino acid(s)
ATP	adenosine 5'-triphosphate
bp	base pair(s)
BSA	bovine serum albumin
C. elegans	*Caenorhabditis elegans*
CCT	chaperonin containing TCP-1 protein
cct	chaperonin containing *tcp-1* gene
cDNA	DNA complementary to coding strand
cpm	counts per minute
dATP	deoxyadenosine 5'-triphosphate
dCTP	deoxycytidine 5'-triphosphate
dGTP	deoxyguanosine 5'-triphosphate
dH_2O	distilled water
DNA	deoxyribonucleic acid
dNTP	dATP, dCTP, dGTP, dTTP
DTT	dithiothreitol
dTTP	deoxythymidine 5'-triphosphate
E. coli	*Escherichia coli*
ECL	enhanced chemiluminescence
EDTA	ethylenediamine tetraacetic acid
GTP	guanosine 5'-triphosphate
HSE	heat shock element
HSP	heat shock protein
hsp	heat shock protein gene
IPTG	isopropyl-β-D-thiogalactopyranoside
kb	kilobase pair(s)
kDa	kilodalton(s)
L1-L4	four *C. elegans* larval stages
mAb	monoclonal antibody
MDa	megadalton(s)
MES	2-[N-morpholino]ethanesulfonic acid

M_r	molecular mass
mRNA	messenger RNA
MW	molecular weight
NG	nutrient growth (medium)
NP	50 mM NaCl, 50 mM sodium phosphate
nt	nucleotide
pAb	polyclonal antibody
PAGE	polyacrylamide-gel electrophoresis
PCR	polymerase chain reaction
PMSF	phenylmethylsulfonyl fluoride
PND	25 mM sodium phosphate pH 7.0, 25 mM NaCl, 0.5 mM DTT
PVDF	polyvinylidene difluoride
RNA	ribonucleic acid
RNAse	ribonuclease
SDS	sodium dodecyl sulphate
SL	splice leader
smHSP	small heat shock protein
SSPE	180 mM NaCl, 1 mM EDTA, 10 mM NaH_2PO_4; pH 7.4
Taq	*Thermus aquaticus*
TB	terrific broth
TBE	90 mM Tris-borate pH 8.3; 2 mM EDTA
TBS-T	25 mM Tris-HCl, 140 mM NaCl, 0.05% Tween 20; pH 7.4
tcp	*t*-complex polypeptide gene
TCP-1	*t*-complex polypeptide-1 protein
TE	10 mM Tris-HCl, pH 8.0; 1 mM EDTA
TEDKM	50 mM Tris pH 7.4, 0.1 mM EDTA, 1 mM DTT, 50 mM KCl, 10 mM $MgCl_2$
TEND	50 mM Tris-HCl, 0.1 mM EDTA, 50 mM NaCl, 1 mM DTT; pH 7.5
TER	10 mM Tris-HCl, pH 8.0; 1 mM EDTA; 1 μg/ml RNAse A
Tris	tris (hydroxymethyl) aminomethane
Tween 20	polyoxyethylene-sorbitan monolaurate
X-GAL	5-bromo-4-chloro-3-indolylgalactosidase
YAC	yeast artificial chromosome

ACKNOWLEDGMENTS

I would like to give my warmest thanks to my supervisor, Peter Candido, for giving me the opportunity to work on projects that have been very interesting and exciting. Throughout my degree, I have benefited tremendously from many helpful discussions with my lab colleagues, Don, Mei, Dave, Tracy, Bruce, Brian, Sandra, Eve, and Emily. Many of these people have been my friends for many years, and the work environment they created was always productive and enjoyable at the same time.

Anyone working with *C. elegans* knows that researchers from the *C. elegans* community are very communicative, helpful, and generous. The *C. elegans* genomic DNA yeast YAC library and cosmids were kind gifts from John Sulston and Alan Coulson (Sanger Centre, Cambridge, UK), and the *cct* cDNA clones were provided by Robert Waterston (Dept. of Genetics, Washington University, St. Louis). Richard Durbin and Steve Jones (St. Louis) have been helpful in locating and deciphering information from the *C. elegans* database ACeDB.

Research would not be as rewarding if there were no collaborations. I would like to thank Keith Willison (Institute of Cancer Research, Chester Beatty Laboratories, London, UK) for providing samples of his UM1 antibody, as well as Bruce Gordon and Brian Ma (UBC) for helping out with some smHSP purifications, molecular weight determinations, and aggregation assays. Peter also contributed to my research by performing the injections needed to create transgenic strains. A very special thanks to Ronald Melki (Laboratoire d'Enzymologie et Biochimie Structurales, CNRS, Gif-sur-Yvette, France) for supplying [^{35}S]-labeled actin and tubulin in addition to a sample of purified bovine testis CCT, and for providing me with sedimentation and fluorescence quenching data on some of the smHSPs. Gérard Batelier's (CNRS) expert help with the sedimentation velocity measurements is also appreciated.

Most importantly, I would like to thank my wife Tracy for her boundless enthusiasm for my career in health sciences. But above all, *merci de m'aimer pour qui je suis et de m'avoir montré qu'il y a plus que la science dans la vie.*

CHAPTER I— Studies on the structure, function, and expression of *C. elegans* CCT

Protein folding is one of the most important process in living organisms, as it produces the three-dimensional conformation required by proteins for their specific properties. In this chapter we explore various aspects of a eukaryotic molecular chaperone that has only recently come to light, but whose function appears essential in assisting the proper folding of two of the most abundant cellular proteins, namely the cytoskeletal elements actin and tubulin.

I. INTRODUCTION

Protein folding

The process of protein folding, or the acquisition of tertiary structure, has long been believed to be a spontaneous event, guided strictly by the information contained within the amino acid sequence of a protein. Early work on protein folding by Anfinsen using ribonuclease A demonstrated that if this protein was completely unfolded in denaturant and then diluted into a buffer, it could spontaneously regain full activity (Anfinsen, 1973). Although many purified proteins can refold *in vitro* under certain conditions, protein misfolding and aggregation is a frequent and major problem which rarely occurs *in vivo* (Gething and Sambrook, 1992). The reason is that unfolded polypeptides expose core hydrophobic amino acid side chains which tend to associate with each other incorrectly both inter- and intra-molecularly, resulting in the formation of aggregates (Hendrick and Hartl, 1993). Although the extent of aggregation can sometimes be controlled in the test tube by lowering the concentration of the refolding protein or lowering the temperature, the physiological relevance of *in vitro* refolding experiments is now regarded with caution, for two major reasons. The first reason concerns the environment in which protein folding occurs within the cell. Not only is the concentration of unfolded, nascent chains in the cytoplasm very high (approximately 35 μM in *E. coli*, for example; Ellis and Hartl, 1996), but molecular crowding by the bulk of the cellular proteins is

predicted to cause a tremendous increase in molecular association constants over those in dilute solution (Hartl, 1996). Secondly, because of the cooperativity of the folding process, the formation of stable tertiary structures requires the presence of a complete polypeptide or at least a complete protein domain (Hartl *et al.*, 1994). Since the polypeptide chain is synthesized *de novo* in an extended conformation, unproductive associations of the nascent chain with itself or other proteins would be strongly preferred over the correct folding pathway unless a specific machinery were present during most of the folding process to prevent off-pathway reactions. The components of this machinery are termed molecular chaperones.

Molecular chaperones

The term 'molecular chaperone' was first used to describe the unique function of the nuclear protein nucleoplasmin in assisting chromatin assembly (Laskey *et al.*, 1978). This term was later applied more generally to a range of cellular proteins whose role is to promote the folding and assembly of unfolded and partially unfolded forms of other proteins (Ellis, 1987). Chaperones serve many functions that stem from their ability to recognize and modulate the state of folding within cells. The basic, revised definition of a molecular chaperone is "any protein that binds to and stabilizes an otherwise unstable form of another protein, and by controlled binding and release, facilitates its correct fate *in vivo*, be it folding, oligomeric assembly, transport to a particular subcellular compartment, or disposal by degradation" (Hartl, 1996). Numerous reviews on the subject of molecular chaperones are available (Morimoto *et al.*, 1990; Gething and Sambrook, 1992; Welch, 1993; Georgopoulos and Welch, 1993; Hendrick and Hartl, 1993; Parsell and Lindquist, 1994; Buchner, 1996; Hartl, 1996; Martin and Hartl, 1997). The various roles for some of the well-known chaperones are illustrated in **Figure 1**.

The involvement of molecular chaperones during and following cellular stresses will be discussed in *Chapter II*, where studies on HSP16-2, a strictly stress-inducible small HSP, are presented.

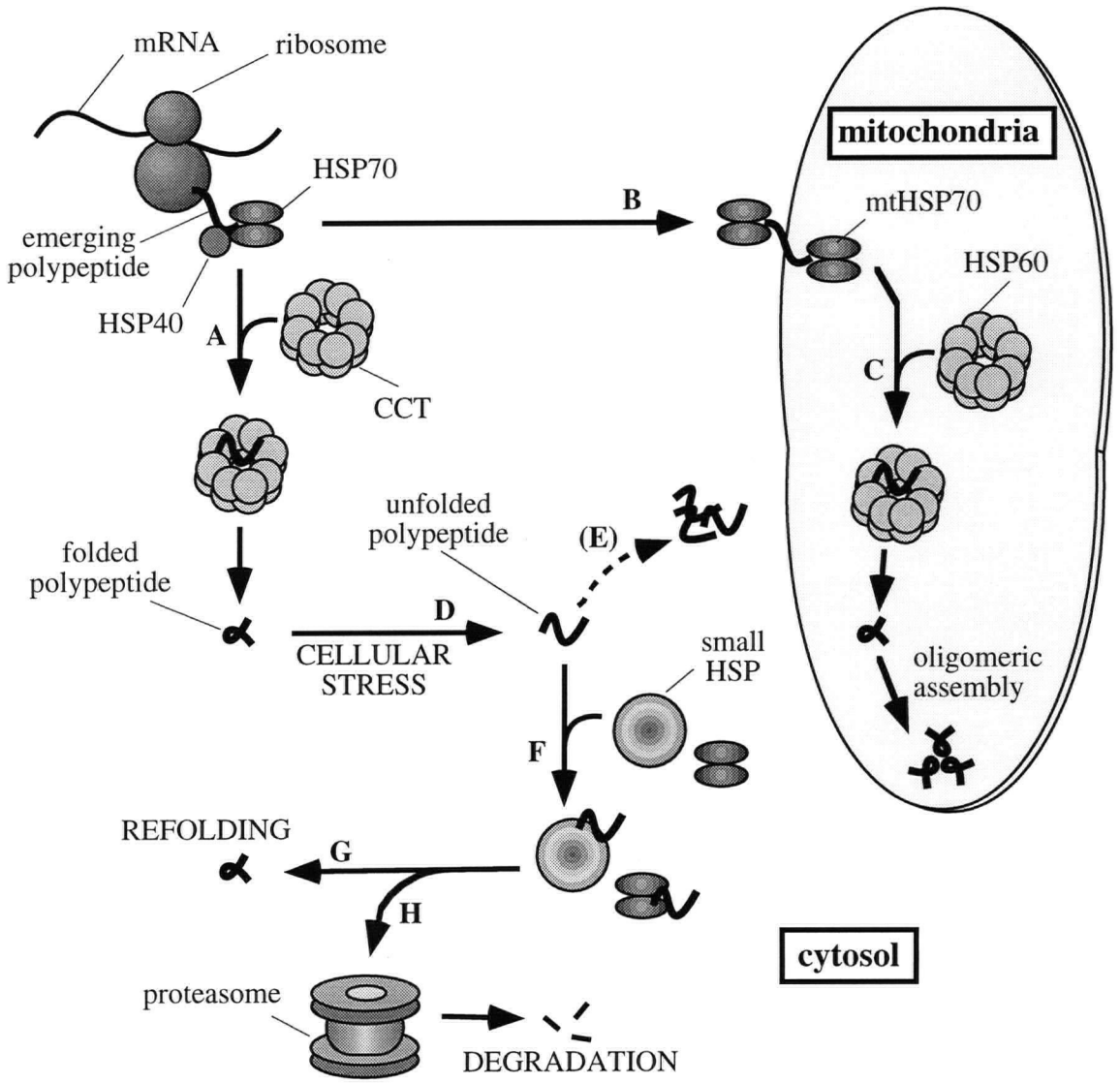

Figure 1. Summary of some chaperone functions in the cell. The folding of some nascent polypeptide chains in the eukaryotic cytosol requires a specific machinery consisting of HSP70, its partner HSP40, and CCT. HSP40 and HSP70 (dimer) first interact with the emerging polypeptide, preventing its premature folding and aggregation (**A**). The partially folded protein is then passed on to CCT for folding to its native state. Proteins destined for the mitochondria require HSP70 and HSP40 to remain in a translocation-competent state (**B**), and mitochondrial HSP70 (mtHSP70) and HSP60 for proper folding and oligomeric assembly inside the organelle (**C**). When cells are subjected to stress, some proteins become damaged and unfolded (**D**), which may result in their aggregation and loss of function (**E**). Alternatively, these proteins interact with various chaperones such as small HSPs, HSP70, and HSP104 (**F**). Either through the direct action of these chaperones, or by further intervention of other chaperones, the unfolded proteins may be refolded (**G**). Alternatively, the damaged proteins may be degraded via the ubiquitin- and proteasome-dependent degradation pathway (**H**).

One of the well-studied functions of chaperones is their ability to assist in the folding of *de novo* synthesized proteins. A number of proteins have been found to associate with nascent chains in the eukaryotic cytosol, and are believed to be components required to ensure the proper folding of the polypeptide emerging from the ribosome. The first component which is thought to interact with nascent chains is the nascent-chain-associated complex (NAC), which is a heterodimer of 33 and 21 kDa subunits. NAC shields the first ~33 residues adjacent to the peptidyl transferase site and prevents the association of the ribosome with the endoplasmic reticulum (ER) membrane unless the polypeptide contains a signal sequence recognized by the signal-recognition particle (SRP) (Wiedmann *et al.*, 1994; Wang *et al.*, 1995). NAC may also be involved in recruiting two chaperones involved in maintaining the nascent polypeptide in a folding-competent conformation, HSP70 and its co-chaperone HSP40. Protein translocation across the ER and mitochondrial membranes also requires the participation of HSP70 and HSP40, which together maintain the polypeptide in a translocation-competent conformation (Hendrick *et al.*, 1993; Höhfeld and Hartl, 1994).

HSP70 and HSP40 have been co-purified with ribosome-bound polypeptide chains, and recognize polypeptides less than 85 residues in length (Beckmann *et al.*, 1990; Hendrick *et al.*, 1993; Frydman *et al.*, 1994a). HSP40 is believed to recruit HSP70 onto the nascent chain (Frydman *et al.*, 1994a), where it regulates the ATPase activity of HSP70 (Höhfeld *et al.*, 1995). Yet another factor involved in the HSP70/HSP40 reaction cycle is Hip (HSP70-interacting protein), which itself has chaperone activity and can modulate the activity of HSP70 (Höhfeld *et al.*, 1995). Together, these chaperones maintain the aggregation-sensitive nascent chains in a folding-competent conformation through their co-translational association (Hartl, 1996). After a sufficient length of polypeptide destined for the cytosol has been produced, it is transferred by HSP70/HSP40 to a specialized class of molecular chaperone termed 'chaperonin' for eventual folding to its native state.

Chaperonins

The term 'chaperonin' denotes a family of sequence-related proteins of ~60 kDa found in eukaryotic mitochondria and chloroplasts, and in eubacteria such as *E. coli* (Hemmingsen *et al.*, 1988). These ubiquitous proteins were later shown to exist in the eukaryotic cytosol (Ellis, 1990; Gupta, 1990) and in archaebacteria (Trent *et al.*, 1991). Chaperonins form a distinct class of ATP-dependent molecular chaperones involved in assisting *de novo* protein folding (Hendrick and Hartl, 1993; Horwich and Willison, 1993; Frydman and Hartl, 1996; Ellis and Hartl, 1996; Hartl, 1996; Martin and Hartl, 1997).

Chaperonin evolutionary relationships

Two chaperonin families are known, and can be classified on the basis of evolutionary relationships, structures, and functions. One family (Group I) is represented by eubacterial GroEL, mitochondrial Hsp60, and plastid Rubisco subunit-binding protein (RuBP). The eukaryotic Hsp60 and RuBP chaperonins share a high degree of deduced amino acid sequence identity with GroEL (45-60%), presumably because they are localized within organelles believed to originate from the endosymbiotic capture of a proteobacterium and cyanobacterium, respectively (Gray, 1992; Viale and Arakaki, 1994). In addition to their sequence similarity and shared eubacterial lineage, the so-called classical chaperonins are composed of one or two types of subunits, possess a common quaternary structure consisting of 14 subunits arranged as two stacked toroids with 7-fold rotational symmetry, and usually require an ~10 kDa co-chaperonin (termed GroES or chaperonin 10) for function (Hemmingsen *et al.*, 1988; Lubben *et al.*, 1990; Martin *et al.*, 1993; Horwich and Willison, 1993).

The other family (Group II) consists of eukaryotic cytosolic and archaebacterial chaperonins. In the eukaryotic cytosol, the chaperonin named CCT (Chaperonin Containing TCP-1) or TRiC (TCP-1 Ring Complex; Frydman *et al.*, 1992) is encoded by 8 members of a *Cct* multigene family which shares 25-36% pairwise predicted amino acid sequence identity between members (Kubota *et al.*, 1994; Kubota *et al.*, 1995a; Stoldt *et al.*, 1996). An additional testis-specific *Cct* gene was recently identified (Kubota *et al.*, 1997). TCP-1 (CCTα) was the

first protein from the cytosolic chaperonin to be identified (Lewis *et al.*, 1992; Yaffe *et al.*, 1992). The murine and bovine CCT protein subunits (denoted CCTα, β, γ, δ, ε, etc.) assemble to form a hetero-oligomeric double-ring complex with 8- or 9-fold rotational symmetry (Frydman *et al.*, 1992; Gao *et al.*, 1992; Lewis *et al.*, 1992; Marco *et al.*, 1994). Because of the great number of variations in naming the CCT chaperonin genes and subunits, a consistent nomenclature has been proposed (Stoldt *et al.*, 1996), where genes are named *cct1*, *cct2*, etc., subunits are designated Cct1p, Cct2p, etc., and the complex is called CCT. However, to be consistent with the accepted *C. elegans* nomenclature (Hodgkin, 1995), the *C. elegans* genes are designated as *cct-1*, *cct-2*, etc., the proteins they encode as CCT-1, CCT-2, etc., and the complex is referred to as CCT.

Remarkably, the subunits of the eukaryotic cytosolic chaperonin are very closely related to a subunit of the archaebacterial chaperonin TF55 (32-39% identity), and are only weakly similar to GroEL (Kubota *et al.*, 1994). The considerable similarity between the eukaryotic cytosolic and archaebacterial chaperonins agrees with phylogenetic analyses which suggest that the eukaryotic cell nucleus evolved from an archaebacterial ancestor (Iwabe *et al.*, 1989; Rivera and Lake, 1992). The evolution of the CCT/TF55 family is also consistent with an alternative chimeric model for the origin of the eukaryotic cell nucleus (Gupta, 1995), which proposes that a fusion between a thermoacidophilic archaebacterium and a Gram-negative bacterium gave rise to a pro-eukaryotic cell (Gupta and Singh, 1994; Irwin, 1994). The quaternary structures of the TF55 chaperonins from the archaebacteria *Sulfolobus shibatae* and *Sulfolobus solfataricus*, double toruses with 9 subunits per ring, are also more similar to CCT than to GroEL (Trent *et al.*, 1991; Knapp *et al.*, 1994). An abundant chaperonin isolated from the hyperthermophile *Pyrodictium occultum* is composed of two types of subunits, like TF55, but seems to possess mostly 8 rather than 9 subunits per ring (Phipps *et al.*, 1991, 1993). Another distinguishing feature of the eukaryotic cytosolic and archaebacterial chaperonins is that they do not appear to associate with a chaperonin-10-like co-chaperonin. Recently, Guagliardi *et al.* (1994, 1995) have demonstrated that the *S. solfataricus* chaperonin can prevent the thermal aggregation as well as fold several thermophilic and mesophilic enzymes *in vitro*. Hence, the eubacteria,

archaebacteria, and eukaryotes all possess one or more evolutionarily related chaperonins whose ubiquitous function is to assist protein folding.

Function of Group I chaperonins

Functional studies on chaperonins provided the first evidence that protein folding within cells is a chaperone-dependent process. The *E. coli* chaperonin GroEL was originally shown to participate in the morphogenesis of bacteriophage λ and T4 head structures, suggesting a role in protein assembly (Georgopoulos *et al.*, 1973; Sternberg, 1973). Several years later, the rubisco subunit binding protein (RuBP) was identified as a component associating with newly-translated large subunits of rubisco in the chloroplast, implying a role in protein folding and assembly (Barraclough and Ellis, 1980), and is now thought to have a broader scope of action in this organelle (Lubben *et al.*, 1989).

A general role for GroEL in folding newly translated proteins appears likely (Viitanen *et al.*, 1992; Horwich *et al.*, 1993). For example, it was shown that under non-permissive conditions, a number of cytoplasmic proteins including citrate synthase, ketoglutarate dehydrogenase, a maltose-binding protein, and polynucleotide phosphorylase, were translated but failed to reach native form in an *E. coli* strain producing a temperature-sensitive mutant GroEL (Horwich *et al.*, 1993). Furthermore, a 2D gel analysis of GroEL-deficient cells shows that approximately 30% of the protein species are affected. The folding of polypeptides within the GroEL cavity has been extensively studied. GroEL cooperates with GroES, a single heptameric ring of ~10 kDa subunits that binds asymmetrically to GroEL, capping one opening of the cylinder (Saibil, 1996). The substrate interacts with GroEL through multiple ATPase cycles of GroES binding and release (Hayer-Hartl *et al.*, 1995). Folding occurs in iterative steps in which the polypeptide is sequestered in the GroEL cavity, prevented from undergoing aggregation or other off-pathway reactions (Mayhew *et al.*, 1996). ATP binding and hydrolysis triggers the opening of the GroEL-GroES cage, at which point the folded polypeptide leaves; alternatively, incompletely-folded polypeptide rebinds for a further round of folding and release (Martin *et al.*, 1993; Weissman *et*

al., 1995; Burston *et al.*, 1996). The most recent reviews on chaperonin-assisted protein folding are those of Hartl (1996) and Martin and Hartl (1997).

Eukaryotic mitrochondrial HSP60 performs a function analogous to that of GroEL, and has been implicated in the folding and assembly of many polypeptides—for example, the assembly of newly imported wild-type HSP60 subunits is not observed in intact cells or isolated mitrochondria of the yeast HSP60-defective mutant *mif4* (Cheng *et al.*, 1989, 1990). It also was found that the subunits of ornithine transcarbamylase and citrate synthase were found in the mitochondrial matrix compartment at their mature size, but were lacking biological activity: on extraction with nonionic detergents, the proteins were found in the insoluble fractions, suggesting that they had not properly folded, and had instead aggregated upon entry into the matrix. Similarly, Ostermann *et al.* (1989) found that HSP60 was implicated in the ATP-dependent folding of proteins in the mitochondrial matrix. In addition to defective biogenesis of imported proteins in HSP60-deficient mitochondria, the folding of at least one mitochondrially-encoded protein, a ribosomal component, is also affected (Horwich *et al.*, 1992).

Unlike the eubacterial and organellar chaperonins, the scope of action of the eukaryotic cytosolic chaperonin CCT may be more restricted, and details concerning its function are discussed in a separate section below.

Structure-function studies on GroEL and GroES

The only three-dimensional structure of a chaperonin available is that of *E. coli* GroEL, which has been solved by X-ray crystallography to a resolution of 2.8 Å (Braig *et al.*, 1994). The quaternary structure of the chaperonin consists of a porous cylinder made from two back-to-back heptameric rings. In addition, the structure of GroEL complexed with a non-hydrolyzable form of ATP reveals the location of a novel nucleotide-binding pocket whose primary sequence is conserved among chaperonins (Boisvert *et al.*, 1996). Together with comprehensive mutation-function studies which have defined numerous critical residues involved in all aspects of chaperonin activity (Braig *et al.*, 1994), the above findings provide significant insight into the mechanism of polypeptide binding and release of this chaperonin.

The bacterial chaperonin monomer is divided into three domains which form a bilobate structure: the amino- and carboxy-terminal portions of the protein make up the equatorial domain, the central region forms the apical domain, and the intermediate region links the two domains. Residues required for inter-subunit contacts and ATPase activity are localized mainly in the equatorial and intermediate domains. As might be expected, residues involved with co-chaperonin interaction and polypeptide binding map almost exclusively to the apical domain, which form the ends of the cylinder. Mutations which produce defective release or folding of the bound polypeptide are found in the apical and equatorial domains of GroEL.

The crystal structures of two different GroES heptamers are also known (Hunt *et al.*, 1996; Mande *et al.*, 1996). The overall structure of the heptamer is dome-shaped, and it has been shown by electron microscopy to form a cap over the top of one of the two polypeptide binding chambers of GroEL (Martin *et al.*, 1993). GroES is believed to interact in *cis* with the GroEL ring enclosing the folding polypeptide (Weissman *et al.*, 1995; Burston *et al.*, 1996). Folding is believed to be initiated within the GroEL-substrate-GroES ternary complex, and for some substrates may be completed prior to the release of GroES following ATP hydrolysis (Weissman *et al.*, 1996). The surface of the interior cavity provided by GroES is very hydrophilic. Therefore, the role of GroES, in addition to modulating the cooperativity of ATP hydrolysis by GroEL (Gray and Fersht, 1991), may be to assist the folding of proteins by binding to hydrophilic regions of substrate proteins, while avoiding interactions with hydrophobic patches, which eventually form the interior core of the substrate protein (Mande *et al.*, 1996).

Structure of Group II chaperonins

In contrast with GroEL, the crystal structures of the Group II chaperonins have not been determined. However, observations of CCT and TF55 by electron microscopy suggest that their quaternary structures are very similar to each other and superficially similar to that of GroEL. First, the compositions of CCT and archaebacterial chaperonins are more complex, consisting of 7-9 and 2 different subunits, respectively. Second, these chaperonins display 8- or sometimes 9-fold rotational symmetry compared with 7-fold for GroEL/HSP60. The most detailed three-

dimensional view of a Group II chaperonin has been obtained with the TF55-related complex from the archaebacterium *Pyrodictium occultum*, by means of random conical tilt reconstructions from electron micrographs (Phipps *et al.*, 1993). The chaperonin structure contains two eight-membered rings composed of equal amounts of two polypeptides of 56 and 59 kDa, whose arrangement within the complex is unknown. In contrast, TF55 isolated from *Sulfolobus solfataricus* by Knapp *et al.* (1994) and recombinant *Thermoplasma acidophilum* chaperonins (Waldmann *et al.*, 1995c) consist exclusively of nine-membered rings. In the centre of the chaperonin is a large cavity about 6.7 nm in diameter, larger than that of GroEL (4.7 nm). Unlike GroEL, its cavity is partially blocked by a mass which appears to be weakly connected to the main body (Phipps *et al.*, 1991).

CCT is an ~900 kDa heteromeric complex consisting of an assembly of 7-9 polypeptides of 53-65 kDa (Lewis *et al.*, 1992; Frydman *et al.*, 1992; Rommelaere *et al.*, 1993; Kubota *et al.*, 1994). The subunit composition of CCT varies somewhat depending on its source (Kubota *et al.*, 1994; Hynes *et al.*, 1995). As with the archaebacterial chaperonins, the only data available on the CCT quaternary structure has been obtained by electron microscopy (em). Initially, visual inspection of the electron micrographs of murine CCT by Lewis *et al.* (1992) suggested that it consisted of 8 or 9 subunits per ring. However, more thorough em analyses of CCT structures reveals that they are likely to consist solely of eight-membered rings (Marco *et al.*, 1994; Waldmann *et al.*, 1995b). Most likely because of the additional subunits in each ring, the pore size of CCT, approximately 6.0 nm, is larger than that of GroEL (Marco *et al.*, 1994).

In a review article by Kim *et al.* (1994), a detailed primary sequence alignment of the seven known members of the CCT protein family (α, β, γ, δ, ε, ζ, and η) and *E. coli* GroEL was used to assess domain-specific structural similarities between different CCT subunits and GroEL. A high level of conservation among all chaperonin proteins was observed in the region which corresponds to the equatorial, or ATP-binding domain of GroEL. In contrast, little sequence similarity was seen within the region corresponding to the apical domain, or polypeptide-binding region, of GroEL: not only had the seven CCT subunits substantially diverged from GroEL in this region, but they were also surprisingly different from each other, suggesting that each

subunit migh have different structural and/or functional properties. Similarly, on the basis of amino acid sequence alignments and secondary structure predictions, Waldmann *et al.* (1995a) suggested that the equatorial domain of CCTs and GroEL were likely to be similar, and that the apical domains of these chaperonins may share a common, albeit significantly divergent fold.

Function of CCT in vitro and in vivo

A number of reviews describing the structure, function, and expression of CCT have appeared (Horwich and Willison, 1993; Willison and Kubota, 1994; Kim *et al.*, 1994; Kubota *et al.*, 1995b; Stoldt *et al.*, 1996; Lewis *et al.*, 1996; Hartl, 1996). In contrast to the Group I chaperonins, there is considerable evidence that CCT may play a more specialized role in the folding of proteins within the eukarytic cytosol. Two highly abundant cytoskeletal protein families, actins and tubulins, are known to be the major physiological substrates folded by CCT (Yaffe *et al.*, 1992; Sternlicht *et al.*, 1993; Melki and Cowan, 1994; Ursic *et al.*, 1994; Chen *et al.*, 1994). Melki and Cowan (1994) measured the relative affinities of many unfolded proteins for both HSP60 and CCT, and found that CCT appears to be more selective in its choice of target proteins, having greater affinity for actins and tubulins compared to other noncytoskeletal proteins. Interestingly, Tian *et al.* (1995) showed that HSP60 and GroEL could bind unfolded actin and tubulin, but unlike CCT, could not release them in their properly folded conformation. Mutations in many yeast genes encoding CCT subunits result in exclusively cytoskeletal phenotypes, such as disorganized or disrupted actin and tubulin filaments (Ursic *et al.*, 1991, 1994; Chen *et al.*, 1994; Miklos *et al.*, 1994; Vinh and Drubin, 1994; Schmidt *et al.*, 1996; reviewed in Stoldt *et al.*, 1996). Interestingly, CCT has been shown to be associated with the centrosome, where it is required for mediating the growth of microtubules initiated from this structure (Brown *et al.*, 1996). Overall, these results suggest that the increased complexity of the hetero-oligomeric CCT complex may have evolved to deal with particularly aggregation-prone proteins such as actins and tubulins (Kim *et al.*, 1994).

It is also possible that CCT may be involved in folding a broader range of newly synthesized polypeptides. The cytosolic chaperonin, in conjunction with HSP70 and the DnaJ

homolog HSP40, is required for folding firefly luciferase as it emerges from ribosomes (Frydman *et al.*, 1994b, 1996). CCT can refold chemically denatured firefly luciferase *in vitro* whereas GroEL/GroES can bind the unfolded protein but apparently cannot refold it to its native state (Frydman *et al.*, 1992). An association of CCT with an intermediate in the assembly of hepatitis B virus capsids has also been observed (Lingappa *et al.*, 1994). The relative ability of GroEL, HSP60, and CCT to bind an unfractionated mixture of labeled, unfolded *E. coli* proteins was recently assessed (Tian *et al.*, 1995). It was found that the pattern of proteins recognized by each chaperonin was very similar, although the overall amount of proteins bound to CCT was approximately 10-fold lower compared with GroEL.

It is now evident that the chaperone-mediated protein folding pathway in eubacteria parallels the eukaryotic *de novo* folding pathway. In a landmark paper by Langer *et al.* (1992), the sequential action of DnaK, DnaJ, and GroEL was shown to be required for the efficient folding of newly synthesized polypeptides. In the eukaryotic cytosol, the same chaperone system (HSP70, HSP40, and CCT) is involved in folding *de novo* synthesized firefly luciferase and actin (Nimmesgern and Hartl, 1993; Frydman *et al.*, 1994, 1996). However, in contrast to the CCT-mediated folding of actin (Gao *et al.*, 1992; Melki *et al.*, 1993, 1994), the mechanism by which CCT folds tubulin is substantially more complex. Indeed, four different cofactors (A, C, D, and E) in addition to CCT are required for the correct folding of tubulin *in vitro* (Gao *et al.*, 1993, 1994; Melki *et al.*, 1996; Tian *et al.*, 1996). As β-tubulin is synthesized *de novo*, CCT interacts most strongly with a stretch of ~120 amino acids situated in the core (middle) region of tubulin, and the N- and C-terminal regions of β-tubulin are thought to fold back onto the β-tubulin core region (bound to CCT), permitting its release from the chaperonin complex (Dobrzynski *et al.*, 1996).

Expression and localization of CCT

Because of the complex subunit composition of CCT, little information regarding the expression of the corresponding genes in higher organisms is available. In general, it appears that the spatial and temporal distribution of CCT subunits corresponds with specific

requirements for folded actin or tubulin. The first subunit to be studied, CCTα (*i.e.*, TCP-1 or CCT-1), is known to be abundant in mouse testis, and is expressed at lower levels in almost all cell types (Willison *et al.*, 1989, 1990). There also exists a murine testis-specific CCT subunit (Kubota *et al.*, 1997). Another process apart from spermatogenesis which requires high rates of tubulin synthesis has been documented for *Tetrahymena*, where CCTγ is upregulated during reciliation (Soares *et al.*, 1994). The same subunit (TRIC-P5, or CCTγ) is known to be expressed at the two-cell stage in mouse embryos, suggesting an important function for this protein during the rapid cell division occurring in early development (Sévigny *et al.*, 1995). In a neuronal cell line, CCTα specifically co-localizes with actin at the extreme periphery of growth cones, where the unassembled, globular form of actin and assembly-competent filamentous forms are found. In contrast, other subunits (CCTβ, ε, γ) are restricted to the perikaryal cytoplasm of these cells, where cytoskeletal proteins are first synthesized (Roobol *et al.*, 1995). These data strongly suggest that CCT subunits do not necessarily assemble into a single type of hetero-oligomeric complex. Indeed, a homo-oligomeric CCTα particle from mammalian brain was reported by Martin *et al.* (1993).

The expression of several *cct* genes has been described in two vertebrates, a salamander (axolotl) and in *Xenopus laevis*. In *Xenopus*, the expression patterns of two CCT subunits are developmentally regulated during embryogenesis, as evidenced by increased expression of CCTα and CCTγ in differentiating neural and muscle precursor cells (Dunn and Mercola, 1996). More specifically, the transcripts for CCTα and CCTγ are enriched in cranial neural crest cells during embryogenesis, as well as in the developing central nervous system (CNS) and skeletal and cardiac muscle. At least in the CNS and muscles, the need for abundant expression of *cct* genes is consistent with their potential requirement for actin and tubulin biogenesis. Similarly, temporal and spatial regulation of TCP-1 in axolotl is evident (Sun *et al.*, 1995). At an early stage of development, *TCP-1* transcripts accumulate in developing brain and neural tube. At a somewhat later stage, strong expression is seen in the brain, spinal cord, and somites by whole-mount *in situ* hybridization studies and RT-PCR. The authors note that the expression of *TCP1* correlates with the expression of actin and myosin during early development.

C. elegans as a model organism

The free-living soil nematode *Caenorhabditis elegans* is an anatomically and genetically simple multicellular organism (Wood, 1988). It is one of the preferred model systems for the study of fundamental biological problems. Because the nematode is self-fertilizing, has a short life cycle of about 3 days at room temperature, and is easily cultured on plates or in liquid media, genetic manipulations using classical Mendelian approaches are possible. *C. elegans* can also be transformed with cloned DNA to produce stable transgenic lines (Mello *et al.*, 1991). The small size (1 mm length for the adult), small cell number (959 somatic cells in the hermaphrodite), invariant cell lineage and transparency of the organism have allowed the entire cell lineage to be defined (Sulston and Horvitz, 1977; Sultson *et al.*, 1983), and the complete wiring diagram of the nervous system has been determined at the ultrastructural level (White *et al.*, 1986). Targeted gene disruptions, although still not as simple as in *S. cerevisiae*, are made possible by the use of transposon insertion and imprecise excision (Plasterk and Groenen, 1992).

Of particular interest for molecular studies is the existence of a virtually complete physical map of the genome, and the rapid progress on sequencing of the *C. elegans* genome. At this writing, about two thirds of the genome has been sequenced through a consortium of two laboratories based in St. Louis, MO, and Cambridge, England (Wilson *et al.*, 1994), and completion is projected for late 1998. The sequences of cosmids are deposited in Genbank as they are completed and are therefore available to researchers. In addition, the cosmids, as well as a huge collection of cDNAs isolated in order to identify expressed genes, are distributed freely. The availability of a major part of the genome sequence allows *C. elegans* researchers to readily study entire protein families, or entire pathways, if desired.

The present study

The hetero-oligomeric eukaryotic cytosolic CCT represents the most complex chaperonin discovered to date. By making use of available cDNA sequence tags and the *C. elegans* genome sequencing project, characterization of five genes that encode subunits of the complex was greatly facilitated. All five genes were shown to be expressed throughout development. One of

the genes, *cct-1*, was isolated and sequenced. The *cct-1* transcript was shown to involve *cis*- and *trans*-splicing events to yield the mature 1.9-kb mRNA species. The ability to make transgenic *C. elegans* carrying promoter-*lacZ* fusion constructs made it possible to determine the expression pattern of *cct-1* within the context of an entire multicellular animal.

The CCT complex was purified by sucrose gradient fractionation and ATP-agarose chromatography, and the presence of two of the subunits (CCT-1 and CCT-5) was confirmed by Western blot analysis with polyclonal antibodies generated against C-terminal peptides. The subunit composition of the *C. elegans* CCT was shown to be very similar to that of bovine CCT, suggesting that the structure of the chaperonin complex is highly conserved in the animal Kingdom. The affinity of CCT for denatured actin appears to be lower than that of a related chaperonin from *C. elegans*, HSP60.

II. MATERIALS AND METHODS

2.1 Bacterial strains and media

The *E. coli* strains used for propagating plasmids and phage are listed in **Appendix I**. YT plates were used to grow the various *E. coli* strains, and Terrific Broth (TB) liquid medium was used for culturing the bacteria for the subsequent isolation of plasmid DNA or overexpressed protein. Both liquid and solid media were supplemented with the appropriate antibiotic(s) and were prepared as reported in Sambrook *et al.* (1989).

2.2 Molecular biological techniques

2.2.1 Gel electrophoresis and isolation of DNA fragments

Restriction enzyme digestion of DNA was usually carried out in a 20 µl reaction mixture containing 0.5-3.0 µg of DNA, 2 µl of 10X enzyme buffer supplied with the enzyme, and 1-10 units of restriction endonuclease enzyme(s). Restricted DNA fragments were fractionated on an agarose gel (0.4-2.0%) in TBE buffer (45 mM Tris-base, 45 mM boric acid, 2 mM EDTA; pH 8.0). Visualization of DNA bands under UV light was facilitated by the inclusion of 0.25 µg/ml ethidium bromide in the gel. Restricted DNA fragments were excised from the agarose gel and purified using the Qiaex™ Gel Extraction Kit (Qiagen Inc.).

2.2.2 Ligations

For most ligations, about 50 ng (25 fmol) of plasmid vector DNA and a 2-5 fold molar excess of insert DNA were ligated in a 20 µl reaction mixture containing 50 mM Tris-HCl (pH 7.8), 10 mM $MgCl_2$, 10 mM DTT, 1 mM ATP, 25 µg/ml BSA, and 0.25 Weiss units (cohesive-end ligation) or 2.5 Weiss units (blunt-end ligation) of T4 DNA ligase. Removal of vector DNA 5′ phosphoryl groups, when required to prevent self-ligation, was carried out by adding 4 units of calf intestinal alkaline phosphatase to the restriction digest reaction. The phosphatase enzyme was removed using the Qiaex Gel Extraction Kit.

2.2.3 Transformations

Competent DH5α subcloning efficiency cells purchased from BRL were typically used for transformations, although sometimes competent cells were prepared using the method of Hanahan (1983). Competent *E. coli* cells were transformed with 5 µl of ligation reaction by heat shock. Transformed cells were spread on YT plates containing the appropriate antibiotic(s) and incubated overnight at 37°C for colony growth. When required, X-Gal (50 µl of 20 mg/ml stock) and IPTG (10 µl of 100 mM stock) were spread onto the plates to differentiate recombinants (white) from nonrecombinants (blue), as described by Messing (1983).

2.2.4 Purification of plasmid and cosmid DNA

For isolating plasmid DNA suitable for restriction enzyme digests, subcloning, and sequencing, a slightly modified plasmid miniprep protocol from that of Morelle (1989) gave the best and most consistent results. A 2 ml bacterial culture harbouring plasmid or cosmid DNA was grown overnight at 37°C in TB medium supplemented with the appropriate antibiotic (Sambrook *et al.*, 1989). The cells were harvested in a 1.7 ml microcentrifuge tube, and resuspended in 200 µl of a 50 mM glucose, 10mM EDTA, 25 mM Tris-HCl pH 8.0 solution. After a 2 minute incubation, 400 µl of lysis buffer (0.1 N NaOH and 1% SDS) was added, and the tube mixed gently by inversion. After a 2-minute incubation, 300 µl of 7.5 M ammonium acetate was added, and the tube contents mixed well by inversion and incubated on ice for 10 minutes. Cellular debris, high molecular weight RNA and chromosomal DNA were then pelleted by centrifugation (10000 x *g*) at room temperature for 8 minutes. To precipitate the DNA, 700 µl of supernatant and 420 µl of isopropanol were mixed together and incubated for 10 minutes. The DNA was pelleted by centrifugation for 10 minutes, washed briefly with 70% ethanol, dried at room temperature for 10 minutes, and then dissolved in 40-60 µl TER buffer (10 mM Tris-HCl, pH 8.0; 1 mM EDTA; 1 µg/ml RNAse A).

2.2.5 Double stranded DNA sequencing

For most subcloning and sequencing procedures, restriction digest or PCR DNA fragments were ligated into pBluescript® II KS(+) (Stratagene) and sequenced by the dideoxy chain termination method of Sanger *et al.* (1977) using reagents from the Sequenase® Version 2.0 sequencing kit (U.S. Biochemical). The double stranded plasmid DNA (15 µl or at least 5 µg) was denatured for 5 minutes at room temperature by the addition of 2 µl of freshly prepared 2M NaOH, in the presence of 1 µl (1 pmol) of sequencing primer. A list of primers used for sequencing and/or PCR is given in **Appendix II**. The template DNA and primer were precipitated by the addition of 100µl of 95% ethanol and 8 µl of 5 M ammonium acetate (pH 7.8), mixing, and incubation at -70°C for 15 minutes. After centrifugation, the pellet was washed in 70% ethanol and air dried. Annealing of the primer to the template DNA was accomplished by resuspending the DNA in 10 µl 1X reaction buffer, and incubating at 37°C for 20 minutes. The remaining protocol was performed exactly as described in the Sequenase® Version 2.0 user's manual.

2.2.6 Polymerase chain reaction

Selective amplification of various DNA sequences was routinely performed using the polymerase chain reaction (PCR) (Saiki *et al.*, 1988). Typical reaction conditions are outlined in **Appendix III**. The 50 µl reactions were overlaid with light mineral oil, and inserted into a thermocycler block (TwinBlock™ System by Ericomp Inc.) preheated to 95°C. The thermal cycling program usually consisted of a 95°C denaturation step (3 minutes) followed by 30 cycles of 95°C for 30 seconds, 48-55°C for 30 seconds, and 72°C for 30-90 seconds. After a final extension step at 72°C for 10 minutes, 20 µl aliquots were analyzed on a 1.5 or 2.0% TBE agarose gel.

2.2.7 Preparation of DNA, RNA and first strand cDNA

Genomic DNA was isolated from *C. elegans* embryos as described by Emmons *et al.* (1979). Total RNA was prepared from staged nematodes by lysis in guanidine hydrochloride and

separation on a CSCl gradient (Antonucci, 1985). Alternatively, a mini-scale isolation of RNA (using a few hundred nematodes) was carried out (Mei Zhen, Ph. D. thesis, University of British Columbia, 1995). First strand cDNA was prepared from 10-20 µg of total RNA according to Jones and Candido (1993).

2.2.8 Southern and DNA dot blots

Aliquots of *C. elegans* genomic DNA (10 µg) or cosmid DNA (500 ng) were digested overnight with one or more restriction enzyme(s) and electrophoresed on a 0.7% TBE agarose gel. Prior to transfer, gels were soaked in 0.25 N HCl for 10 minutes, denaturation solution (1.0 M NaCl, 0.5 M NaOH) for 2 x 15 minutes, and neutralization solution (1.5 M NaCl, 0.5 M Tris-HCl, pH 7.4) for 2 x 15 minutes. Denatured DNA was then transferred to a Hybond™-N nylon membrane (Amersham) by capillary action using 10X SSPE (1.8 M NaCl, 10 mM EDTA, 100 mM NaH_2PO_4; pH 7.4). For dot blots, plasmid DNA (about 50 ng) or cosmid DNA (about 150 ng) was denatured with 0.1 volume of 3 M NaOH for 30 minutes at 65°C, and then neutralized by the addition of SSPE to a final concentration of 5X. The entire denatured DNA solution was spotted in 3 µl aliquots on a Hybond™-N nylon membrane previously soaked in 5X SSPE, air dried, and placed on top of 2 sheets of dry filter paper.For both methods, DNA was crosslinked to the nylon membranes by UV crosslinking (approximate exposure: 120 mJ/cm^2), or by baking the membrane at 80°C for 30 minutes.

2.2.9 Northern blots

The fractionation of RNA through an agarose gel containing formaldehyde was performed as described by Sambrook *et al.* (1989). Total cellular RNA samples (20 µg) were fractionated on a 1.2% formaldehyde gel alongside 5 µg of 0.24-9.5 kb RNA ladder molecular weight markers (BRL). After electrophoresis, the gel was rinsed in dH_2O for 15 minutes and the RNA was then transferred to a Hybond™-N nylon membrane by capillary action using 20X SSPE. The RNA was immobilized on the nylon membrane by UV crosslinking. RNA molecular weight markers were visualized by staining the membrane section containing the markers with 0.02%

methylene blue dye in 0.3 M NaOAc pH 5.5 (Herrin and Schmidt, 1988). If removal of the radiolabeled probe was required, the membrane was stripped in 0.1X SSPE, 0.1% SDS at 100°C for 5 minutes.

2.2.10 Preparation of radiolabeled DNA probes

DNA (25-50 ng) was uniformly labeled with [α-^{32}P]dATP or [α-^{32}P]dCTP using random hexadeoxyribonucleotides (Pharmacia) and Klenow enzyme (Pharmacia) as described by Feinberg and Vogelstein (1983). Alternatively, probes were random-primer labeled with [α-^{32}P]dCTP using the ^{T7}QuickPrime™ kit from Pharmacia. The radiolabeled probes were purified by chromatography on 1-ml Sephadex G50 spun columns to remove unincorporated dNTPs.

2.2.11 Nucleic acid hybridization conditions

Southern and Northern blots were pre-hybridized at 42°C for 1 hour in hybridization solution (final composition for 10 ml: 50% (v/v) deionized formamide, 5X SSPE, 0.5% (w/v) SDS, 5X Denhardt's reagent (diluted from a 50X stock consisting of 10 µg/ml each of Ficoll, polyvinylpyrrolidone, and BSA), and 0.5 mg/ml heparin). Denatured probe (0.1 ml; 1-6 X 10^7 cpm) was then added to the fresh hybridization solution and allowed to hybridize to the target DNA or RNA overnight at 42°C. Membranes were washed twice in 250 ml of 0.1X SSPE/0.1% SDS at room temperature for 15-30 minutes. For more stringent washes, membranes were washed twice in 250 ml of 0.1X SSPE/0.1% SDS at 65°C for 15 minutes. Membranes were exposed to X-OMAT™ AR film (Kodak) with an intensifying screen for autoradiography.

2.3 General protein and immunological techniques

2.3.1 Denaturing and native polyacrylamide gel electrophoresis

Denaturing, discontinuous SDS-PAGE of protein samples (Laemmli, 1970) was carried out on a Bio-Rad Mini-PROTEAN II gel. Gels (7.5%-15% acrylamide) and protein samples were prepared as described by Laemmli (1970). Native gels (4.5% acrylamide) were made with 80 mM MES pH 6.8 and 1 mM EGTA, and run on a Bio-Rad mini gel apparatus in the same

buffer at a constant power of 5 W for 1.5 hours. The running buffer in the upper and lower tank chambers was mixed every 30 minutes. For actin folding reactions, gels were supplemented with 1 mM ATP/ 1 mM $MgCl_2$, and the running buffer contained 0.1 mM ATP and 1 mM $MgCl_2$. Samples were supplemented with glycerol to 20% before loading.

2.3.2 Polyclonal antibody production

Peptides whose sequences match those of the 15 last residues of *C. elegans* CCT-1 (KLDKQEPLGGDDCHA-COOH) and CCT-5 (KIDDVRVPDDERMGY-COOH), respectively, were obtained from API (Alberta Peptide Institute). Each peptide came conjugated to KLH (for immunization) and BSA (for affinity purification). For each antigen, one rabbit was immunized with 0.5 mg of the KLH-conjugated peptide in Freund's complete adjuvant. New Zealand White rabbits were then boosted with 0.5 mg of the KLH-conjugated peptide in Freund's incomplete adjuvant after two weeks, and then once more after a further 3 weeks before sacrificing (bleeding) the rabbit two weeks later. Antiserum was prepared by allowing the blood to clot overnight at 37°C, precipitating the IgG with 45% ammonium sulfate, and dialyzing the resuspended salt-IgG pellet against TBS (25 mM Tris-HCl, 140 mM NaCl; pH 7.4).

2.3.3 Affinity purification of antibodies

The polyclonal antibodies (pAbs) were affinity purified on an Affi-Gel 10 resin coupled with the appropriate BSA-conjugated peptide according to the manufacturer's instructions. Antibodies were eluted with 0.1 M glycine pH 2.5, and immediately neutralized with 15 µl 1M Tris base per ml of eluant. Fractions containing antibody (monitored by A_{280}) were pooled and dialyzed against TBS.

2.3.4 Western blot analysis

Approximately 10 µg of total *C. elegans* protein extract (solubilized in Laemmli sample buffer), or ≤1 µg of partly purified or purified chaperonin was separated by SDS-PAGE, soaked in transfer buffer (25 mM Tris, 192 mM glycine, 10% methanol) for 10 minutes, and transferred

onto an Immobilon™-P PVDF membrane (Millipore) in transfer buffer for 1 hour at 250 mA or overnight at 50 mA. Following transfer, the membrane was blocked for 1 hour in TBS-T (TBS supplemented with 0.05% Tween 20) supplemented with 10% skim milk powder (Carnation). The membrane was briefly washed with TBS-T, and incubated with primary antibody (usually 1:3000 to 1:10000 dilution of purified and unpurified anti-CCT-1 or anti-CCT-5 antibodies, respectively) for 1 hour. After 3 washes with TBS-T (5 minutes each), the membrane was incubated with a 1:10000 dilution of Amersham peroxidase-labeled anti-rabbit antibody for 1 hour, and washed as before. Immunodetection was carried out using Amersham's enhanced chemiluminescence (ECL) kit.

2.3.5 Miscellaneous

Protein concentrations were determined with the Bio-Rad protein assay kit using bovine IgG as standard.

2.4 Purification of Chaperonin Containing TCP-1 (CCT)

Large-scale isolation of *C. elegans* embryos was performed as described in **Appendix IV**. *C. elegans* CCT was purified essentially as described by Lewis *et al.* (1992). A post-nuclear supernatant of frozen *C. elegans* embryos (50% v/v in 250mM sucrose, 10mM Tris-HCl, pH 8.0, 10mM $MgCl_2$) was prepared by homogenizing thawed embryos using a Potter Elvejhem homogenizer, and pelleting the cell debris at 12000 x *g*. Protease inhibitors (100 µg PMSF, 2 µg antipain, 2 µg aprotinin, and 1 µg pepstatin A, all per ml; 1 mM EDTA) were added to the thawed embryos before homogenization. Approximately 2.5-ml aliquots of the supernatant were loaded onto 36.5-ml 10-40% (w/w) sucrose gradients (made in 50 mM KCl, 50 mM Tris-HCl pH 7.4, 1 mM DTT, 0.5 mM EDTA) and centrifuged in a SW28 rotor at 26000 rpm for 18 hrs at 4°C. A total of 19 2-ml fractions were collected from the bottom of the polyallomer centrifuge tubes (Beckman), and 15 µl aliquots from each fraction was assayed for CCT-1 by Western blotting. Positive fractions were dialyzed against TEDKM buffer (50 mM Tris-HCl pH 7.4, 50 mM KCl, 1 mM DTT, 0.1 mM EDTA, 10 mM $MgCl_2$) and loaded onto a column containing

ATP-agarose resin (Sigma) equilibrated with the same buffer. After washing the column with 3 column volumes of TEDKM/ 100 mM NaCl buffer, ATP-binding proteins were eluted with three column volumes of TEDKM/ 100 mM NaCl/ 10 mM ATP/ 10 mM $MgCl_2$. The second and third fractions were dialyzed against TEDKM buffer diluted 10-fold with dH_2O, and 200 µl aliquots were concentrated approximately 10-fold by vacuum centrifugation.

2.5 Construction and analysis of transgenic nematodes

2.5.1 Preparation of construct for injection

To make a *cct-1*-promoter-*lacZ* expression construct, the ~3.7 kb *Hin*dIII restriction fragment upstream of the internal *cct-1 Hin*dIII site was cloned from the cosmid T05C12 (pBS-*cct-1* [*Hin*dIII-*Hin*dIII] clone). A nematode expression vector containing the β-galactosidase gene (pPD16.43 vector; Fire *et al.*, 1990) was used to fuse, in frame, the 5'-end (promoter region) of the *cct-1* gene fused to the β-galactosidase coding region, and to add the 3'-untranslated region of *cct-1,* as described below. First, the pPD16.43 vector was cut with *Eag*I and *Stu*I (16.43.ES). The 3'-end of *cct-1* was restricted with *Bgl*I and *Pst*I, and subcloned into pBluescript cut with the same enzymes. From the latter vector, a *Hin*cII/*Eag*I fragment was isolated, and subcloned into 16.43.ES, creating pPD16.43.3'. A fragment containing the 5'-end of *cct-1* was then made by amplifying the pBS-*cct-1* [*Hin*dIII-*Hin*dIII] clone with the *cct-1*-specific oligo MIC5 (see **Appendix II**) and the pBS vector primer T3. The amplified product and 16.43.3' were then cut with *Hin*dIII and *Sal*I and ligated together, forming pPD16.43.5'.3'. This construct therefore contained 2.7 kb of upstream noncoding region, the first intron in the *cct-1* gene, followed by 32 amino acids of the *cct-1* coding region fused in-frame to the nuclear localization signal (NLS) and β-galactosidase gene, as well as approximately 1000 bp of *cct-1* 3'-noncoding region (including the polyadenylation signal). This vector was tested for expression in transgenic strains (below).

2.5.2 Injection of the construct

The construct was prepared by the regular plasmid DNA isolation protocol, and was resuspended in distilled water at a concentration of 200 ng/µl. The plasmid marker pRF4 (Mello *et al.*, 1991) was co-injected at the same concentration into the gonad of the Bristol N2 strain. Transformed progeny, identified by their rolling phenotype caused by the mutant collagen encoded by pRF4, were transferred to separate plates to determine if the extrachromosomal array was passed on to subsequent generations. Transient lines were frozen in liquid nitrogen as described in Lewis and Fleming (1995), and are listed in **Appendix V**.

2.5.3 Histochemical detection of β-galactosidase in transgenic lines

Strains containing the *cct-1*-promoter-*lacZ* construct were stained according to Fire *et al.* (1992). The animals were dried *in vacuo* on a microscope slide, permeabilized with acetone, and incubated with 75 µl of staining solution overnight at 37°C in a moist chamber. The stained animals were mounted in 80% glycerol, 20 mM Tris (pH 8.0), and 200 mM sodium azide, and then examined by Nomarski microscopy. The cell types were identified on the basis of their position (relative to the animal and other cells), size, and shape, based on published *C. elegans* anatomy and cell lineage (Wood, 1988).

2.6 Sequence alignments and secondary structure predictions

Amino acid sequences were deduced using the Macintosh program DNA Strider 1.2 (Christian Marck). Multiple amino acid sequence alignments were assisted by the program MacDNASIS Pro v3.2 (Hitachi Software Engineering Co.), and refined manually to minimize the number of gaps/insertions within the alignment, and to take into account predicted secondary structures. Secondary structure predictions for the chaperonin proteins were made with the program PHD (1995 version). PHD scans the SWISSPROT database for sequences similar to the input sequence, and generates a multiple sequence alignment which is then used by a three-level neural network algorithm for making predictions at better than 70% accuracy (Rost and Sander, 1993, 1994).

III. RESULTS

3.1 Sequence analysis of five CCT proteins

3.1.1 Sequence determination of five *cct* cDNAs from a multigene family

As an adjunct to the genomic sequencing of *C. elegans*, a complementary project has provided investigators with a large collection of sequence tags from a sorted cDNA library (Waterston *et al.*, 1992). For each cDNA clone, a single sequence read from the 5' end is made available through ACeDB (the genome database of *C. elegans*, accessible through NCBI, EMBL, and GenBank), and the clones themselves are freely available. Four different λSHLX2 phage harbouring the *C. elegans cct* cDNAs encoding CCT-1, CCT-2, CCT-4, and CCT-5 were obtained from this library; these clones correspond to cm08g10, cm17c1, cm15e11, and cm13e8, respectively. The BLASTX scores (Altschul *et al.*, 1990) for the predicted protein sequences encoded by the cDNAs showed them to be significantly similar to murine CCTα (Kubota *et al.*, 1992) and CCTβ, CCTγ, and CCTε (Kubota *et al.*, 1994).

The pRatII plasmids containing the *cct* cDNAs (pRatII-*cct-1*, pRatII-*cct-2*, pRatII-*cct-4*, and pRatII-*cct-5*) were excised from the phage DNA using the 'popout' *E. coli* strain BM25.8 (Palazzolo *et al.*, 1990). The plasmid DNAs were isolated and used to transform competent DH5α *E. coli* for efficient propagation of the plasmids. *Not*I/*Apa*I fragments containing the full-length cDNAs were isolated from the pRatII plasmids and subcloned into pBluescript (pBS) vectors cut with *Not*I/*Apa*I, yielding pBS-*cct-1*, pBS-*cct-2*, pBS-*cct-4*, and pBS-*cct-5*. The pBS vectors containing the *cct* cDNAs were digested with multiple restriction enzymes, and the fragments generated were subcloned into pBS for sequencing using the primers T3 and T7, as well as some gene-specific primers. The entire cDNAs (approximately 1.9 kb each) were sequenced in this manner. Sequence coverage included all of both strands for *cct-1*, and both strands for the other *cct* cDNAs except in some regions where the sequence was clearly unambiguous. The deduced amino acid sequence of *C. elegans* CCT-6 was obtained by translating the open reading frames of the *cct-6* gene sequence determined by the *C. elegans* genome sequencing project (Wilson *et al.*, 1994).

3.1.2 Primary structure analyses of five CCT proteins

The open reading frames of the *cct-1*, *cct-2*, *cct-4*, *cct-5*, and *cct-6* genes encode proteins of 58.8 kDa (549 aa), 57.0 kDa (529 aa), 58.4 kDa (540 aa), 59.4 kDa (542 aa), and 58.9 kDa (539 aa), respectively. Kubota *et al.* (1994) reported that members of the murine CCT protein family are as closely related to the archaebacterial protein TF55 as they are to other members of the CCT family. Sequence analysis of the five *C. elegans* CCT proteins and TF55 corroborate this observation. An amino acid sequence alignment of the *C. elegans* CCT proteins with TF55 (**Figure 2A**) reveals that members of the *C. elegans* CCT protein family share 23-35% pairwise predicted amino acid sequence identity between each other and 31-35% sequence identity to TF55 (**Figure 2B**). The *C. elegans* proteins CCT-1, 2, 4, 5, and 6 share 66%, 66%, 63%, 68%, and 67% amino acid sequence identity with the orthologous mouse CCTα, β, δ, ε, and ζ subunits, respectively. Similarly, various CCT proteins from humans, yeast, and *Drosophila* share between 62-68% amino acid sequence identity with their *C. elegans* orthologs. The strong similarity between the CCT orthologs spans the entire protein sequence, and the calculated MWs of the orthologs are nearly identical.

Some sequence motifs that are conserved in nearly all chaperonins, including the classical chaperonins (Lewis *et al.*, 1992) and members of the CCT/TF55 protein family (Kim *et al.*, 1994; Kubota *et al.*, 1994), are also conserved in the *C. elegans* CCT protein family (**Figure 2A**). One highly conserved sequence is GDGTT, centered on position 110 of the *C. elegans* CCT and TF55 alignment. This sequence was proposed to form part of a putative ATP-binding domain based on limited sequence homology to the cAMP-dependent protein kinase family (Lewis *et al.*, 1992; Kubota *et al.*, 1994). Mutational analysis of the aspartic acid residue present within this sequence confirms that it is required for ATP hydrolysis and polypeptide release (Fenton *et al.*, 1994).

A

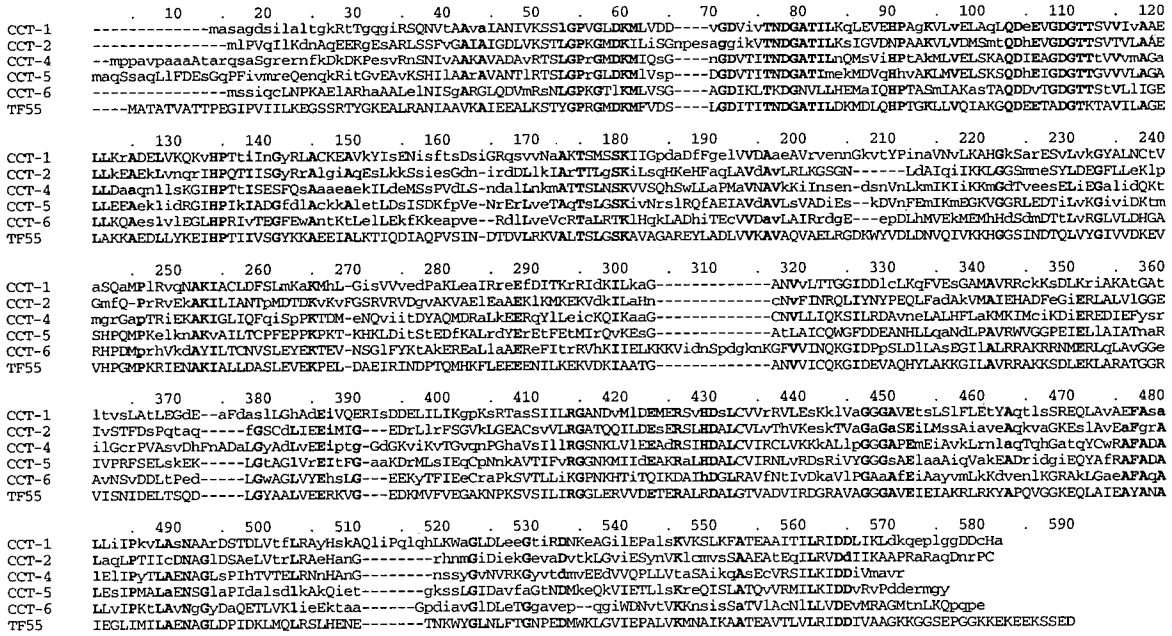

B

	CCT-1	CCT-2	CCT-4	CCT-5	CCT-6	TF55
CCT-1	*549*	8(27)	5(13)	5(14)	7(32)	4(14)
CCT-2	34	*529*	6(18)	6(13)	8(27)	5(13)
CCT-4	29	30	*540*	3(7)	6(25)	4(9)
CCT-5	30	29	30	*542*	6(20)	2(4)
CCT-6	25	29	22	28	*539*	5(20)
TF55	38	36	39	38	33	*552*

Figure 2. Multiple alignment of five *C. elegans* CCT proteins and TF55. **A.** Single-letter amino acid designations for each *C. elegans* CCT protein are shown in uppercase if they are identical to the orthologous mouse CCT protein at the same respective position (the TF55 sequence is shown entirely in uppercase). Amino acids which are identical at five of six positions in the *C. elegans* CCT and TF55 proteins are shown in bold to denote highly conserved positions. Dashes indicate gaps introduced to maximize the number of identical or conserved residues aligned between the CCT and TF55 amino acid sequences. The numeric scale represents relative amino acid positions in the alignment. **B.** A summary of the percentage amino acid identities of the *C. elegans* CCT proteins and TF55 is shown below the diagonal. The total number of gaps required for the pairwise alignments, and the total number of spaces within the gaps (in parentheses) are shown above the diagonal. The size of each protein in amino acids is shown along the diagonal. The sequences of the nucleotide and deduced amino acid sequences of the *C. elegans cct* genes are available in Genbank, under the following accession numbers: CCT-1 (U07941), CCT-2 (U25632), CCT-4 (U25697), CCT-5 (U25698), and CCT-6 (U13070).

The sequence (I/V)T(K/N)DG (positions 75-79), conserved in all chaperonins, is also located near the ATP-binding region in GroEL. Another conserved region, LGP(K/R)G, is centered on position 55 and is the site of a known temperature-sensitive mutation in yeast TCP1β (Miklos *et al.*, 1994). Lastly, a highly conserved V(P/A/Y)GGG motif (positions 443-447), is present in the *C. elegans* CCT proteins in the somewhat modified (V/L)(P/A/Y)G(G/A)(G/A) form. The triple-glycine motif is part of a tubulin-binding domain present in the microtubule-associated MAP2 and tau proteins, and is the site of a temperature-sensitive mutation in a yeast mutant (*tcp1-1*) which is synthetic-lethal in combination with the tubulin *tub2-402* mutation (Lewis *et al.*, 1988; Ursic *et al.*, 1994).

3.1.3 Predicted secondary structures of CCTs and other chaperonins

The structural and functional information available on GroEL facilitates a more thorough analysis of the CCT/TF55 chaperonin family structure and function. Kim *et al.* (1994) demonstrated that the primary amino acid sequence of the CCT proteins and GroEL are much more conserved in their equatorial (ATP-binding) domains than in their apical (polypeptide binding) domains. The fact that residues within the apical region of the CCT subunits were poorly conserved suggested that the polypeptide binding domains of the CCT subunits had diverged in response to the eukaryote's increasing variety of substrates to fold, or to specialize in the folding of specific sets of proteins, such as tubulins and actins.

Important questions regarding the structure and function of CCT/TF55 proteins remain (Kim *et al.*, 1994). Do individual CCT/TF55 members share the same fold or have they all diverged from one another, especially in their polypeptide binding domain? Do the classical and CCT/TF55 chaperonins share evolutionarily conserved secondary and tertiary structures? Lastly, are differences in substrate affinities, folding properties, and requirement for a co-chaperonin in the GroEL/Hsp60 and CCT chaperonins due to changes in secondary and/or tertiary structures of the presumed polypeptide binding domain?

To provide some insight into these questions, alignments of the primary and predicted secondary structures of the five *C. elegans* CCT members along with two murine CCTs, TF55,

GroEL, Hsp60 and RuBP were performed, and rooted to the known GroEL secondary structure (**Figure 3**). The defined secondary structure of GroEL provided an important internal standard with which to compare the predicted structures of the two chaperonin families. Secondary structure predictions were performed with the program PHD, which uses information from homologous amino acid sequences to make predictions with an overall accuracy of greater than 70% (Rost and Sander, 1993, 1994).

Since the GroEL/Hsp60/RuBP chaperonin family is highly conserved (44-55% amino acid sequence identity), it was expected that the predicted secondary structures of the members would be very similar. Indeed, the alignment of the Group I chaperonins clearly shows that their predicted secondary structures are almost identical. However, while PHD predicts almost identical secondary structures for GroEL, Hsp60, and RuBP, the predicted secondary structure of GroEL is very similar, but not identical to the known secondary structure of this chaperonin. PHD correctly predicted 11 out of 19 β-sheets and 16 out of 18 helices; the low prediction rate for β-sheets seems to be due to the relative inability of the algorithm to correctly predict β-sheet structures which are immediately adjacent to a helix (only 1 out of 5 such β-sheets was predicted). Therefore, although the secondary structure predictions are only an approximation of the true secondary structure, they are nonetheless useful for detecting conserved secondary structures within related proteins.

The alignment of the CCT and TF55 proteins suggests that the secondary structures of these chaperonins are very closely related. Except for a few minor differences, the predicted secondary structures of these chaperonins are virtually identical. Moreover, the predicted secondary structures of the *C. elegans* and mouse orthologues are completely superimposable (not shown). On this basis, the structural backbone of the CCT/TF55 chaperonin family appears to have been evolutionarily conserved, despite the divergence in primary amino acid sequence of each member.

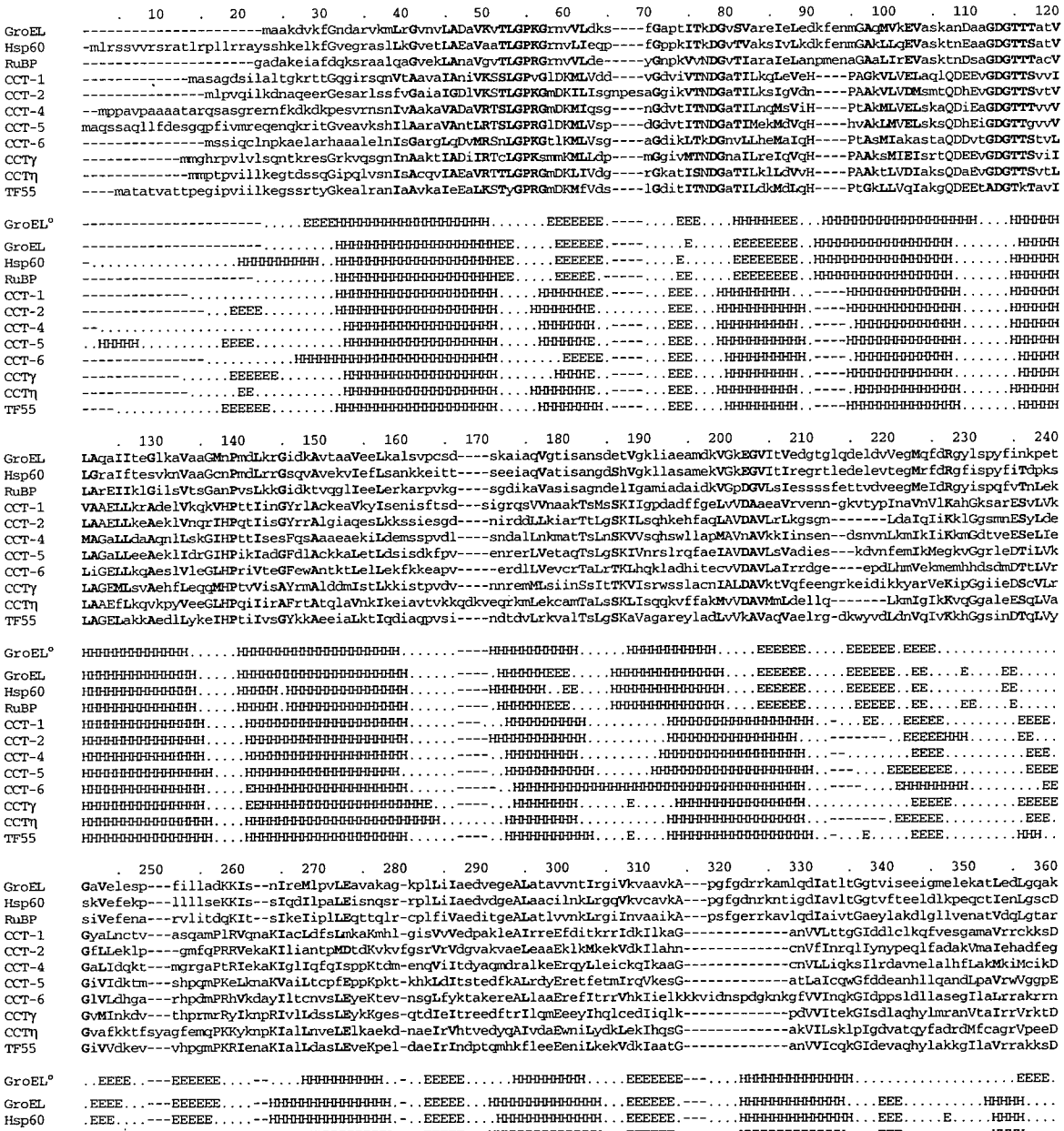

Figure 3. Multiple alignment of the deduced amino acid sequences and predicted secondary structures of the GroEL/Hsp60/RuBP and CCT/TF55 chaperonin families. The *C. elegans* CCT family (CCT-1, 2, 4, 5, and 6) and two murine CCTs (CCTγ and η) are shown in the alignment. GroEL, Hsp60, and RuBP, as well as TF55 are also included. Amino acids in uppercase or bold uppercase indicate conserved amino acids present in 7 or 9 of the 11 chaperonins, respectively. Conserved amino acids were placed in the following groups: A, G; M, I, L, V; D, E; K, R; S, T; N, Q; F, W, Y. Predicted secondary structure alignments are shown below the amino acid sequences. The known GroEL secondary structure (GroEL°) is shown for comparison. Protein conformations are indicated as follows: dots represent coils, turns, or bends; H, α helix; E, β-sheet. Dashes indicate gaps introduced in the protein primary and predicted secondary structures. Numbers in brackets represent the number of truncated amino acids from the ends of some sequences. Chaperonin sequences (with accession numbers) used in this alignment are as follows: GroEL [X07850] and RuBP [X07851] (Hemmingsen *et al.*, 1988); Hsp60 [M33301] (Reading *et al.*, 1989); murine CCTγ [Z31556] and η [Z31399] (Kubota *et al.*, 1994); TF55 [X63834] (Trent *et al.*, 1991).

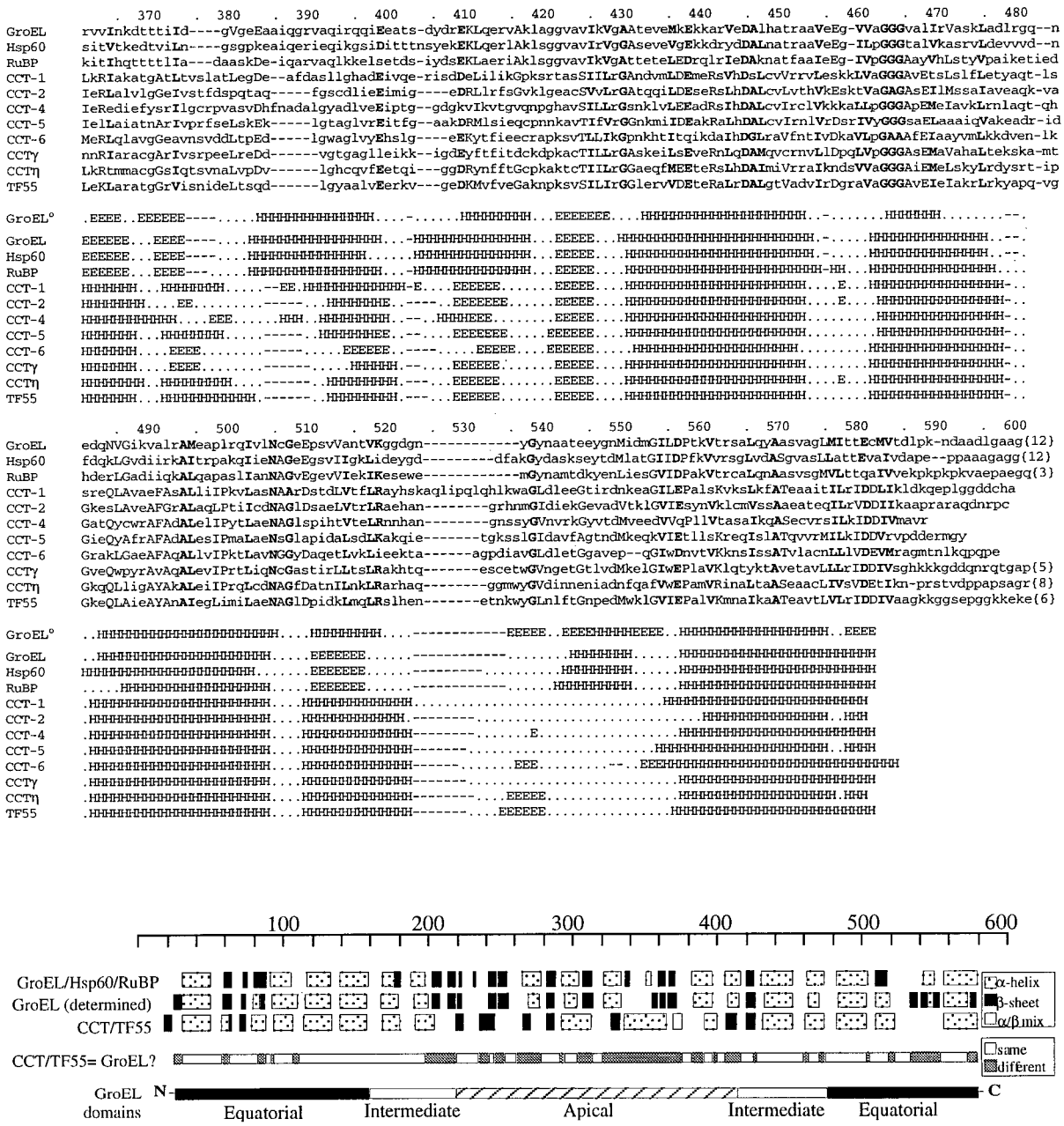

Figure 3 cont'd. A summary of chaperonin predicted secondary structures is depicted below the alignments. Secondary structures (helix is shown dotted, β-sheet in black, and combination of helix/β-sheet in white) predicted in all members of the GroEL/Hsp60/RuBP family, or in five or more members of the CCT/TF55 family are shown aligned with the known GroEL secondary structure. Below, regions where the CCT/TF55 family are different from the determined GroEL secondary structure are highlighted in gray, identical regions in white. Also shown are the relative positions of the three domains found in GroEL. All of the secondary structures, the CCT/TF55-GroEL structure comparison, and the GroEL domains are aligned against a scale (1-600) which corresponds to the amino acid sequence positions in the sequence alignment.

Although the two chaperonin families (Group I and II) are evolutionarily related, basic differences in their primary amino acid sequence, quaternary structure, substrate specificity, and requirements for a co-chaperonin suggest that some alterations in their secondary structures would be required. The results obtained indicate that important similarities, as well as differences, exist between the predicted secondary structures of the two families. Comparison of the predicted secondary structures of the CCT/TF55 family members with the determined GroEL secondary structure (**Figure 3**) reveals significant correspondence in their structures. The entire equatorial domain (two halves), the C-terminal intermediate domain, and the left half of the N-terminal intermediate domain are very similar in the CCT/TF55 family and GroEL. These regions are rich in helical structures, and comprise residues required for ATP binding and hydrolysis, as well as for making inter-subunit contacts.

Significant differences between the predicted secondary structures of the CCT/TF55 family and the known GroEL secondary structure are present in the second half of the N-terminal intermediate domain and most but not all of the apical domain. These two regions encompass a cluster of β-sheet structures (positions 199-373) which contains 10 of the 19 β-sheet structures of GroEL. This region is also predicted to be rich in β-sheets in the CCT/TF55 family, but the positions of 4 of its 6 β-sheets do not coincide with the β-sheets of GroEL. In contrast, 8 out of 10 β-sheets are correctly predicted in the GroEL/Hsp60/RuBP proteins. Also, the region where a β-sheet and an extended helical structure is predicted in CCT/TF55 (positions 329-367) consists of a helix, an extended loop and two β-sheets in GroEL.

3.2 Isolation of genomic *cct-1*

Southern blot analysis of *C. elegans* genomic DNA reveals that *cct-1* is a single copy gene (**Figure 4**). In order to isolate genomic *cct-1*, the cDNA was used to screen a polytene membrane containing ordered yeast artificial chromosome (YAC) clones representing approximately 90% of the *C. elegans* genome (Waterston *et al.*, 1992). Two overlapping YAC clones (Y50H5 and Y50D9) mapping to chromosome II hybridized to the *cct-1* probe (**Figure 5A**).

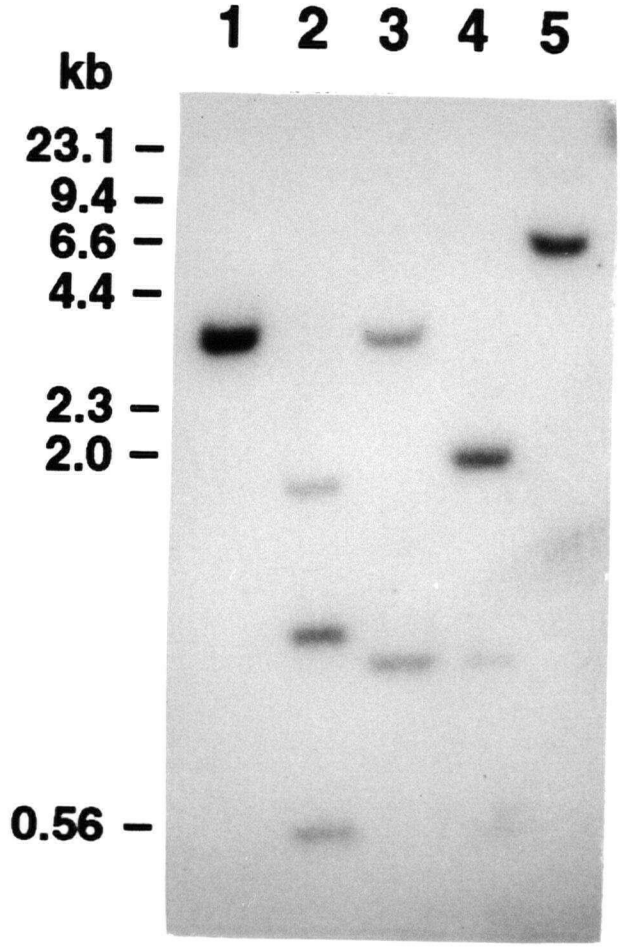

Figure 4. Southern blot analysis of *C. elegans cct-1*. Genomic DNA was digested with *Pst*I (1), *Eco*RI (2), *Hin*dIII (3), *Dra*I (4), and *Xho*I (5), and probed with ^{32}P-labeled *cct-1* cDNA under stringent hybridization conditions.

Cosmids spanning the overlapping YAC clones were obtained and screened by dot blot analysis using the same probe; one of the cosmids, T05C12, was found to contain the gene of interest (**Figure 5B**).

A Southern blot of the T05C12 cosmid DNA digested with *Pst*I, *Pst*I/*Xho*I, *Eco*RI, and *Hin*dIII was hybridized to a *cct-1* probe (**Figure 5C**). The restriction map patterns of the cosmid and genomic *cct-1* gene were found to be identical. Consequently, a 3.7 kb *Pst*I restriction fragment was isolated from the cosmid DNA, subcloned into pBluescript, and sequenced. The open reading frame sequence of the *cct-1* gene was found to be identical to that of the cDNA. As shown in **Figure 5D**, the *cct-1* gene locus was mapped to cosmid T05C12 on the central (gene-rich) region of chromosome II, between *fer-15* and *rol-6*.

The *C. elegans cct-1* gene sequence is shown in **Figure 6**. Sequence analysis of *cct-1* shows that the coding region is divided into 5 exons and 4 introns. The region upstream from the translation start site contains a distinctive degenerate sequence repeated five times: NAAANATTTTTATTTTTA. The repeats contain a core sequence with nucleotides (nt) present in 4 or 5 of the five repeats (underlined), and more variable nt present in 3 of the repeats (not underlined; N means any nt). Three of these repeats are separated by 5 and 7 nt and are proximal to the *trans*-splice site (see **section 3.6**). The repeats do not match any known transcription factor consensus binding site. Also present upstream from the start codon are two potential TATA boxes and a CCAAT box (Jones *et al.*, 1987). No HSE consensus sequences, which are involved in the transcriptional regulation of *HSP* genes (Sorger, 1991), are present. The 3'-untranslated region of the gene contains a putative polyadenylation signal, AATGAA, present 13 nt upstream from the polyadenylation site defined by the cDNA sequence. Lastly, a potential transcription stop signal (Vandenbergh *et al.*, 1991) consisting of an imperfect 13 bp inverted repeat is present 26 nt downstream from the polyadenylation site.

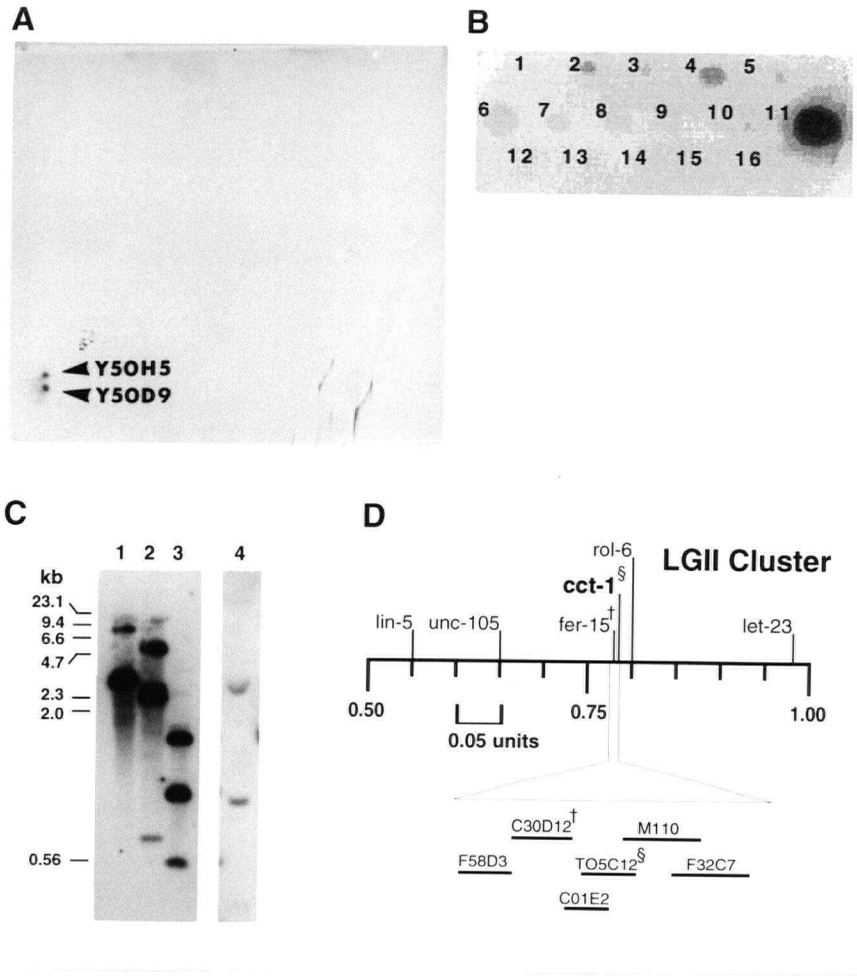

Figure 5. Isolation of *cct-1* from the cosmid T05C12. **A.** Detection of two cross-hybridizing, overlapping YACs (Y50H5 and Y50D9) in an ordered YAC filter (Waterston *et al.*, 1992) using ^{32}P-labeled *cct-1* cDNA as a probe. **B.** Cosmid DNA samples spanning the two YACs were probed in a dot blot using the same probe. Listed in order, the cosmids were: DH11, C09D2, C08B11, C04H4, B0223, C24E1, C30D12, C30G9, ZK656, ZK658, T05C12, T05H10, F10E8, ZK660, T07C3, and F49C2 (the positive cosmid, number 11, is underlined). **C.** Southern blots of T05C12 cosmid DNA digested with *Pst*I (1), *Pst*I-*Xho*I (2), *Eco*RI (3), and *Hin*dIII (4) were probed with ^{32}P-labeled *cct-1* cDNA. **D.** Map position of *cct-1* relative to cosmids surrounding T05C12 as well as other genetic markers on chromosome II.

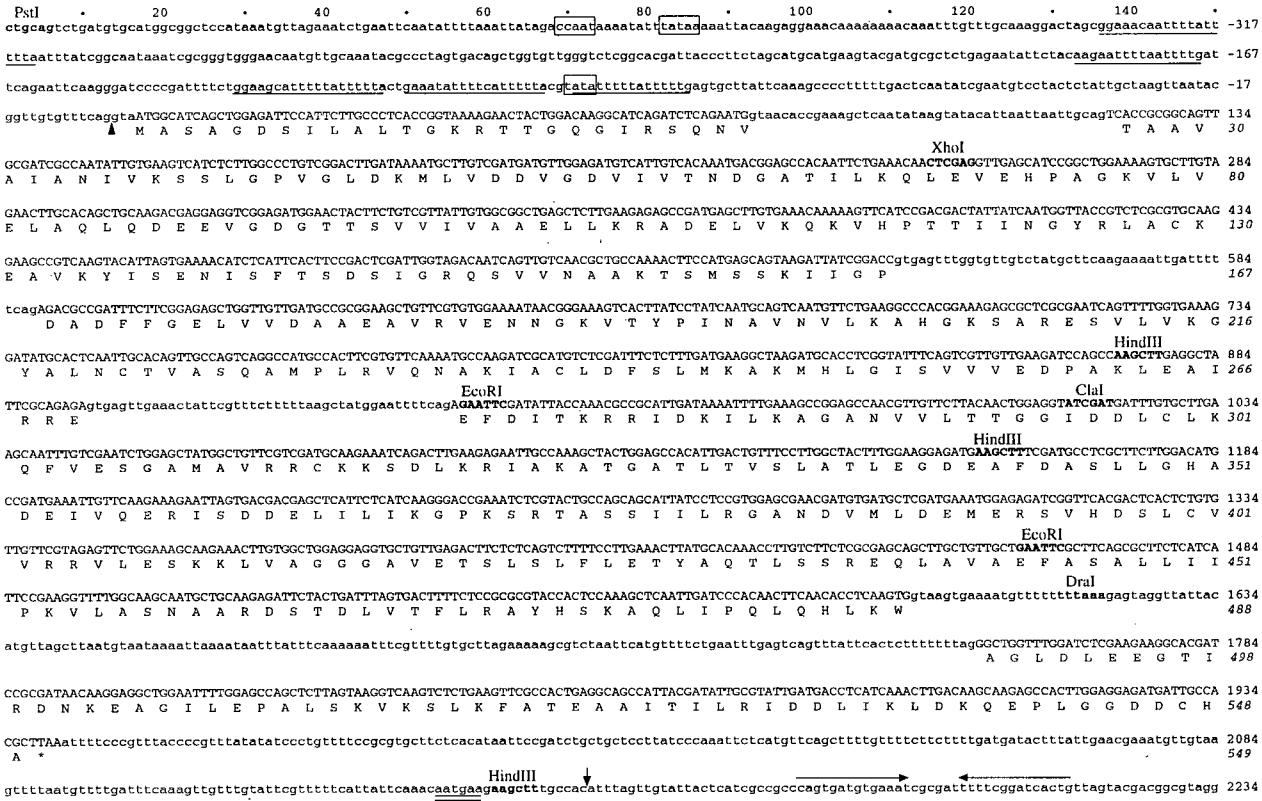

Figure 6. Nucleotide and amino acid sequence of *C. elegans* genomic *cct-1*. Part of the 3.7-kb *Pst*I restriction fragment isolated from the cosmid T05C12 is shown here. The nucleotide (nt) and amino acid numbering are indicated on the right side of the sequence; the first nt (+1) begins at the start codon (A in ATG), and negative numbering begins upstream of the start codon. Exons are in uppercase type, and have the corresponding aa residue indicated for each codon; introns are shown in lower case type. Five repeats within the non-coding promoter region are singly underlined. Putative CCAAT and TATA consensus sequences are shown boxed. The SL1 *trans*-splicing site is indicated by an arrow pointing up. The likely polyadenylation signal (AATGAA) is double underlined, and the respective polyadenylation site is shown by an arrow pointing down. An inverted repeat downstream of the polyadenylation site is denoted by two horizontal arrows. The accession number for *C. elegans cct-1* is U07941.

3.3 Physical map positions of five *cct* genes

Many *C. elegans* genes are transcribed as polycistronic mRNAs, much like bacterial operons (Krause and Hirsh, 1987). Processing of the individual transcripts requires *trans*-splicing to splice leader RNAs (SL1 and SL2; reviewed in Blumenthal, 1995). In theory, operons may serve to coordinate the expression of genes with related functions or which assemble into an oligomeric complex, as is the case with CCT. Both *cct-1* and *cct-2* were mapped by hybridization to a filter containing overlapping ordered yeast artificial chomosome (YAC) clones representing about 90% of the *C. elegans* genome (Waterston *et al.*, 1992), and *cct-4*, *cct-5*, and *cct-6* were identified in the genome sequencing project. The five *C. elegans cct* genes are located on chromosomes II and III (**Figure 7**). Three genes, *cct-1*, *cct-2*, and *cct-4* are between 50 and 300 kb apart on chromosome II, and thus are unlikely to be part of a single transcriptional unit. Likewise, the two genes on chromosome III, *cct-5* and *cct-6*, are widely separated from each other.

3.4 Expression of *cct* genes throughout nematode development

The expression levels of the five *C. elegans cct* genes throughout development were examined by Northern blot analysis. Total RNA (approximately 20 µg) prepared from the nematode's six major life cycle stages was separated on a 2.2 M formaldehyde-1.2% agarose gel and transferred to a Hybond-N membrane. The membrane was then sequentially hybridized to individual *cct* cDNAs, autoradiographed, and then stripped before the next hybridization. As a control for RNA loading, the membrane was also hybridized to a ^{32}P-labeled *actin-1* probe which hybridizes to at least four actin genes in *C. elegans*, that, overall, are expressed at the same approximate level during development (Krause and Hirsh, 1986). Northern blot signal intensities were quantified by densitometry, and the expression levels of the *cct* genes were then normalized to the actin control. **Figure 8** summarizes the results from the Northern blot analysis. Each *C. elegans cct* gene is expressed at a similar level throughout development. An mRNA transcript of approximately 1.9 kb, which closely matches the sizes of the cDNAs (1.8-2.0 kb), is present for each gene during all life stages.

A

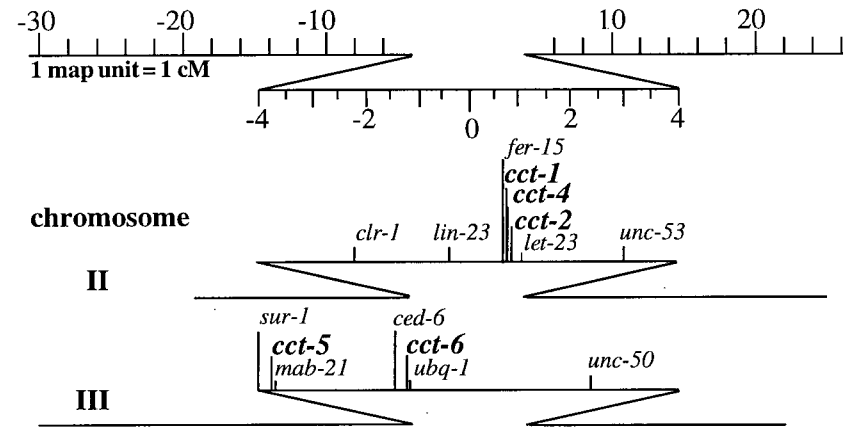

B

gene	cosmid(s)	YACs	chromosome	determined
cct-1	T05C12	Y50H5, Y50D9	II	this study
cct-2	T21B10	Y55H12, Y50B6	II	this study
cct-4	K01C8		II	genome seq.
cct-5	F25F2/C07G2		III	genome seq.
cct-6	F01F1, W04D12		III	genome seq.

Figure 7. Physical map positions of five *C. elegans cct* genes. **A.** The *cct* genes, marked in bold and shown with some genomic landmarks, are distributed on two of the five *C. elegans* autosomes. Precise locations of the genes on the physical map can be found in the *C. elegans* ACeDB database (Richard Durbin and Jean Thierry-Mieg). Each map unit corresponds to more than 1.5 Mb in the gene-rich, central chromosomal clusters of *C. elegans* (Sulston *et al.*, 1992). **B.** Summary of *cct* gene mapping to cosmids and/or YACs. "genome seq." refers to genes already mapped and sequenced by the *C elegans* sequencing consortium.

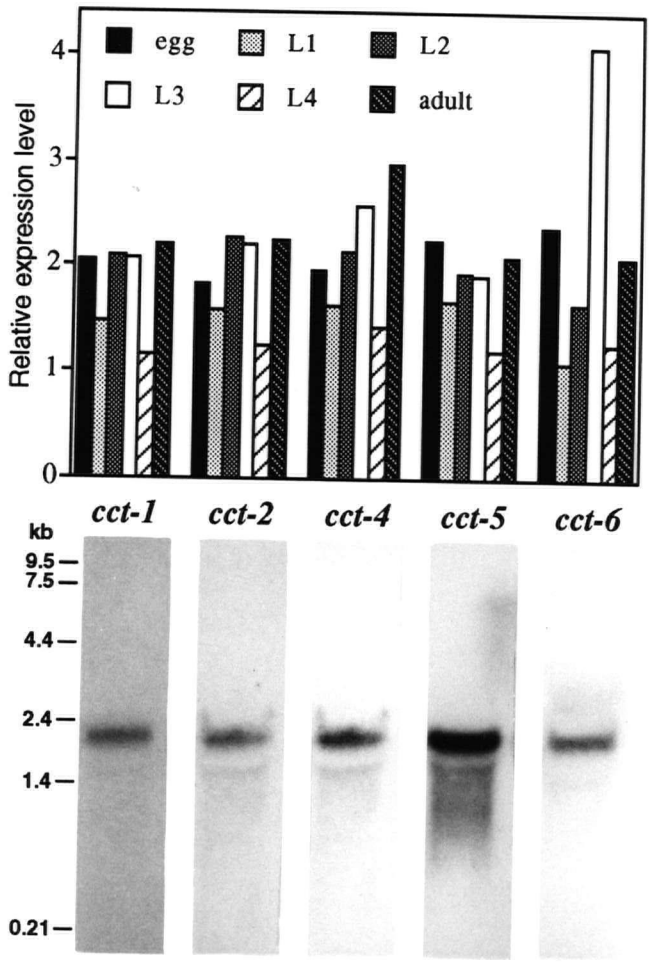

Figure 8. Northern blot analysis of five *C. elegans cct* genes. RNA from each major developmental stage (embryo, L1-L4 larvae, and adult) was separated on a 1.2% denaturing agarose gel and transferred to a Hybond-N membrane. The membrane was then sequentially hybridized to five *cct* cDNAs and a control *actin-1* probe. After each hybridization and autoradiography, probes were stripped from the membrane. The bar graph shows relative mRNA levels of each *cct* gene during the developmental stages. Expression levels are normalized with respect to the *actin-1* control probe. Below the graph are representative Northern blot autoradiograms of each gene at the L4 larval stage, with the sizes of the RNA molecular weight markers indicated on the left.

3.5 Expression of *cct-1* after heat-shock treatment

A characteristic difference between yeast *cct-1* and other chaperonin genes is that the level of RNA transcript is not upregulated following heat-shock treatment; rather, there appears to be a decrease in the amount of transcript produced during heat-shock (Ursic and Culbertson, 1992). A Nothern blot containing RNA samples isolated from heat-shocked (2 hours at 30°C and 30 minute recovery at room temperature) and control nematode embryos was successively hybridized to ^{32}P-labeled *cct-1* cDNA, *actin-1*, and *hsp16-48* probes (**Figure 9**). The relative signal intensity from the *cct-1* (**Figure 9A**) compared with the *actin-1* (**Figure 9B**) probing of the control and heat-shocked RNAs is somewhat weaker, indicating that *C. elegans cct-1* expression is not heat-inducible and might be slightly lower. The *actin-1* probe serves as a loading control, as it is expressed at a similar level during heat-shock; a control probing (**Figure 9C**) shows that the RNA from the heat-shocked nematodes but not the control nematodes hybridizes strongly to the strictly heat-inducible *hsp16-48* gene (Jones *et al.*, 1989).

3.6 *cct-1* undergoes both *cis*-splicing of its introns and *trans*-splicing to SL1

Inspection of the *cct-1* cDNA sequence immediately upstream of the methionine start codon revealed part of the SL1 *trans*-splice RNA leader sequence, which is spliced onto many *C. elegans* gene transcripts (Krause and Hirsh, 1987). To determine if *cct-1* is *trans*-spliced to the SL1 or SL2 RNA leaders, PCR was performed on a *C. elegans* embryo cDNA library using an SL1 and SL2 primers in conjunction with an internal *cct-1* primer (MIC3, complementary to nt 242-227 on the genomic DNA sequence). A DNA fragment amplified with these primers was identified as *trans*-spliced *cct-1* by sequencing (**Figure 10**). Therefore, the beginning of the fully processed mRNA sequence is 5'-<u>GGTTTAATTACCCAAGTTTGAG</u>GTA***ATG***, where the underlined nt are derived from the SL1 RNA leader, which is *trans*-spliced at the splicing consensus signal (TTTCAG), and ***ATG*** is the start codon. In addition, the four introns in *cct-1* are absent from the cDNA sequence, indicating that these introns are *cis*-spliced from the RNA transcript.

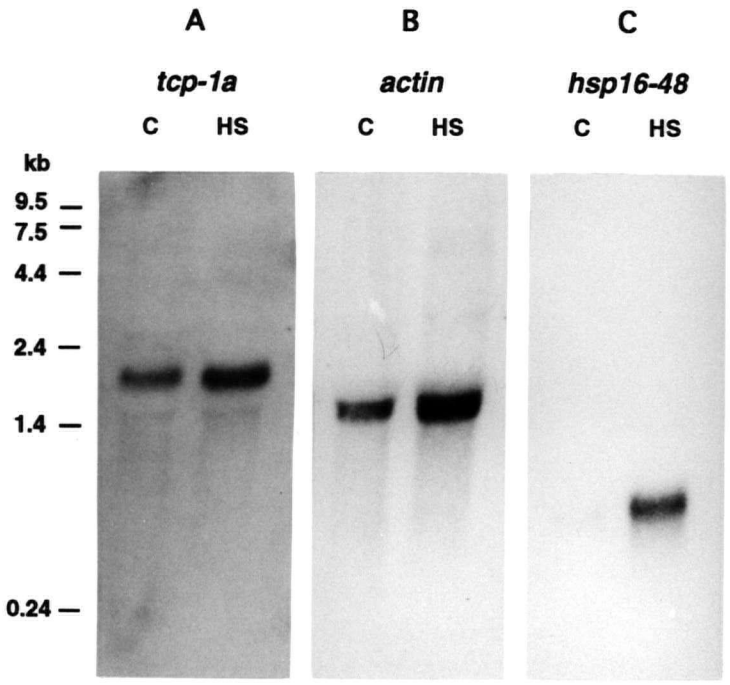

Figure 9. Northern blot analyses of heat-shocked *C. elegans* RNA. A Northern blot prepared with embryonic total RNA from control (C) or heat-shocked (HS) nematodes was sequentially hybridized to ^{32}P-labeled *cct-1* (A), *actin-1* (B), and *hsp16-48* (C) probes. After each hybridization and autoradiography, probes were stripped from the membrane.

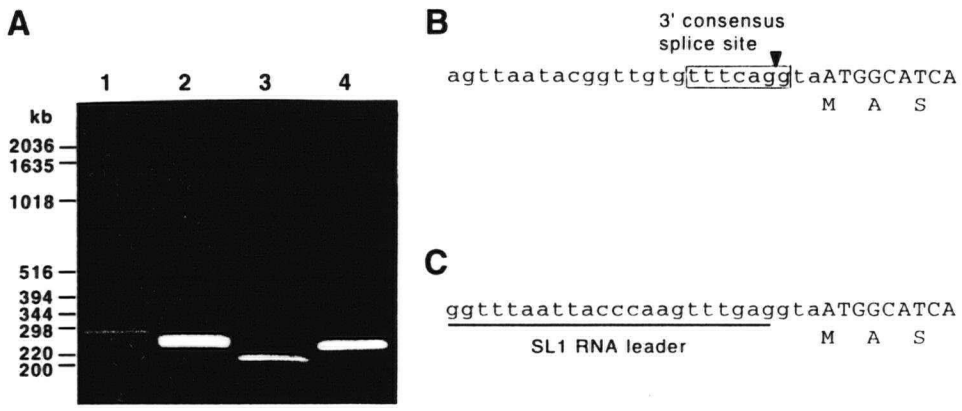

Figure 10. The *cct-1* primary transcript is *trans*-spliced to the splice leader-1 (SL1) RNA. **A.** Three amplified fragments were obtained when *C. elegans* embryo first strand cDNA was used in a PCR reaction containing a primer with the SL1 sequence and an internal *cct-1* primer (MIC 3). One major product was obtained when the PCR was carried out with an SL2 primer and the same *cct-1* internal primer. Shown here are the individual products re-amplified from the SL1 reaction (lanes 1-3) and the SL2 reaction (lane 4), and analyzed on a 1.5% agarose gel. Upon isolation, subcloning, and sequencing of all four fragments, it was found that only one of them (lane 2) was trans-spliced *cct-1* cDNA. **B.** Sequence of *cct-1* near the trans-splicing site. The consensus splice site is boxed, and the initiating methionine and two additonal amino acids are shown below the DNA sequence. **C.** Sequence of the 5'-end of *cct-1* cDNA, with the SL1 sequence underlined.

3.7 Expression pattern of *cct-1*-promoter-β-galactosidase fusion transgene

In order to determine the spatial expression pattern of the *cct-1* gene, an additional ~2 kb of upstream sequence from the *Pst*I site was cloned (see *Materials and Methods*). An expression construct harbouring the entire 5'-noncoding region (~2.7 kb) and ~1 kb of 3'-noncoding region (including the polyadenylation signal), which is likely to contain the promoter and/or regulatory elements of the *cct-1* gene, was created (**Figure 11A**). To monitor expression from the *cct-1* promoter, the first 32 amino acids of the CCT-1 protein was fused in-frame with the SV40 nuclear localization signal (NLS) and β-galactosidase as a marker. The NLS is used to restrict the localization of the marker enzyme to the nucleus, thereby assisting in the identification of cell types. This construct was then injected into *C. elegans*, and four stable lines carrying extrachromosomal arrays of the construct were isolated (see **Appendix V**). The expression of the *cct-1*-promoter-β-galactosidase fusion transgene was monitored by permeabilizing the nematodes with acetone and staining with X-GAL. The staining pattern of selected nematodes is shown in **Figure 11B**.

In the transgenic strains analyzed, expression of the marker enzyme occurs throughout development, from embryos to adults. This result was expected given that *cct-1* transcripts are detectable during all life stages. Note that because the constructs are propagated as extrachromosomal arrays, not all cells or tissues will contain the vector construct and therefore staining will differ from animal to animal. However, specific staining patterns in embryos and larvae/adults were reproducibly obtained in the four independent strains. Late-stage embryos expressed the transgene, often in pairs of closely-associated cells, or sometimes in a greater number of cells. Expression in larvae was particularly strong in the head region near the pharynx, where numerous muscle and neuronal cells are present. Similarly, tail expression was prominent near the anal sphincter, a site also rich in the same cell types. Many cells from the ventral nerve cord and nerve ring stained prominently. Occasionally, expression of the β-galactosidase marker was visible in hypodermal in larvae and in some vulval cells of adults.

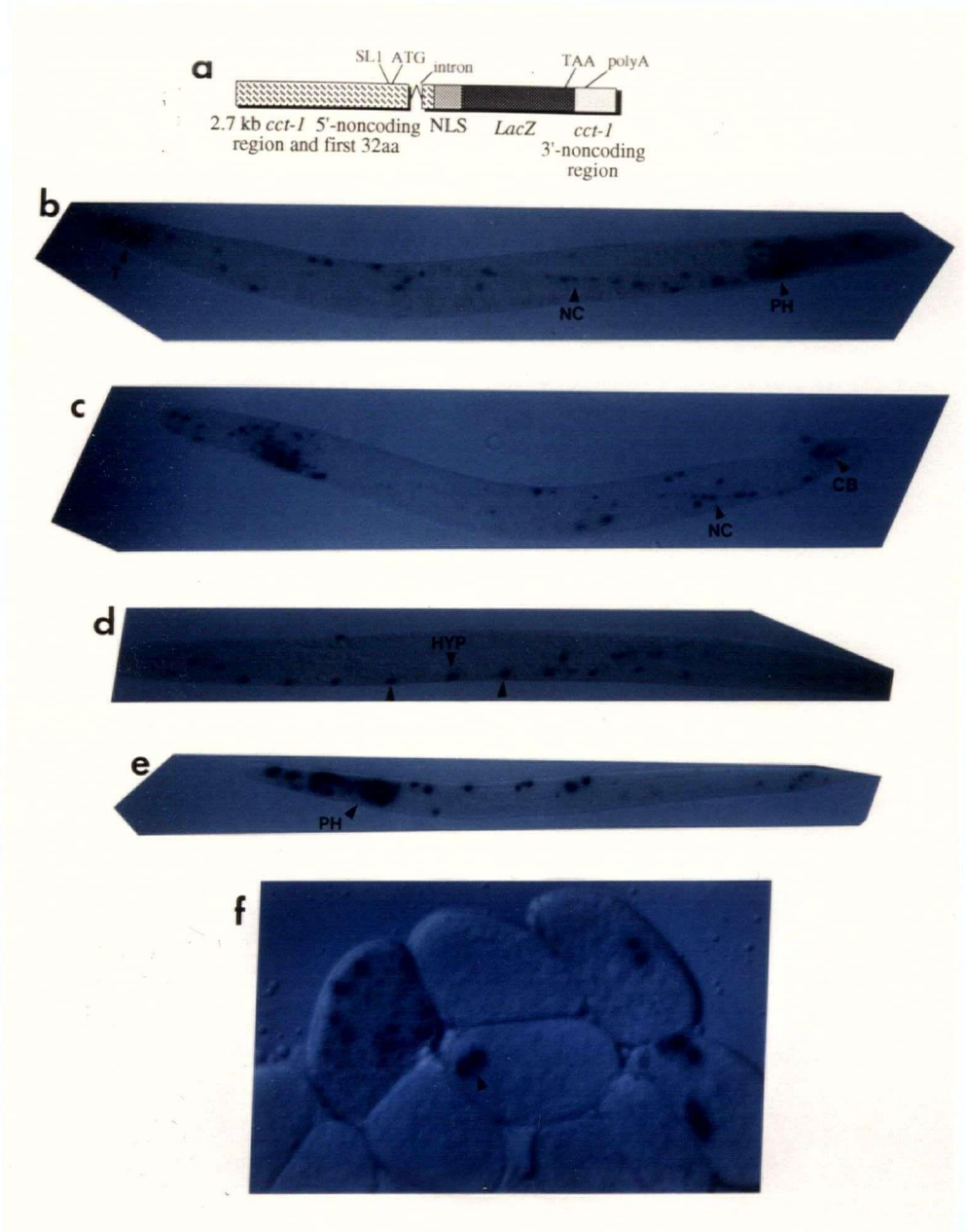

Figure 11. Localization of *cct-1* transgene expression. **a.** Schematic of the construct used to monitor *cct-1* promoter-driven expression of β-galactosidase. The construct contains ~2.7 kb of 5'-noncoding region and ~1 kb of 3'-noncoding region, and the first intron of *cct-1*. The vector encodes a translational fusion of the first 32 aa of the CCT-1 protein and the SV40 nuclear localization signal (NLS) and β-galactosidase coding region. Transgenic nematodes carrying extrachromosomal arrays of the above construct were dessicated, permeabilized with acetone, and stained with a solution containing X-GAL. **b.** L4 hermaphrodite larva showing staining in pharyngeal (PH) and head region, in the nerve cord (NC), and in the tail (T). **c.** L4 male staining in the head region (left), NC, and reproductive organ in tail, copulatory bursa (CB). **d.** Young larva showing staining in hypodermal (HYP) cells. **e.** L2 or L3 showing intense staining in PH. **f.** embryos showing staining.

3.8 Purification of CCT and analysis of protein subunits

In order to obtain sufficient quantities of starting material for purifications, over 100 g of embryos were isolated from 2 separate 20-liter nematode fermentor cultures (see **Appendix IV**). Embryos rather than adult nematodes were used because of the gut protease contamination which occurs when adults are homogenized. A purification of CCT from adults resulted in a substantial amount of proteolytically-degraded CCT protein (not shown), which was avoided when embryos were used. Interestingly, a similar 30 kDa proteolytic fragment of CCTε is observed in some preparations of mouse testis CCT (Hynes *et al.*, 1995), perhaps indicating the presence of a common proteolytically-sensitive region in the CCT subunits. To help in the detection of CCT subunits during and after the purification of the chaperonin complex, polyclonal antibodies against peptides corresponding to the last 15 amino acids of *C. elegans* CCT-1 and CCT-5 were produced. Both antibodies specifically recognize proteins of approximately 59 kDa in whole nematode extracts (**Appendix VII**).

The CCT complex appears to be largely cytosolic. Preparations of cytosolic and nuclear fractions from embryos showed that the majority of the CCT is in the cytosol, although there may be a small amount in the nucleus (not shown), as has been previously observed (Joly *et al.*, 1994). Isolation of CCT from embryos involved a two-step purification, the first being a size separation on 10-40% sucrose gradients, followed by affinity purification on an ATP-agarose column. Sucrose gradients (2-8) were poured and a 2.5 g aliquot of cleared embryonic protein extract was applied to each gradient and centrifuged at 26000 rpm for 18 hours. Nineteen 2-ml fractions were collected from the bottom of each gradient and assayed for the presence of CCT-1 by Western blotting (**Figure 12A**). Positive fractions were dialyzed and applied to a column containing ATP-agarose resin. After extensive washing, the ATP-bound proteins were eluted using 10 mM ATP. The fractions containing CCT were dialyzed against a low salt buffer and concentrated by vacuum centrifugation. The CCT complex was also purified by a combination of sucrose gradient fractionation, ion-exchange chromatography, and ATP-agarose chromatography, but this yielded a substantially lower amount of CCT without greatly

increasing the purity as judged by silver staining (data not shown; CCT binds to DEAE Sephacel resin and is eluted at 450-550 mM NaCl concentrations).

The purified CCT complex contains at least 7 visible polypeptides when separated on a single-dimension 7.5% SDS-gel (**Figure 12B**). These range in size from 52-65 kDa, and appear to be present in approximately equimolar amounts. When *C. elegans* and bovine testis CCT (kind gift from R. Melki) preparations are analyzed in parallel on an SDS-gel, the number and molecular weights of the polypeptides present appear essentially identical, suggesting that the subunit composition and stoichiometry of the CCT complexes from evolutionarily distant organisms are very similar. Even the contaminants from both preparations are similar. Both contain HSP70, which is known to associate specifically with CCT (Lewis *et al.*, 1992). Actin, a known substrate for CCT, is likely to be present in both preparations. HSP60, whose size and ATP-binding activity are almost identical to those of CCT, represents another contaminant. The presence of HSP70 and HSP60 in the *C. elegans* CCT purified by both of the above described methods was confirmed by Western blotting (not shown; HSP70 was detected with a mAb against HSP70/HSC70, and HSP60 was detected with a pAb against moth HSP60; both are from *StressGen*).

Two CCT subunits, CCT-1 and CCT-5, were detected in the purified CCT preparation by Western blot analysis with the purified anti-CCT-1 and anti-CCT-5 pAbs (**Figure 12C**). These two proteins were previously shown to be present in both murine and bovine CCT (Kubota *et al.*, 1994). In addition, several CCT-related subunits within the complex were identified by Western blot analysis with the UM1 pAb (kindly provided by Keith Willison), which cross-reacts with all murine CCT subunits (Hynes *et al.*, 1995; also see **Appendix VII**). The reactivity of the *C. elegans* CCT complex subunits toward these three antibodies further suggests that the CCTs from different organisms possess similar subunit species.

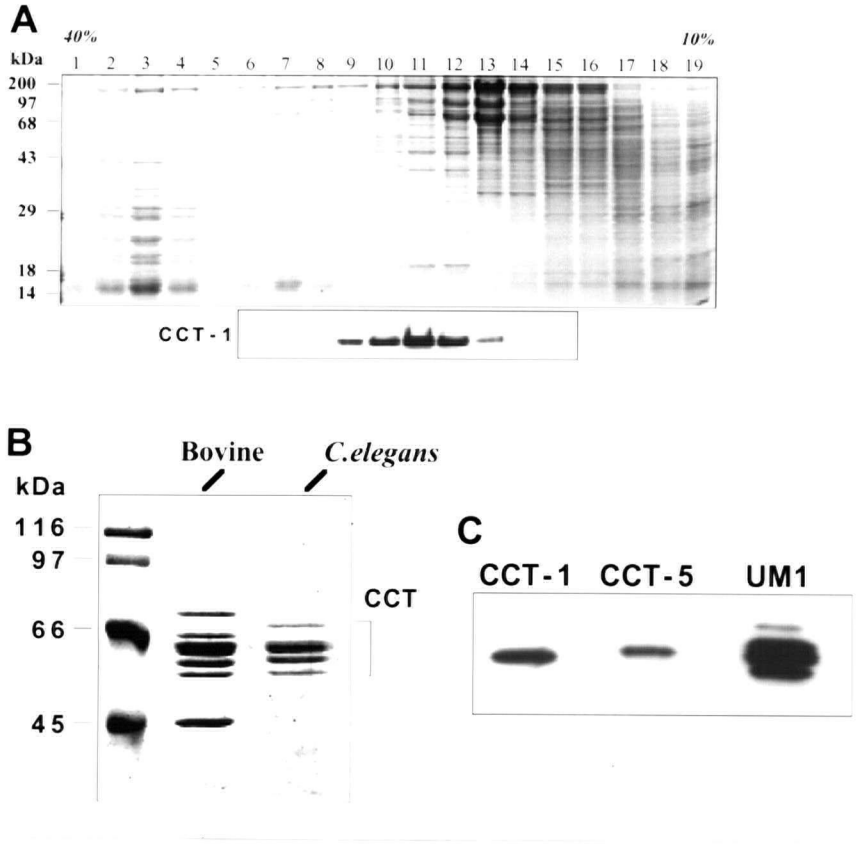

Figure 12. Purification *C. elegans* CCT and identification of subunits. **A.** SDS-PAGE of 10 µl aliquots from 2 ml sucrose gradient fractions (left to right corresponding to decreasing sucrose concentrations). Aligned below the gel are the corresponding sucrose gradient fractions (6-15) probed with the anti-CCT-1 antibody. Fractions containing the most CCT-1 (9-12) were isolated and dialyzed against TEDKM buffer (see *Materials and Methods*) before loading onto an ATP-agarose column equilibrated in the same buffer. ATP-binding proteins were then eluted with ATP, and concentrated by vacuum centrifugation. **B.** A fraction of the *C. elegans* CCT preparation (10 µl) was analyzed on a 9% SDS-gel in parallel with partially purified bovine testis CCT (obtained from Ronald Melki). Protein MW markers are indicated on the left of the gel. The 2 prominent polypeptides not associated with the bovine CCT complex are HSP70 (~70 kDa) and actin (~45 kDa) (R. Melki, personal communication). **C.** This panel shows the cross-reactivity of the *C. elegans* CCT complex with the *C. elegans* anti-CCT-1 and anti-CCT-5 pAbs, as well as the pAb which recognizes a conserved region in CCTs, UM1 (supplied by Keith Willison and described in Hynes *et al.*, 1995).

3.9 Affinity of CCT for denatured actin

The fact that only very small amounts of *C. elegans* CCT could be purified greatly limited the functional assays which could be carried out. Therefore, an assay involving the binding of the chaperonin to [^{35}S]-labeled, denatured actin was chosen because of its convenience and sensitivity. First, the purified *C. elegans* CCT was separated by electrophoresis on a 4.5% native gel (**Figure 13A**). Rather than a single migrating species, three Coomassie-stainable bands are observable (Bands A, B, and C). Bands A and B are approximately of equal intensity, and band C is approximately one-fifth the intensity of the others. By Western blotting, Band A was shown to contain CCT-1 and CCT-5, and therefore likely represents the CCT complex. The mobilities of *C. elegans* and bovine testis CCTs on the native gel are identical, further confirming the identity of Band A. The third band cross-reacts with an anti-HSP60 antibody, and therefore is likely to contain the co-purified HSP60 contaminant. The identity of Band B is unknown, although it is apparent that the bovine testis CCT preparation contains a small amount of material with the same mobility on the native gel.

Bovine and *C. elegans* CCTs were incubated with [^{35}S]-labeled, urea-denatured actin (a kind gift from R. Melki) and separated on a 4.5% native gel (**Figure 13B**, lanes 1 and 2). After autoradiography (lanes 4 and 5), it is apparent that an actin-binding activity is associated specifically with bovine CCT (lane 4). In contrast, an actin-binding activity is found almost exclusively with the HSP60-containing Band C in the *C. elegans* CCT preparation (lane 5). A substantially lower amount of radiolabelled actin is also found associated with the CCT-containing Band A. In order to diminish the actin-binding activity associated with the HSP60 contaminant, the CCT preparation was immunodepleted of HSP60 using an excess of *StressGen*'s anti-moth HSP60 (lane 3). Indeed, the immunodepleted reaction mixture had little labeled actin associated with Band C (which contains HSP60), and had a correspondingly (slightly) larger amount of actin associated with the CCT-containing Band A (lane 6). It should be noted that the bovine CCT preparation refolded a portion of the denatured actin in the presence of ATP (lane 4; arrow shows native actin species). Neither the untreated or immunodepleted *C. elegans* preparation yielded native actin (lanes 5 and 6).

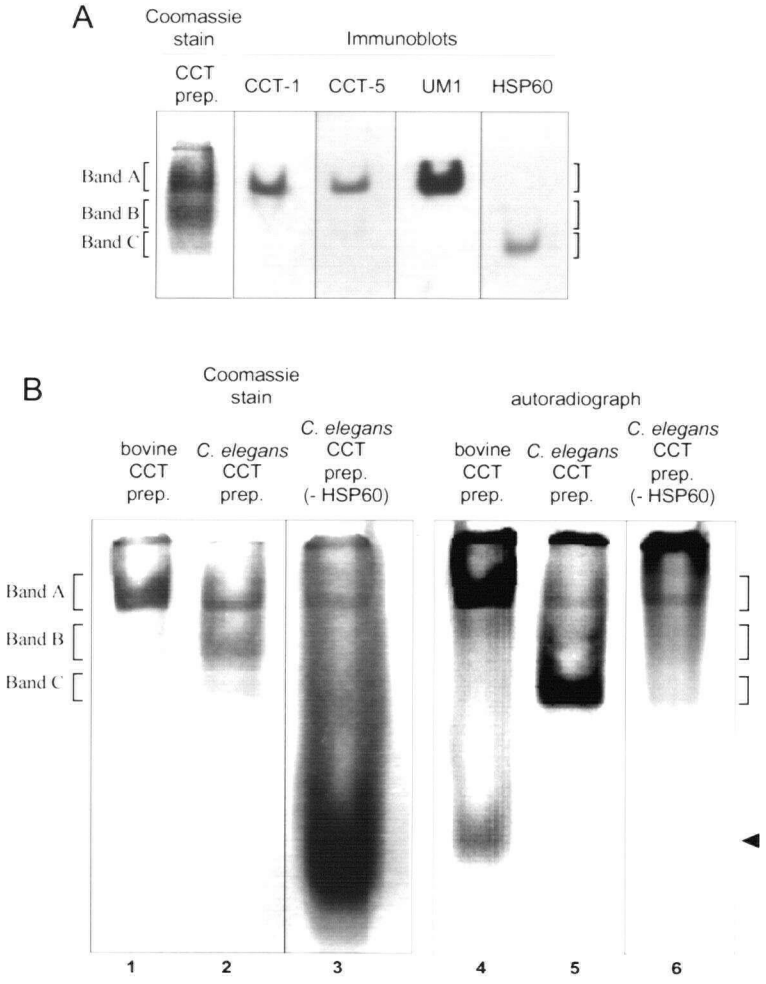

Figure 13. Native gel analysis and affinity of CCT and HSP60 for denatured actin. **A.** Separation of ~10 µg *C. elegans* CCT preparation on a 4.5% native gel. Three species can be detected (Bands A, B, and C) by Coomassie staining. Immunoblot analysis of the same preparation with antibodies against CCT-1, CCT-5, UM1, and HSP60 are shown aligned with the Coomassie-stained gel. **B.** Binding/refolding assays using [^{35}S]-labelled denatured actin. Bovine CCT (lanes 1 and 4) or *C. elegans* CCT (lanes 2, 3, 5, and 6) preparations were incubated in an ATP-containing buffer with identical amounts of labelled, unfolded actin and separated on 4.5% native gels. The *C. elegans* CCT preparation in lanes 3 and 6 was first immunodepleted of HSP60. Lanes 1-3 show the Coomassie-stained gel, and lanes 4-6 show the autoradiograms of lanes 1-3, respectively. The arrow points to native actin (lane 4).

IV. DISCUSSION

A novel eukaryotic cytosolic chaperonin

Our understanding of the mechanisms by which chaperonins facilitate the folding of newly synthesized proteins, as well as proteins translocated across biological membranes, has dramatically increased since the identification by Hemmingsen *et al.* (1988) of the homologous genes encoding GroEL/ES and RuBP, proteins which could chaperone protein folding and assembly *in vivo*. Moreover, the recent identification (Lewis *et al.*, 1992; Gao *et al.*, 1992; Frydman *et al.*, 1992) of a eukaryotic cytosolic chaperonin structurally and functionally similar to the Group I chaperonins has generated tremendous interest in the field of protein folding (Ellis, 1992). The unique multimeric nature (Frydman *et al.*, 1992; Lewis *et al.*, 1992) and possible heterogeneous subunit composition (Creutz *et al.*, 1994; Roobol *et al.*, 1995) of the CCT complex make it a particularly interesting and challenging chaperonin model system to study.

The cct multigene family of C. elegans

The genes encoding CCT subunits are common to all eukaryotes, including yeast (Ursic and Culbertson, 1991), *Drosophila* (Ursic and Ganetzky, 1988), vertebrates (human, mouse, bovine, *Xenopus*, axolotl, etc.; reviewed in Willison and Kubota., 1994; Kubota *et al.*, 1995b), plants (Ehmann *et al.*, 1993), and protozoa (Soares *et al.*, 1994; Maercker and Lipps, 1994). So far, the full complement of *cct* genes (8 different genes) have been sequenced in mouse (Kubota *et al.*, 1994, 1995a) and yeast (reviewed in Stoldt *et al.*, 1996). A testis-specific mouse chaperonin gene is also known (Kubota *et al.*, 1997).

In this study, five members of the *C. elegans cct* multigene family were characterized. The *C. elegans cct* genes studied thus far (*cct-1*, *cct-2*, *cct-4*, *cct-5*, and *cct-6*) are well conserved across species, displaying 62-69% predicted amino acid sequence identity with mouse, human and yeast orthologs. Also, sequence motifs and residues conserved in all chaperonins are conserved in the *C. elegans* CCT family, including those known to be involved in the ATPase

function of GroEL. The *C. elegans* CCT subunits are 23-35% identical to each other, and 31-35% identical to one of the two archaebacterial chaperonin subunits, TF55. From an evolutionary perspective, phylogenetic analyses of CCT proteins and TF55 point to an early divergence of the gene family—as early as two billion years ago, or approximately as old as the origin of eukaryotes (Willison *et al.*, 1994; Kubota *et al.*, 1994, 1995b). It has been remarked that the amino acid substitution rate of TCP-1 is nearly constant and that it evolves as slowly as the highly conserved protein cytochrome *c* (Kubota *et al.*, 1995b).

Genomic mapping data on several human and mouse *Cct* genes (reviewed in Kubota *et al.*, 1995b) is also consistent with an early divergence of this gene family. No clusters of CCT subunit genes are known in any organism including yeasts and mammals. Although it is interesting that three of the five *C. elegans cct* genes are somewhat closely associated on chromosome II (see **Figure 7**), the distance between the *cct* genes on the two different chromosomes argues against the possibility that they are transcribed as polycistronic messages, as a few known genes with related functions are in *C. elegans* (Blumenthal, 1995).

Taken together, these findings imply that the *cct* genes diverged from one or perhaps two ancestral genes common to both eukaryotes and archaebacteria to encode proteins with conserved, specialized functions. Indeed, attempts to rescue yeast strains deficient in a particular *Cct* gene by overexpression of a yeast *Cct* homolog have revealed that each *Cct* gene examined has an irreplaceable function(s) in this organism (Chen *et al.*, 1994). Moreover, in the present study, attempts at rescuing a yeast *cct-1* mutant (DUY4; Ursic and Culbertson, 1991) with the *C. elegans cct-1* gene were not successful (not shown). These results suggest that not only are different CCT subunits functionally distinct but that homologous genes from different organisms, although closely related (61% amino acid sequence identity between yeast and *C. elegans* CCT-1), require compensatory mutations in other subunits for proper assembly or activity of the CCT complex. There is presently no evidence that the different subunits carry out different functions on their own; instead, a single functional CCT complex containing the eight different subunits is likely to be required for carrying out its chaperone activity.

Structure of C. elegans CCT complex

The quaternary structures of the mammalian CCT complexes are known to be well conserved, most likely consisting of 8 or 9 subunits per ring (Lewis *et al.*, 1992; Frydman *et al.*, 1992; Marco *et al.*, 1994). The subunit composition of different mammalian CCT complexes has been extensively investigated. Two-dimensional polyacrylamide gel electrophoretic analysis of mouse and bovine CCTs shows that each complex contains nine subunit species (Kubota *et al.*, 1994). In contrast, eight subunits of rabbit reticulocyte lysate CCT were identified using an HPLC purification method (Rommelaere *et al.*, 1993). Human HEp-2 and mouse F9 cells were shown to contain only seven subunit species (Lewis *et al.*, 1992; Kubota *et al.*, 1994), and Roobol and Carden (1993) also noted differences in the number of subunits present in rodent testis and brain CCT preparations. These data suggest that the subunit composition of CCT may vary between different cell or tissue types. In contrast, the structure of the CCTs from different organisms has received much less attention. Thus far, only cucumber (Ahnert *et al.*, 1996) and *S. cerevisiae* (Miklos *et al.*, 1994) CCT complexes have been isolated. Both were shown to contain TCP-1 (CCT-1) and the yeast chaperonin contained CCTβ (CCT-2) in addition. Although it is claimed that the CCT complexes isolated in the above studies are comparable to those of mammalian CCTs, no direct (side-by-side) comparisons were made.

To assess whether the subunit composition of CCT is similar between highly diverged organisms, it was of interest to determine the makeup of the *C. elegans* CCT complex and compare it with a mammalian counterpart. A large-scale preparation of *C. elegans* embryos provided enough starting material for the two-step (sucrose gradient fractionation and ATP-agarose chromatography) purification of CCT, as first described by Lewis *et al.* (1992) to isolate murine testis CCT. The much lower concentration of CCT in *C. elegans* embryos compared with testis made it very difficult and impractical to add an additional purification step. Consequently, the *C. elegans* CCT was not purified to near-homogeneity, and several contaminants were shown to be present, including HSP60 and HSP70 by immunoblotting, and a 45 kDa protein (most likely actin). More importantly however, at least seven polypeptides between 53-65 kDa are distinguishable in the *C. elegans* preparation, which is precisely the range of subunit sizes

observed by SDS-PAGE for both mouse and bovine CCT (Gao *et al.*, 1992; Lewis *et al.*, 1992; Frydman *et al.*, 1992; Kubota *et al.*, 1994). A side-by-side comparison of bovine and *C. elegans* CCTs shows the subunit composition of these evolutionarily distant CCT complexes to be remarkably similar. Interestingly, similar contaminants were present in the partially-purified bovine CCT complex and *C. elegans* CCT (HSP70 and actin; R. Melki, personal communication). The *C. elegans* CCT preparation also contains some HSP60 (see below). The presence of HSP70 'contaminants' in CCT preparations may be biologically relevant because it cooperates with CCT during protein folding (Frydman *et al.*, 1994, 1996). Indeed, HSP70 is specifically immunoprecipitated with anti-TCP-1 antibodies (Lewis *et al.*, 1992).

Surprisingly, native gel analysis of the CCT preparation revealed *three* distinct species, of which the slowest migrating is most likely CCT, as it corresponded in mobility to bovine CCT and contained CCT-1 and CCT-5 (detected by specific antibodies against the C-termini of the two corresponding *C. elegans* chaperonin subunits) as well as polypeptides recognized by the UM1 antibody, which recognizes a region conserved in CCT subunits (Hynes *et al.*, 1995). Interestingly, the second fastest migrating species is approximately equal in abundance to the first, but it is not recognized by any of the CCT-specific antibodies, suggesting that it is unrelated to CCT. The identity of this species therefore remains unknown. The fastest migrating species reacted with an anti-moth HSP60 antibody, and therefore is likely to be (or to contain) HSP60.

Secondary structure analysis of C. elegans CCTs and other chaperonins

The unique hetero-oligomeric structure of CCT and divergent primary structure of each CCT subunit suggest that Group II chaperonins may be significantly different structurally from each other and from Group I chaperonins. Perhaps contrary to expectations, analysis of the *C. elegans* and murine CCT proteins revealed that all the members have nearly identical predicted secondary structural folds, despite displaying limited pairwise sequence identity between members (23-35%). This observation suggests that the divergence in the primary structures of the CCT subunits has not resulted in major alterations in their secondary or tertiary

structures, but has allowed for significant variability in amino acid composition, perhaps resulting in diversification of function.

Most of the highly conserved regions within chaperonins are probably involved in ATP hydrolysis (Fenton *et al.*, 1994; Kim *et al.*, 1994; Lorimer, 1995). The analysis presented here provides evidence that the secondary structures within the equatorial and part of the intermediate domains of the Group I and II chaperonins are very similar and therefore likely to have been evolutionarily conserved. This finding suggests that the ATPase function of the two chaperonin families is maintained through the conservation of secondary and perhaps also tertiary structures, as well as residues critical for ATP binding and hydrolysis. Interestingly, a number of residues known to affect GroEL ATPase activity (*e.g.*, residues at positions 180-182 in **Figure 3**) are not conserved in the CCT/TF55 family but are present within regions predicted to have equivalent secondary structures.

On the other hand, the predicted secondary structures of the CCT proteins in the region encompassing part of the N-terminal intermediate domain and most of the apical domain are substantially different from the known GroEL secondary structure. Therefore, the differences predicted for the polypeptide binding domain of the CCT subunits and GroEL may account for the different range of target polypeptides which can be bound to and folded by the two chaperonins. Also, differences in primary structure are likely to account for some of the specificity. For example, hydrophobic residues within the apical domain which are known to be involved in polypeptide binding are not all conserved between the CCT subunits and GroEL (Kim *et al.*, 1994; this study). However, a few important secondary structures required for polypeptide binding may be conserved between the two groups of chaperonins (*e.g.*, the helix centered on position 298). Furthermore, the three β-sheet structures predicted in the apical domain of the CCT proteins (beween positions 220-270) may form a structural backbone analogous to the GroEL β-sheets present between positions 205-260 (see **Figure 3** alignment). In GroEL, these β-sheets are located on the outside surface of the apical domain and do not appear to contain residues critical for polypeptide binding (Fenton *et al.*, 1994); hence, their role

may be strictly structural in character, and could be performed in the CCT proteins by a proximal but different, non-conserved region of the protein.

The predicted secondary structure of TF55 closely matches that of the CCT members, which along with their shared primary and quaternary structures, further demonstrates that CCT proteins and TF55 constitute a family of closely related chaperonins. However, the scope of action of the two chaperonins may be different. Whether CCT folds mainly tubulins and actins *in vivo* is still unclear, but the heat-inducible TF55 chaperonin probably folds a large number of substrates, and prevents the denaturation of many proteins during cellular stress (Phipps *et al.*, 1991; Guagliardi *et al.*, 1994). Since the predicted secondary structures of TF55 and the CCT subunits are nearly identical, it is likely that their tertiary structures are also very similar, and that it is the differences in exposed amino acids within their polypeptide binding domains which are responsible for their (apparently) different substrate specificities.

The lack of requirement for a co-chaperonin such as GroES by CCT and TF55 may be due to differences in primary structures within the apical domain, since the residues required for polypeptide binding are also required for GroES interaction with GroEL (Fenton *et al.*, 1994). However, it is also possible that the differences between the predicted CCT/TF55 and known GroEL secondary structures may be functionally significant. An intriguing possibility is that the CCT/TF55 chaperonins incorporate a chaperonin-10-like functionality within their apical domains. Through random conical tilt reconstruction of the *Pyrodictium occultum* archaebacterial chaperonin complex from electron micrographs, Phipps *et al.* (1993) were able to detect a solid mass partially occluding the central channel, in a location analogous to where the co-chaperonin binds (Saibil, 1996).

Denatured actin-binding activities in C. elegans CCT preparations

The eukaryotic cytosolic chaperonin CCT is known to interact with unfolded actin and promote its folding in the presence of ATP *in vitro* (Gao *et al.*, 1992; Rommelaere *et al.*, 1993; Melki and Cowan, 1994), and *in vivo* (Sternlicht *et al.*, 1993). The ability of *C. elegans* CCT to

interact with this target protein was assessed by diluting [^{35}S]-labelled, urea-denatured actin into the CCT preparation, and monitoring binary complex formation after separation on native gels.

Unexpectedly, a relatively 'minor' component of the CCT preparation (the fastest migrating of three species) was clearly the most active in binding to the denatured actin. Interestingly, this species is likely to be HSP60, a mitochondrial chaperonin which co-purified with CCT. While it cannot be discounted that the CCT in the preparation was damaged during the purification procedure, or was lacking the proper conditions for binding to the denatured substrate, two publications aimed at comparing the differences in the affinities and specificities of HSP60 and CCT provide evidence that the data obtained in the above experiment supports what is currently known about the two chaperonins.

In a study by Melki and Cowan (1994), it was found that the cytoplasmic chaperonin had a higher relative affinity for actin folding intermediates which formed within a few minutes of dilution from denaturant, whereas HSP60 had a correspondingly higher affinity than CCT for actin conformers which are present immediately after dilution of the denatured actin. Given this observation, it should therefore be expected that HSP60 whould have a higher affinity than CCT in the actin-binding experiment performed with the *C. elegans* CCT preparation, which was the case. Furthermore, the above authors also reported that the relative affinity of CCT compared to HSP60 for denatured β-actin (the same substrate used in the present studies) was slightly less than one-half. Tian *et al.* (1995) suggest that the ability of CCT to bind various unfolded substrates is lower by a factor of approximately 10-fold compared with HSP60. Interestingly, HSP60 is unable to fold actin or tubulin to their native state, unlike CCT, and this observation is consistent with the fact that no folded actin was generated by the *C. elegans* CCT preparation whereas bovine CCT was able to refold some of the actin (**Figure 13B**). Overall, the above data suggest that HSP60 has a higher affinity for unfolded substrate, and therefore is likely to outcompete CCT in substrate binding *in vitro*. Whether this is biologically important in the function of CCT and HSP60 *in vivo* is unknown, but the fact that CCT but not HSP60 nor GroEL can refold actin and tubulin may indicate true functional differences between Group I and Group II chaperonins.

Expression of cct genes in C. elegans and other organisms

The expression of *C. elegans cct* genes at all stages suggests that each gene encodes a protein whose function(s) may be required throughout nematode development. Since CCT is involved in cytoskeletal protein folding, it is possible that the expression of the *C. elegans cct* genes roughly parallels the expression of the major cytoskeletal genes tubulin and actin. In support of this hypothesis, actin genes (Krause and Hirsh, 1986) and at least one tubulin gene (Fukushige *et al.*, 1993) are indeed known to be expressed constitutively throughout *C. elegans* development. A direct correlation between the expression of *Tetrahymena pyriformis TpCCTγ* and tubulin genes during ciliogenesis has been documented (Soares *et al.*, 1994). In addition, constitutive expression of the five *C. elegans cct* genes may also signify that all are required to form a functional CCT complex.

The finding that the *C. elegans cct-1* promoter drives the expression of a reporter gene in muscle and neuronal cells is entirely consistent with the expression pattern of CCT subunit genes in *Xenopus laevis* (Dunn and Mercola, 1996) and in the axolotl *Ambystoma mexicanum*, a salamander (Sun *et al.*, 1995). These data are likely to reflect the increased need for folding actin and tubulin by CCT in these tissues (Roobol *et al.*, 1995; Dunn and Mercola, 1996).

Interestingly, the *Cctg* gene of *Xenopus* is expressed in all tissues examined but is particularly abundant in the ovary (Walkley *et al.*, 1996). No β-galactosidase staining in the gonad of the adult transgenic *C. elegans* can be detected. On the one hand, this finding is unexpected since developing oocytes would be expected to require the presence of CCT for the folding of cytoskeletal proteins, which would be needed in great quantity given the tremendous amount of cell divisions occuring. On the other hand, the lack of expression in *C. elegans* germ cells is not surprising given that the activity of a germline specific factor (PIE-1) blocks new gene expression in the early embryonic germ lineage (Seydoux *et al.*, 1996; Mello *et al.*, 1996). Thus, CCT-1 may be present (or even abundant) in germ cells but would be detectable only by whole-mount immunostaining with the anti-CCT-1 antibody.

Northern blot analysis of RNA samples from control and heat shocked *C. elegans* reveals that *cct-1* expression is not increased and may be slightly decreased in heat-shocked nematodes.

It was also noted by Ursic and Culbertson (1992) that yeast *TCP-1* expression was slighly repressed following a heat shock treatment, implying that this chaperonin was not a member of the HSPs like most other molecular chaperones. Sun *et al.* (1995) showed that the transcription of *TCP-1* was also repressed in heat-shocked axolotl embryos. Similarly, the *Tetrahymena* homolog of *Cctg* is not heat-inducible (Soares *et al.*, 1994). Despite these findings, it is possible that CCT may play a role in protecting certain proteins from unfolding during biological stresses, as has been shown to be the case with HSP60. Although only induced approximately two-fold during stress conditions, *in vivo* experiments demonstrated that HSP60 was required to prevent the thermal inactivation of a protein (dihydrofolate reductase) imported into mitochondria (Martin *et al.*, 1992). Also, chaperonins are the main proteins expressed under conditions of heat shock in thermophilic Archaea, which suggests that they play an important role in the thermotolerance of these organisms (Conway de Macario and Macario, 1994). Remarkably, the *Pyrodictium occultum* archaebacterial chaperonin constitutes approximately 73% of the total soluble protein at 108°C, approximately 10°C above its optimal growth temperature (Phipps *et al.*, 1991).

Future studies

One of the primary goals of studying CCT is to understand its function *in vivo*. *C. elegans* is an excellent model organism in which to study the role(s) that this chaperonin play(s) within a complex, multicellular organism. In collaboration with Ronald Plasterk, a strain containing a Tc1 transposon insertion near *cct-1* was uncovered. The site of this Tc1 insertion was determined to be between the stop codon and polyadenylation signal (see **Appendix VI**). Using a well-established technique of screening for imprecise excisions of Tc1 (Plasterk and Groenen, 1992), a *cct-1* knockout could be generated using this strain. The resulting phenotype might itself be very interesting, and disruption of *cct-1* would also provide an avenue for attempting rescues with mutant forms of *cct-1* (some of which may be temperature sensitive, or have specific defects and therefore display a range of phenotypes). Alternatively, or in parallel with such experiments, lethals mapping near *cct-6* (isolated by David Baillie, Simon Fraser

University) could be investigated by injecting wild-type *cct-6* into these strains in an attempt to rescue the lethal phenotype and identify mutations in this gene. Similarly, other *cct* genes mapping near known lethals could be possible targets for rescue experiments. To date, chaperonin mutants have been uncovered only in yeast and prokaryotes. Therefore, the isolation and characterization of a *C. elegans* strain carrying a mutant *cct* gene might yield the first significant insight into the function of this molecular chaperone in higher eukaryotes.

One of the persisting mysteries concerning CCT is its complex subunit composition compared with the Group I and archaebacterial chaperonins. It is possible that some *cct* genes are differentially regulated and that the subunit composition of CCT may differ depending on the stage of development or localization within different tissues. Consequently, CCT variants may have different affinities for its substrates. A thorough analysis of the spatial and temporal expression of all of the *cct* genes within *C. elegans* would be possible as soon the entire genome sequence becomes available, and would likely provide useful information concerning this possibility. Meanwhile, the promoters of five *cct* genes are available. By making *cct* promoter-*lacZ* fusion constructs comparable to the *cct-1* promoter-*lacZ* construct analyzed in this study, a detailed comparison of the expression patterns of all *cct* genes is possible. Furthermore, *in situ* immunostaining studies on staged nematodes would provide complementary data on the localization of CCT proteins in the organism; this could be done starting with the anti-CCT-1 and anti-CCT-5 polyclonal antibodies developed in this study.

CHAPTER II— Structure-function studies on *C. elegans* HSP16-2 and HSP12.6

Organisms are frequently subjected to environmental stresses which must be dealt with in order to prevent cellular damage. Protection at the molecular level requires a specific set of proteins termed stress or heat shock proteins. In the present chapter, studies on the structure and function of two small heat shock proteins provide insight on how this family of chaperones assembles into large multimeric complexes which can interact with structurally compromised proteins.

I. INTRODUCTION

Small HSP family

The small HSPs (smHSPs) and α-crystallins form a highly divergent protein family with members present in Eukarya, Archaea, and Bacteria (Caspers *et al.*, 1995; Bult *et al.*, 1996). α-crystallin is a highly abundant protein in eye lenses, and is usually found as large aggregates consisting of two types of related subunits, αA and αB (Groenen *et al.*, 1994). It is also present to a lesser extent in various tissues outside the lens (Bhat and Nagineni, 1989; Kato *et al.*, 1991). The evolutionary relatedness between α-crystallins and smHSPs was first noted by Ingolia and Craig (1982), and is restricted to a conserved ~85-amino acid α-crystallin domain (Ingolia and Craig, 1982; Russnak *et al.*, 1983; Wistow, 1985). Among the prominent molecular chaperone families (including HSP104, HSP90, HSP70, HSP60, and HSP40), the smHSP family is the most structurally diverse, ranging in size from 17-26 kDa in plants, 20-27 kDa in vertebrates, 20-24 kDa in *Drosophila*, 24-43 kDa in yeast, and 16-21 kDa in bacteria (Ingolia and Craig, 1982; Bossier *et al.*, 1989; Caspers *et al.*, 1995; Waters *et al.*, 1996; Wotton *et al.*, 1996). The first archaebacterial smHSP, an 18-kDa protein most closely related to plant cytosolic smHSPs, was recently uncovered by the sequencing of the *Methanococcus jannaschii* genome (Bult *et al.*, 1996). The N-terminal domains and C-terminal extensions of smHSPs, which flank the

evolutionarily conserved α-crystallin domains, differ substantially in length and amino acid sequence and account for most of the structural diversity between different members.

All organisms cope with changes in their environment, including exposure to elevated temperatures and environmental pollutants such as heavy metals and toxins, by increasing their levels of stress proteins (Lindquist and Craig, 1988; Morimoto *et al.*, 1990). Although many smHSPs are present during development under physiological conditions, smHSPs are among the most highly inducible HSPs during heat shock or other stresses (Arrigo and Landry, 1994).

In plants, some smHSPs are induced more than 200-fold under stress conditions, and the accumulation of the proteins is proportional to the temperature and duration of the stress (Waters *et al.*, 1996). Following the stress event, smHSPs persist for long time periods, having half-lives of 30-50 hours (Chen *et al.*, 1990; DeRocher *et al.*, 1991). This suggests that their function is probably critical during the recovery period (Waters *et al.*, 1996). In mammalian cells, induction of smHSPs is typically 10-20-fold, and in the lens, HSP27 and αB-crystallin represent about 0.2-1% and 2-10% of total proteins, respectively (Arrigo and Landry, 1994). In the yeast *Saccharomyces cerevisiae*, both HSP26 and HSP42 accumulate to high levels during heat shock, although HSP42 is present at lower levels during physiological conditions (Wotton *et al.*, 1996)

Transcriptional activation of smHSP genes is thought to be the major regulatory mechanism by which smHSPs preferentially accumulate after stresses in *Drosophila*, *C. elegans*, *yeast*, plants, and *Xenopus* (Arrigo and Landry, 1994). The induction of smHSPs during heat shock or other stresses is mediated by the binding of the heat shock transcription factor (HSF) to repeats of the regulatory DNA sequence termed heat shock element (HSE) (Morimoto *et al.*, 1990). HSE repeats are present upstream of all known stress-induced smHSP genes. It is likely that in many cases, there are other regulatory elements influencing smHSP gene expression. It is now well established that smHSPs are regulated not only by environmental stressors, but also by a variety of other environmental and developmental cues (Arrigo and Landry, 1994; Waters *et al.*, 1996). Thus, the expression of plant smHSPs is regulated, in the absence of heat stress, in developing embryo (Coca *et al.*, 1994; Vierling and Sun, 1989), during germination (Vierling and Sun,

1989), pollen development (Bouchard, 1990), fruit maturation (Fray *et al.*, 1990), and cold storage (Van Berkel *et al.*, 1994). In *Drosophila*, the spatial and temporal expression patterns of four of the known smHSP genes (Ingolia and Craig, 1982) have been extensively characterized (Arrigo and Landry, 1994). Not only are some smHSPs produced during different life stages (embryos, larvae, pupae, and adults), but the localization of these proteins differs during development. In constrast, the genes are expressed in almost all tissues following heat shock (Arrigo and Tanguay, 1991).

Small HSP family of C. elegans

During the early and mid 1980's, two cDNAs encoding small HSPs (Russnak *et al.*, 1983) and four genes encoding two different classes of smHSPs (Russnak and Candido, 1985; Jones *et al.*, 1986) were isolated. These genes (*hsp16-1*, *hsp16-2*, *hsp16-41*, *hsp16-48*) were shown to contain a region highly homologous to a conserved sequence in the α-crystallin and *Drosophila* small *hsp* genes. Until recently, no additional small *hsp* genes had been isolated, but the *C. elegans* genome sequencing project has now uncovered 11 novel genes which are clearly related to the small *hsp* gene family (**Figure 14**). The smHSPs can be subdivided into three classes based on size alone. Class I smHSPs may be the most abundant and range from 16-18 kDa, which roughly parallels the size of eubacterial, most plant, and archaebacterial smHSPs (Caspers *et al.*, 1995; Bult *et al.*, 1996). Interestingly, the size distribution of the Class I smHSPs is quite narrow (145-159 amino acids), especially in light of the fact that other smHSPs are more than 200 amino acids in length. The *C. elegans* Class II smHSPs are the smallest known members, ranging from 12.2-12.6 kDa. They are so far unique to nematodes, as they have not yet been observed in other organisms. A comparison of their sizes (there are two pairs, of 109 and 110 aa in length) and similar sequence (43-73% overall aa sequence identity between members) suggests that they form a highly conserved, novel family of smHSPs. Class III smHSPs are the largest in size, ranging from 20-30 kDa. In terms of size alone, these are most closely related to higher eukaryote smHSPs (*e.g.*, murine HSP25, *Drosophila* and human HSP27, etc.).

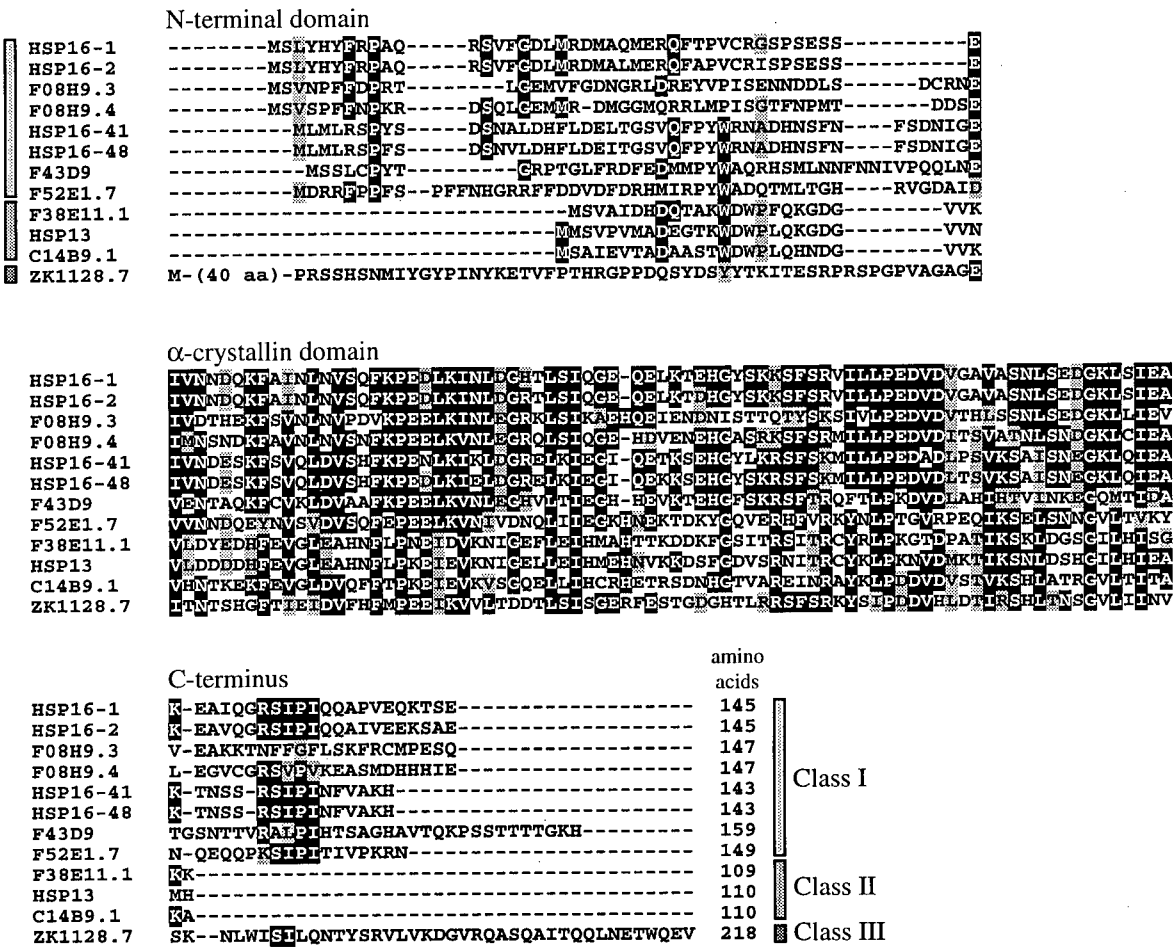

Figure 14. Alignment of *C. elegans* smHSPs. The two smHSPs characterized in this study (HSP16-2 and HSP12.6) are aligned to other members of the *C. elegans* smHSP multigene family. The family can be divided into three classes based on size; Class I smHSPs are between 16-18 kDa (similar to plant and bacterial homologues), Class II smHSPs are the smallest known members of any organism at 12-13 kDa, and Class III smHSPs are 25-30 kDa in size, which is similar to higher-eukaryote smHSPs. The three basic regions of small HSPs, the nonconserved N-terminal domain, the conserved α-crystallin domain, and the C-terminal extension are grouped into separate blocks. The Genbank accession numbers for the *C. elegans* smHSPs are: HSP16-1 and HSP16-48 (K03273), HSP16-2 and HSP16-41 (M14334), F08H9.3 and F08H9.4 (Z77657), SEC-1 (Z35640), F52E1.7 (U41109), HSP12.6 (also known as F38E11.2; Z68342 and U92044) and HSP12.3 (also known as F38E11.1; Z68342), ZK1128.7 (Z47357), C14F11.5 (U39645), and C09B8.6 (U29612). The asterisk at the end of the C14F11.5 coding region indicates that the sequence is predicted to continue by the program *GeneFinder*, but may end at the stop signal present immediately following the putative intron at this location.

A few of the other known nematode proteins also belong to class III smHSPs; for example, there exists immunologically-related 27-kDa smHSPs (p27s) in *D. immitis*, *B. malayi*, *O. volvulus*, *L. carinii*, *A. viteae*, *T. spiralis*, *T. canis*, *T. leonino*, as well as in *C. elegans* (Lillibridge *et al.*, 1996). In *D. immitis*, the hypodermally-localized p27 is developmentally-regulated, but is not upregulated by increased temperatures. A different, constitutively-expressed and heat-inducible 22-24 kDa smHSP from *B. pahangi* was identified by Jecock *et al.* (1992). Yet another nematode smHSP, a 20-kDa protein from the intestinal nematode *N. brasiliensis*, has been found to be developmentally regulated and heat-induced (Tweedie *et al.*, 1993). Homologs of the class II smHSPs have also been uncovered as part of a tag sequenching approach to identify genes expressed in the human filarial nematode parasites *B. malayi and O. volvulus* (Blaxter *et al.*, 1996).

Whereas most HSPs perform necessary functions in non-stressed cells and are also induced following cellular insults (Gething and Sambrook, 1992; Parsell and Lindquist, 1994; Arrigo and Landry, 1994), the *C. elegans* HSP16-class smHSPs are produced only under stress conditions, in a tissue-general manner (Dixon *et al.*, 1990; Stringham *et al.*, 1992; Jones *et al.*, 1986; Candido *et al.*, 1989). More significantly, their expression correlates specifically with the presence of agents which induce protein damage (Jones *et al.*, 1996). A series of compounds closely related to Captan, a commonly used agricultural fungicide, were tested for the induction of β-galactosidase production in a transgenic *C. elegans* harbouring an integrated *hsp16*-promoter-*lacZ* construct. It was found that only compounds possessing N-(trichloromethylthio) or N-(tetrachloroethylthio) groups, which denature proteins by reacting with amino and thiol groups, induced transgene expression. These data on the *C. elegans* HSP16 family strongly suggest that these proteins are produced only under conditions which induce the stress response, which has been shown to be strongly correlated with the presence of proteotoxic agents within the cell (Hightower, 1980; Ananthan *et al.*, 1986)

Structure of small HSPs

Wistow (1985) proposed that the overall structure of α-crystallin consists of two major domains, a globular N-terminal domain and a somewhat larger C-terminal domain, with an exposed C-terminal arm. There is considerable genetic and experimental evidence to support such a model. First, some smHSP genes contain an intron which delineates the N-terminal and α-crystallin domains (King and Piatigorsky, 1983; Russnak and Candido, 1985). Primary structure sequence alignments of smHSPs show the boundary between the nonconserved N-terminal domain and the highly conserved α-crystallin domain to be highly conspicuous, which is suggestive of two separate folding domains. Second, folding-unfolding and NMR studies also support a two-domain structure (van den Oetelaar and Hoenders, 1989; Carver *et al.*, 1993). A computer-modelling study by Groth-Vasselli *et al.* (1995) predicts the α-crystallin monomer to have an elongated, dumbbell-like structure. Based on molecular modelling studies and partial primary sequence similarities, the structure of *E. coli* IbpB, a smHSP, was suggested to resemble the middle region of Caf1M from *Yersinia pestis*, a protein related to the periplasmic molecular chaperone PapD of *E. coli* (Zav'yalov et al., 1995). The crystal structure of PapD is known and consists mostly of β-sheets (Holmgren and Bränden, 1989). Overall, α-crystallin and other smHSPs appear to be composed of >90% β-sheets on the basis of CD spectra (Siezen and Argos, 1983; Merck *et al.*, 1993a).

A common feature of smHSPs is their formation of large oligomeric complexes. The simplest and best characterized smHSP quaternary structure is the 150-kDa trimer of trimers formed by *M. tuberculosis* HSP16.3 (Chang *et al.*, 1996). Plant smHSPs assemble into circular or triangular complexes of 200-300 kDa, or 12 subunits (Lee *et al.*, 1995; Waters *et al.*, 1996), and the typical oligomeric size of α-crystallins and smHSPs from yeast and mammals is between 400 and 800 kDa (Bentley *et al.*, 1992; Groenen *et al.*, 1994). A detailed analysis of recombinant murine HSP25 by hydrodynamic and electron microscopic techniques showed that it consisted of circular, elliptical, triangular, or polygonal 15-18 nm particles of about 730 kDa (32 monomers) (Behlke *et al.*, 1991). Curiously, cardiac α-crystallin appears to possess a central cavity (like chaperonins) (Longoni *et al.*, 1990), a feature not present in other smHSPs studied. The smHSP

quaternary structures are therefore highly diverse. Furthermore, the oligomeric state of mammalian smHSPs depends on various factors, such as the state of phosphorylation and temperature (Siezen *et al.*, 1980b; Van den Oetelaar and Hoender, 1989; Kato *et al.*, 1994). The C-terminal extensions of smHSPs appear relatively unstructured (Carver *et al.*, 1992, 1995a) and are known to undergo numerous modifications, including truncations (reviewed in Groenen *et al.*, 1994). They are therefore likely to be exposed on the surface of the oligomers, and could contribute significantly to maintaining the solubility of the complex (Smulders *et al.*, 1996).

Several contrasting models have been proposed to account for the arrangement of subunits and diversity of α-crystallin aggregates. The review by Groenen *et al.* (1994) addresses these issues in detail, and suggests that although there is as yet no single consistent model for smHSP quaternary structure, it is likely that the smHSP N-terminal domain is buried in the aggregate whereas the C-terminal domain is exposed at the surface, and that all subunits are in equivalent positions within a roughly spherical aggregate. The first quaternary structure models proposed for the α-crystallin aggregate were tetrahedral-based three-layer models which consisted of a core of 13 or 12 subunits, a second layer of 14 or 6 subunits, and a third layer of 16 or 24 subunits, for a total of 43 (Bindels *et al.*, 1979) or 42 (Tardieu *et al.*, 1986) subunits, respectively. These similar models were based on the observation that the approximately 800-kDa α-crystallin (~ 40 subunits) can be dissociated reversibly at various temperatures into particles of smaller sizes (Groenen *et al.*, 1994). Variations of this model have been suggested (Walsh *et al.*, 1991). A micelle-like structure in which the relatively hydrophobic N-terminal domains were oriented toward the interior, providing the driving force for aggregation, was also suggested based on several experimental results (Augusteyn and Koretz, 1987). A later model based on tetrameric building blocks was proposed to explain the observation by Merck *et al.* (1992) that N-terminally-deleted α-crystallin dissociated into dimers/tetramers (Wistow, 1993). Finally, a chaperonin-like structure has been proposed for cardiac α-crystallin (Carver *et al.*, 1994a).

Mechanism of small HSP chaperone function

The first demonstration that smHSPs could function as molecular chaperones came from Horwitz (1992), who showed that αA- and αB-crystallin were highly effective in suppressing the thermally-induced aggregation of β- and γ-crystallins as well as alcohol dehydrogenase. Subsequently, numerous *in vitro* studies have documented the ability of smHSPs to prevent the aggregation of various test proteins at elevated temperatures (Jakob *et al.*, 1993; Merck *et al.*, 1993a; Lee *et al.*, 1995; Chang *et al.*, 1996; Rajaraman *et al.*, 1996). In addition, many (Jakob *et al.*, 1993; Lee *et al.*, 1995) but not all (Horwitz, 1992; Chang *et al.*, 1996) smHSPs appear to promote the refolding of denatured proteins.

The mechanism by which smHSPs recognize and capture aggregation-prone polypeptides is largely unknown. As with other molecular chaperones (*e.g.*, HSP60; Horowitz *et al.*, 1995), there is some evidence that hydrophobic patches in α-crystallin are required for interaction with the hydrophobic regions exposed by unfolded proteins (Raman and Rao, 1994). It has been observed that α-crystallin undergoes a conformational transition at elevated temperatures which results in a marked increase in surface hydrophobicity, and a concomitant increase in chaperone activity (Das and Surewicz, 1995). Therefore, it is likely that the masking and stabilizing of hydrophobic core regions of unfolded proteins by smHSPs is a key aspect of their ability to suppress protein aggregation. It is apparent, however, that electrostatic interactions are also likely to be critical in substrate binding. For example, an $Asp^{69}\rightarrow Ser^{69}$ αA-crystallin mutant was shown to have a substantially reduced protective ability despite its formation of wild-type-like oligomeric complexes (Smulders *et al.*, 1995). Another informative study, on the interaction of α-crystallin with spin-labeled peptides, revealed that the side chains of the peptides were immobilized within a polar environment (Farahbakhsh *et al.*, 1995).

Studies aimed at investigating the structural conformations of polypeptides bound to smHSPs provide inconsistent data on this important aspect of chaperone activity. Carver *et al.* (1995b) demonstrated that α-crystallin does not interact with unfolded, hydrophobic but stable proteins (*e.g.*, reduced and carboxymethylated α-lactalbumin and α-casein), but does complex with grossly unfolded and unstable proteins which are about to

precipitate out of solution. Similarly, Das *et al.* (1995, 1996) suggested that unlike other chaperones, α-crystallin has very low affinity for folding intermediates formed during protein refolding reactions *in vitro* (*i.e.*, protein conformers which are nearly fully denatured), but has a high affinity for aggregation-prone intermediates which are characterized by a very low degree of unfolding. Another study showed that α-crystallin bound to a molten-globule form of carbonic anhydrase, which displays a significant amount of secondary structure but little permanent tertiary structure (Rajaraman *et al.*, 1996).

Unlike some other well characterized molecular chaperones such as HSP60 and HSP70 (Hartl, 1996), little experimental data are available on the site of interaction of the unfolded proteins with smHSPs. In one of the aforementioned studies by Farahbakhsh *et al.* (1995), two spin-labeled peptides (insulin B chain and melittin) were used to demonstrate that these small, largely unstructured polypeptides bound not on the surface or in an interior cavity of the complex, but instead were found to be largely separated in distinctly polar environments. In one of the few studies on a smHSP other than α-crystallin, Lee *et al.* (1997) demonstrated that when a hydrophobic probe (bis-ANS) was incubated with the dodecameric pea HSP18.1 complex, it could be cross-linked specifically to a hydrophobic region within the first half of the α-crystallin domain. Interestingly, a stretch of hydrophobic residues near the end of the α-crystallin domain (GVLTVTV) which is highly conserved among smHSPs was not labeled with bis-ANS, suggesting that this region might be solvent-inaccessible.

Cellular functions of small HSPs

Unlike the HSP60 molecular chaperone family, the smHSPs are unlikely to play a critical role in the folding of nascent polypeptides. One reason is that smHSPs are not encoded in either of the two fully sequenced bacterial genomes (*Haemophilus influenzae* and *Mycoplasma genitalium*), while all of the other classes of chaperones found in prokaryotes and eukaryotes (DnaK/HSP70, DnaJ/HSP40, GroEL/HSP60, GroES/HSP10, and GrpE) are present (Fraser *et al.*, 1995; Fleischmann *et al.*, 1995). Most of these ubiquitous chaperones are involved in folding nascent polypeptide chains. Thus, the function of smHSPs may be restricted to the

protection of the organism from cellular stress by preventing the aggregation of stress-damaged proteins. Consistent with this argument is the fact that one 18-kDa smHSP is indeed found in *Methanococcus jannaschii*, a thermophilic organism whose genome was recently sequenced (Bult *et al.*, 1996). Interestingly, the only other major chaperone present in *M. Jannaschii* is a chaperonin related to other archaebacterial and eukaryotic cytosolic chaperonins. Chaperonins are not only required for protein folding, but have also been shown to play a protective role during stress conditions (Martin *et al.*, 1992).

Given that smHSPs are highly induced under stress conditions, it is not surprising that they are likely to play an important role in induced thermotolerance. This increased resistance of organisms to severe stresses following mild pre-exposures to a similar or different stress is observed in virtually every organism studied (Parsell and Lindquist, 1994). As with other chaperones, including inducible HSP70s (Feder *et al.*, 1996) and HSP104 (Sanchez and Lindquist, 1990; Sanchez *et al.*, 1992), it is well documented that smHSPs play important roles in protecting organisms from stress and in the establishment of thermotolerance (Landry *et al.*, 1989; Lavoie *et al.*, 1993a; Yeh *et al.*, 1994; Arrigo and Landry, 1994).

The repertoire of proteins protected by smHSPs during stress conditions is presently unknown. It is possible that smHSPs nonspecifically recognize and stabilize the bulk of cellular proteins susceptible to unfolding. On the other hand, they may be more specialized, acting on a limited number of target proteins. In the cell, cytoskeletal proteins, which are particularly sensitive to cellular stresses (Welch and Suhan, 1985), appear to be targets for smHSPs. Specific binding of smHSPs to actin and the intermediate filaments desmin, vimentin, and GFAP has been demonstrated (Chiesi *et al.*, 1990; Bennardini *et al.*, 1992; Gopalakrishnan and Takemoto, 1992; Nicholl and Quinlan, 1994). HSP27 has been implicated in regulating the dynamics of actin filaments (Lavoie *et al.*, 1993b; Landry and Huot, 1995), and α-crystallin participates in intermediate filament assembly (Nicholl and Quinlan, 1994). Furthermore, HSP27 and α-crystallin can enhance the survival of cells subjected to heat shock or oxidative stresses by conferring increased stability to actin fibers (Lavoie *et al.*, 1993a, 1995; Huot *et al.*, 1996; Wang and Spector, 1996).

The finding that smHSPs can modulate cytoskeleton dynamics is consistent with the fact that many smHSPs can inhibit actin polymerization (Miron *et al.*, 1991; Benndorf *et al.*, 1994; Rahman *et al.*, 1995). Many factors influence the equilibrium between actin monomers and filaments *in vitro*, including ATP, divalent cations, and proteins that bind to actin (Vandekerckhove, 1990; Cooper, 1992). It has been proposed by Rahman *et al.* (1995) that a possible site of interaction between smHSPs and actin lies within a region in actin thought to be important for the polymerization of G-actin into F-actin, and for the binding of actin to DNAse I. This hydrophobic sequence motif, G-[V/I]-L-T-$[X]_3$-P, is conserved in actin at residues 61-69, and in α-crystallins and many smHSPs near the end of the α-crystallin domain. Interestingly, labeled bis-ANS (a hydrophobic probe) was not photoincorporated into the equivalent region of pea HSP18.1, suggesting that this region might not be the site of interaction with hydrophobic regions of unfolded polypeptides (Lee *et al.*, 1997). Thus, the conserved motif in smHSPs may have a specialized role in binding to the corresponding sequence in actin, thereby influencing the polymerization of the cytoskeletal protein.

In contrast to the above function of smHSPs, Wang and Spector (1996) have recently shown that α-crystallin and its individual subunits (αA and αB) are able to prevent cytochalasin D-induced *de*polymerization of actin. Furthermore, it was shown that α-crystallin stabilizes actin from dilution-induced depolymerization and enhances polymerization at higher actin concentrations. It was suggested that there is no likely interaction between α-crystallin and actin monomers, as the effect of α-crystallin in enhancing actin polymerization is not apparent before some polymerization has occurred. The reason for the apparently disparate roles of α-crystallin and other smHSPs in influencing actin polymerization is unknown, but as the authors suggest, α-crystallin, like other smHSPs, is clearly able to influence actin dynamics. It should be noted that no link has been made between the above function of smHSPs and their chaperone activity; while it is conceivable that the two activities are functionally related, only the chaperone activity has thus far been shown to be a ubiquitous feature of smHSPs.

One interesting aspect of smHSP chaperone activity is its ATP-independence (Horwitz, 1992; Jakob *et al.*, 1993; Merck *et al.*, 1993a; Lee *et al.*, 1995). During heat shock conditions,

significant changes in energy metabolism occur, including decreases in the cellular levels of ATP (Findly *et al.*, 1983). As a consequence, the recruitment of the smHSPs to protect the cell against the accumulation of unfolding proteins may be advantageous. Since the heat-induced interaction of smHSPs with unfolded proteins is ATP-independent and stable *in vitro*, it is possible that the productive release of the bound protein may occur later (perhaps after the stress condition), and require the assistance of other ATP-dependent molecular chaperones. Recently published studies are shedding light into the fate of the smHSP-bound proteins. Ehrnsperger *et al.* (1997) demonstrated that HSP70, which is present at high concentrations after heat shock, is able to trigger the release of citrate synthase from HSP25 and promote refolding in an ATP-dependent manner. However, the percentage of citrate synthase reactivated with HSP70 was only about 13%, whereas without HSP70, the level of spontaneous refolding was approximately 2%. As the authors suggest, it is likely that co-chaperones (for example, HSP40 and Hip), would participate in this process *in vivo*, increasing the efficiency of the refolding reaction. Indeed, Lee *et al.* (1997) showed that pea HSP18.1-bound firefly luciferase could be folded more efficiently (to 40% of total activity) when incubated with rabbit reticulocyte lysate. Essentially no refolding occurred in the presence of apyrase, which causes a depletion of ATP. Although it is unclear what components are involved in initiating the refolding of the bound protein, the rabbit reticulocyte lysate is known to contain all of the necessary chaperone machinery to fold firefly luciferase synthesized *de novo* and from the chemically-denatured state (Frydman *et al.*, 1994b; Frydman and Hartl, 1996).

The present study

Our laboratory has extensively examined the induction of two classes of *C. elegans* smHSPs by various stresses, both at the transcription and protein levels. Conditions which induce expression invariably promote protein denaturation, and range from heat stress to exposure to many kinds of chemicals, including alcohols, heavy metals, and pesticides. Although it is likely that the smHSPs have a protective function *in vivo*, the details concerning their assembly and mechanism of action is largely unknown. In an effort to understand the structure and function of

smHSPs in general, the *C. elegans* HSP16-2 wild-type protein and various deletion variants were expressed in *E. coli* and purified. HSP16-2 is an ideal small HSP to study for two main reasons. Firstly, a great deal is already known about its expression during cellular stresses. Secondly, it reflects the minimal functional unit for a small HSP, as the minimum size of functional smHSPs is very close to 16 kDa. In brief, structure-function studies on HSP16-2 revealed that there is a strict requirement for an intact N-terminal region for the formation of high-MW complexes which are functional as molecular chaperones. The C-terminal extension is not required for oligomerization or chaperone activity, but appears to be involved in maintaining the solubility of the complex. HSP16-2 forms stable binary complexes with unfolded actin and tubulin, and preferentially interacts with early unfolded intermediates which form along the renaturation or aggregation pathway. The findings of this study are likely to be applicable to other smHSPs, and provide insight into our understanding of the protective function of these chaperones *in vivo*. Lastly, characterization of a unique, stage-specific 12.6-kDa smHSP from *C. elegans* provided supporting evidence for the structure-function model proposed.

II. MATERIALS AND METHODS

2.1 Cloning of *hsp12.6* cDNA and preparation of small HSP constructs

The *hsp16-2* coding region had previously been subcloned into the pRSET A expression vector (Invitrogen) at the *Bam*HI-*Eco*RI site (Jones *et al.*, 1996) for producing H_6HSP16-2 (*i.e.*, wild-type HSP16-2 fused to an N-terminal ~4 kDa polyhistidine-containing fusion tag). A construct designed to express wild-type HSP16-2 was made by excising the *Nde*I-*Bam*HI fragment containing the polyhistidine tag, blunting, and religating. To make the vector encoding $H_6\Delta$1-15 HSP16-2 (a tagged HSP16-2 lacking the first 15 amino acids), the *hsp16-2*-containing clone was amplified with the primers OH2-A and OBM2 (see **Appendix II**), and the *Xho*I-*Eco*RI-restricted PCR product was subcloned into pRSET B (*Xho*I-*Eco*RI). The vector encoding $H_6\Delta$130-145 HSP16-2 (like H_6HSP16-2 but missing the last 16 amino acids) was generated by subcloning the PCR product amplified with the primers OBM1 and OH2-C into pRSET A (*Bam*HI-*Eco*RI). The constructs designed to encode $H_6\Delta$1-32 and $H_6\Delta$1-44 HSP16-2 were made by subcloning the *Pst*I-*Eco*RI fragment of the pH_6HSP16-2 vector into pRSET B (*Pst*I-*Eco*RI), and the *Hpa*I-*Hin*dIII fragment into pRSET B (*Pvu*II-*Hin*dIII), respectively.

The *hsp12.6* coding region was amplified from mixed-stage first-strand cDNA (prepared according to Jones and Candido, 1993) with the primers F38A and F38B and subcloned into *Bam*HI-*Hin*dIII restricted pRSET A vector after restriction with the same enzymes. This expression vector encodes H_6HSP12.6 (HSP12.6 fused at the N-terminus to the pRSET vector polyhistidine-containing tag). To create a vector expressing wild-type HSP12.6, the *Bam*HI-*Hin*dIII cut PCR product was subcloned into the *Bgl*II-*Hin*dIII site of a modified pRSET A vector lacking the polyhistidine-containing *Nde*I-*Bam*HI fragment. The sequence of the cloned cDNA matches the coding region predicted from the genomic DNA.

2.2 Expression and purification of the small HSPs

All expression constructs were transformed into the BL21(DE3) *E. coli* strain (Studier *et al.*, 1990), and 0.5-2.0-liter cultures were grown in TB/Amp medium to an OD_{600} between 0.8-1.0,

induced with 1 mM IPTG, and harvested 3 hours later. Cells were frozen and thawed four times and insoluble inclusion bodies were isolated and washed once in TEND buffer (50 mM Tris-HCl, 0.1 mM EDTA, 50 mM NaCl, 1 mM DTT; pH 7.5). For the purification of the HSP16-2 protein, the inclusion bodies were solubilized in TEND buffer supplemented with 4 M urea, and 2.5 ml of the cleared supernatant was applied to an ~40-ml Sephacryl S-100 column equilibrated with TEND/4 M urea buffer. The peak fractions were then collected and dialyzed overnight in TEND buffer. A 2-ml sample was applied to an ~70-ml Sephacryl S-300 column equilibrated in TEND buffer, and the peak fractions were collected, snap-frozen in a dry-ice-ethanol bath, and kept at -70°C. To purify the polyhistidine-containing proteins, the inclusion bodies were solubilized in UNT buffer (8 M urea, 50 mM NaCl, 50 mM Tris; pH 8.0) and centrifuged at 10000 x *g*. The cleared supernatant was applied to a column containing 0.5-2.0-ml Ni^{2+}-chelate affinity resin (Qiagen) equilibrated in UNT buffer. The column was extensively washed with UNT (pH 8.0) followed by UNT (pH 6.3) buffers, and the protein was eluted with UNT (pH 4.3) buffer. Purified proteins were then dialyzed against TEND buffer and used in assays immediately.

The wild-type and polyhistidine-tagged HSP12.6 recombinant proteins were also produced in *E. coli* BL21(DE3). The cells were resuspended in PND buffer (25 mM sodium phosphate pH 7.0, 25 mM NaCl, 0.5 mM DTT) supplemented with protease inhibitors (2 mM PMSF, 10 µg/ml aprotinin, 10 µg/ml pepstatin A, 10 µg/ml leupeptin, 5 mM EDTA), disrupted by sonication, and the insoluble fraction pelleted by centrifugation at 12000 x *g*. The soluble HSP12.6 was first fractionated by size exclusion chromatography on Sephacryl S200-HR in PND buffer. Peak fractions containing HSP12.6 were collected, then loaded on a BIO GEL® HTP hydroxylapatite column (Bio-Rad). The column was washed with PND buffer, and the bound HSP12.6 was eluted using a 10-300 mM sodium phosphate pH 7.0 gradient made in 25 mM NaCl and 0.5 mM DTT. Positive fractions were then dialyzed extensively against PND buffer and used immediately. N-terminal sequencing of the purified HSP12.6 confirmed its identity and revealed some microheterogeneity at the N-terminus, which was probably due to processing (cleaving) of one or both of the two methionine residues present at the start of the

coding region. The native H_6HSP12.6 protein was purified on a Ni^{2+}-chelate affinity column using PND buffer adjusted to pH 6.3 for washes, and pH 4.3 for elution.

2.3 Molecular weight estimation of the small HSPs

To estimate the sizes of the native smHSP complexes, approximately 5 mg of purified protein was subjected to size exclusion chromatography over a 1.5 x 80 cm Sephacryl S-300HR. The column was first calibrated with the following molecular weight standards: thyroglobulin (669 kDa), ferritin (440 kDa), catalase (232 kDa), bovine serum albumin (67 kDa), ovalbumin (43 kDa), chymotrypsinogen A (25 kDa), and RNAse A (14 kDa). The column was run in TEND buffer at room temperature. Samples were separated on 12.5 % SDS-gels, and the elution volume of each was used to estimate the molecular weight.

The native MW of recombinant HSP12.6 was estimated by size exclusion chromatography on a 1.5 x 100 cm Sephacryl S-200HR column in PND buffer at 4°C. Fractions were collected, separated on 13.5% SDS-gels, and relative amounts of HSP12.6 were determined by densitometry. To estimate the *in vivo* M_r of HSP12.6, a soluble protein extract was prepared by Dounce-homogenizing and sonicating ~1 ml of packed L1-stage larvae in 1.5 ml PND buffer supplemented with protease inhibitiors (2 mM PMSF, 2 mM EDTA, and 10 µg/ml each of aprotinin, pepstatin A, and leupeptin). The entire clarified protein extract was chromatographed on a 1 x 50 cm S-200HR column in PND buffer at 4°C. Fractions were analyzed by Western blotting as described below.

2.4 Production and purification of anti-HSP12.6 antibody

Purified H_6HSP12.6 was dialyzed against TBS and used to immunize rabbits for pAb production. Rabbits were injected with 0.5 mg of antigen in Freund's complete adjuvant, then boosted three times at two-week intervals using the same amount of H_6HSP12.6 in Freund's incomplete adjuvant. Antiserum was affinity purified over H_6HSP12.6 affixed to an Affi-Gel 10 column (Bio-Rad) according to the manufacturer's instructions.

2.5 Western blot analysis of HSP12.6

Synchronous populations of *C. elegans* were obtained as described (Emmons *et al.*, 1979), and nematodes were cultured in liquid medium at 15°C. Protein extracts were prepared by boiling the nematodes in Laemmli 1X sample buffer for 20 minutes. For Western blot analysis, 20 µg of protein extract was separated by electrophoresis on a 13.5% gel, transferred to an Immobilon-P membrane (Amersham), and probed with a 1:500 dilution of the anti-HSP12.6 pAb. Immunoblots were developed using Amersham's enhanced chemiluminescence system.

2.6 Cross-linking of small HSPs

Cross-linking reactions consisted of 1.5 µM HSP16-2 and its variants (based on monomeric size), 15 µM BSA (to minimize spurious cross-linking), and 2 mM of freshly-prepared bis (sulfosuccinimidyl) suberate (BS^3; from Pierce). Protein samples to be cross-linked were first dialyzed in cross-linking buffer (25 mM MES pH 7.5, 25 mM NaCl, 0.5 mM DTT), and reactions were carried out in the same buffer for 30 minutes. Aliquots (5-15 µl) were then electrophoresed on 12% SDS-gels, transferred to a PVDF membrane, and probed with a polyclonal antibody against HSP16-2 (Jones *et al.*, 1996; see also **Appendix VII**). Cross-linking reactions with HSP12.6 were performed under the same conditions with the exception that 0.25 or 1 µM protein was used, and the Western blot was developed using the anti-HSP12.6 pAb.

2.7 Assay for H_6HSP16-2 binding to Ni^{2+}-chelate affinity resin

H_6HSP16-2 was purified by nickel affinity chromatography under denaturing (8M urea) conditions, and dialyzed against a 50 mM NaCl and 50 mM sodium phosphate buffer (pH 8.0) (NP buffer). Two 150 µl samples containing 175 µg of H_6HSP16-2 were prepared, one in NP buffer (Sample 'N' for 'Native') and the other in NP buffer containing 6M urea (Sample 'D' for 'Denatured'). A small amount of Qiagen nickel affinity resin (30 µl) was added to samples N and D. The samples were mixed gently at room temperature for 15 minutes, then washed twice with 500 µl NP buffer (without urea for sample N and with 6M urea for sample D, both adjusted to pH 6.3), and any bound protein was eluted by resuspending the nickel resin pellet with two

50 µl washes of 100 mM EDTA, which chelates the nickel bound to the resin and therefore elutes all the adsorbed proteins. Aliquots (15 µl) of the EDTA wash of sample N and the pH 6.3 and EDTA washes of sample D were separated on a 12% SDS-gel, and stained with Coomassie Blue.

2.8 Thermal aggregation studies

The effect of small HSPs on the thermally-induced aggregation of a 150 nM solution of porcine heart citrate synthase (Sigma) was monitored by light scattering at 320 nm in a Cary 210 Varian spectrophotometer equipped with a thermostated cell compartment pre-heated to 45°C. The appropriate dilutions of citrate synthase and smHSP were made with 50 mM $NaPO_4$ (pH 8.0) buffer. The relative amount of CS aggregation was normalized to the 100% aggregation value obtained when CS was incubated alone.

2.9 Chemical aggregation studies

The effect of HSP16-2 on the chemically-induced aggregation of CS was measured in an SPF-500C™ stirred-cell spectrofluorometer with excitation and emission wavelengths set to 500 nm and a bandpass of 2 nm. CS was denatured in 6 M guanidine hydrochloride for at least 45 minutes and diluted 100-fold in a total volume of 2 ml to give a final monomeric concentration of 200 nM. All aggregation experiments were carried out in 50 mM $NaPO_4$ buffer (pH 7.5), and were normalized as described above.

2.10 Native gel analysis of HSP16-2-actin/tubulin binary complexes

The kinetics of HSP16-2-actin/tubulin binary complex formation was measured by diluting [^{35}S]-labeled 7.5 M urea-denatured actin or tubulin 100-fold (final actin/tubulin concentration, approximately 225 nM) into a solution containing 0.5 mg/ml (1.6 µM) HSP16-2 and immediately mixing well by pipetting up and down. Appropriate dilutions of HSP16-2 were made using 'refolding buffer' (25 mM MES pH 7.5, 25 mM NaCl, and 0.5 mM DTT). At each time point, 20 µl of the reaction mix was mixed in with 5 µl glycerol, and snap-frozen in an

ethanol dry-ice bath. Samples were then separated on native gels (prepared and run as described in the *Materials and Methods* of *Chapter I*), and subjected to autoradiography.

To measure the binding of HSP16-2 to progressively more aggregated forms of actin and tubulin, the following experiments were done. Labeled, denatured actin or tubulin was diluted into 'refolding buffer' for various lengths of time, and an aliquot was added to a tube containing HSP16-2 such that the final volume was 20 µl, and the HSP16-2 concentration was 1.6 µM and that of actin or tubulin approximately 225 nM. The binding was allowed to proceed for 20 minutes at room temperature, and the reaction was snap-frozen after the addition of glycerol to 20%. Samples were then separated on native gels as before.

2.11 Sedimentation velocity and fluorescence measurements

The experiments in this section were performed by Ronald Melki and Gérard Batelier as part of a collaboration, and the methodologies are included here for reference only.

2.11.1 Actin and tubulin purification and labeling

Actin was purified from rabbit muscle acetone powder (Spudich and Watt, 1971; Eisenberg and Kielley, 1974) and isolated as CaATP-G-actin by chromatography through Sephadex G-200 (McLean-Fletcher and Pollard, 1980) at 4°C equilibrated in 5 mM Tris-HCl, pH 7.8, 0.2 mM DTT, 0.2 mM ATP, 0.1 mM $CaCl_2$, 0.01% NaN_3. G-actin (50 µM) was stored on ice and used within two weeks. Pyrenyl-labeled actin and NBD-labeled actin were prepared according to Kouyama and Mihashi (1981) and Detmers *et al.* (1981), respectively. Pure tubulin was prepared from fresh pig brain by three assembly-disassembly cycles (Shelanski *et al.*, 1973) followed by phosphocellulose (Whatman P11) chromatography (Weingarten *et al.*, 1975). Tubulin (100-150 µM) in 0.1 M PIPES, pH 6.9, 1 mM EGTA, 0.5 mM $MgCl_2$ and 1 mM GTP was flash frozen in liquid nitrogen and stored at -80°C. DTAF-labeled tubulin was prepared as described by Mejillano and Himes (1989). Native Pyrenyl- or NBD-actin and DTAF-tubulin were denatured by addition of urea to a final concentration of 7.5 M.

2.11.2 Fluorescence measurements

All measurements were made at 20°C in a Spex fluorolog 2 spectrofluorometer. The excitation monochromator was set at 345, 468, and 492 nm and the emissions recorded at 386, 535, and 517 nm for pyrenyl-actin, NBD-actin and DTAF-tubulin, respectively.

2.11.3 Sedimentation velocity measurements

Sedimentation velocity experiments were carried out with a Beckman Optima XL-A analytical ultracentrifuge equipped with an AN 60Ti four-hole rotor and cells with two-channel 12 mm path length centerpieces. Sample volumes of 400 µl were centrifuged at 60 000 rpm. Radial scans of absorbance at 278 nm were taken at 10-minute intervals. Data were analyzed to provide the apparent distribution of sedimentation coefficients using the programs DCDT (Stafford, 1992) and SVEDBERG (Philo 1994). The partial specific volumes, $\bar{\nu}$, at 20°C, were calculated from the amino acid compositions and the solvent density was 1.00 g/cm^3. The degrees of hydration of the totally unfolded proteins were estimated based on the amino acid compositions by the method of Kuntz (1971) according to Laue *et al.* (1992). The degrees of hydration used for all calculations, 0.316, 0.314, and 0.337 g of H_2O per g of protein, for wild-type HSP16-2, $H_6\Delta$130-145 HSP16-2 and $H_6\Delta$1-44 HSP16-2, respectively, were the result of correcting the calculated degrees of hydration by a factor of 0.7, obtained by comparing degrees of hydration for several proteins in their folded state to that based on their amino acid composition (Lin *et al.*, 1991).

2.12 Miscellaneous

SmHSP protein concentrations were determined using the Bio-Rad Bradford assay kit and IgG as a standard. Citrate synthase concentrations were determined by absorbance at 280 nm using an extinction coefficient of 1.55 X 10^{-5} M^{-1} cm^{-1} (Singh *et al.*, 1970). A heat-shocked *C. elegans* embryo extract was prepared by homogenizing 1 g of embryos (incubated at 30°C for 2 hours and recovered at 15°C for 30 minutes) in a Dounce homogenizer in the presence of 2 ml TEND buffer supplemented with protease inhibitors (2 mM PMSF, 2 µg/ml Leupeptin, 1 µg/ml

Aprotinin, 1 μg/ml Pepstatin A), and clearing the cellular debris by centrifugation at 12000 x *g*. The concentrations of HSP16-2 and $H_6\Delta$130-145 complexes were calculated according to the average of the two molecular masses obtained by sedimentation velocity measurements (317 kDa and 421 kDa, respectively). All other smHSP concentrations were based on the theoretical, monomeric molecular weights.

III. RESULTS

3.1 Structure and function of HSP16-2

3.1.1 Production of HSP16-2 variants for structure-function studies

Although the sizes of smHSPs vary substantially, a detailed sequence comparison of known members suggests that the minimal functional unit consists of a core region of about 85 amino acids (the α-crystallin domain) which is flanked by an N-terminal region of at least 39 residues (in *E. coli* IbpA), and a C-terminal extension of at least 12 residues (in *N. crassa* HSP30). Accordingly, the most compact smHSP characterized to date is *E. coli* IbpA, which has a very short C-terminus of 14 residues and totals 137 amino acids (15.8 kDa). The nematode HSP12 family represents the only known exception to the apparent minimum size restriction of smHSPs. *C. elegans* HSP16-2 (145 amino acids) is only slightly larger than IbpA, and is therefore a good model smHSP for delineating the structural requirements for smHSP oligomerization and chaperone activity in these proteins.

Expression constructs harbouring wild-type HSP16-2 and six derivatives were created (**Figure 15A**). The cDNA encoding HSP16-2 was initially isolated and subcloned into pRSET for the purpose of producing and purifying a polyhistidine-containing fusion protein (H_6HSP16-2), which was used to make anti-HSP16-2 polyclonal antibodies (Jones *et al.*, 1996). An HSP16-2 construct lacking the polyhistidine fusion leader was created for the expression of wild-type HSP16-2. Three additional constructs designed to express polyhistidine-containing N-terminal truncations of HSP16-2 were made. These encode H_6Δ1-15, H_6Δ1-32, and H6Δ1-44 HSP16-2, which lack the first 15, 32, and 44 amino acids of HSP16-2, respectively, but contain a 4-kDa N-terminal polyhistidine-containing region to facilitate purification. Finally, a construct designed to express a polyhistidine-containing variant of HSP16-2 lacking the last 16 amino acids (H_6Δ130-145 HSP16-2) was created. All smHSPs were produced in the *E. coli* BL21(DE3) strain (Studier *et al.*, 1990) and purified from inclusion bodies to ≥90% homogeneity (**Figure 15B**). Wild-type HSP16-2 was purified by a combination of denaturing and nondenaturing size exclusion chromatography, while the polyhistidine-containing smHSPs

were purified by binding to Ni^{2+}-chelate affinity resin and eluting with a low pH buffer. The smHSPs were then dialyzed in an appropriate buffer before use.

An alignment of *C. elegans* HSP16-2 and HSP12.6, as well as other smHSP sequences from various organisms (**Figure 15C**) illustrates the three distinct regions found in smHSPs, and delineates the regions of the HSP16-2 derivatives which are truncated relative to wild-type HSP16-2, HSP12.6, and other smHSPs.

The cDNA encoding HSP16-48, a member of another class of 16-kDa smHSPs in *C. elegans* (Russnak and Candido, 1985) was amplified by PCR from first strand cDNA prepared from total (heat-shocked) RNA, and subcloned into a pRSET vector. The wild-type HSP16-48 protein was produced in *E. coli*, and its size and cross-reactivity toward the anti-HSP16-2 antibody strongly suggests that it represents (probably along with its highly identical homologue, HSP16-41) the lower-MW protein seen in Western blots of stressed nematode extracts probed with the same antibody (see **Appendix VII**). No additional studies were attempted with this protein.

3.1.2 HSP16-2 quaternary structure and subunit orientation

The size of recombinant wild-type HSP16-2 was estimated by gel permeation chromatography on a calibrated Sephacryl S-300HR column. The majority of HSP16-2 elutes as a single peak between the MW markers thyroglobulin (669 kDa) and ferritin (440 kDa), and has an apparent molecular mass of 550 kDa (**Figure 16A** and **16B**). The estimated size of the complex is essentially identical to that of HSP16-2 isolated from a heat-shocked nematode extract (Hockertz *et al.*, 1991). Interestingly, the H_6HSP16-2 protein also assembles into large oligomeric complexes of somewhat larger size (680 kDa), as judged by size exclusion chromatography (**Figure 16B**).

These data suggest that HSP16-2 and H6HSP16-2 contain approximately 34 and 37 subunits, respectively. While gel permeation chromatography provides estimated sizes based on the size and shape (Stoke's radius) of any protein or protein complex, significantly better size estimates can be obtained by sedimentation velocity measurements.

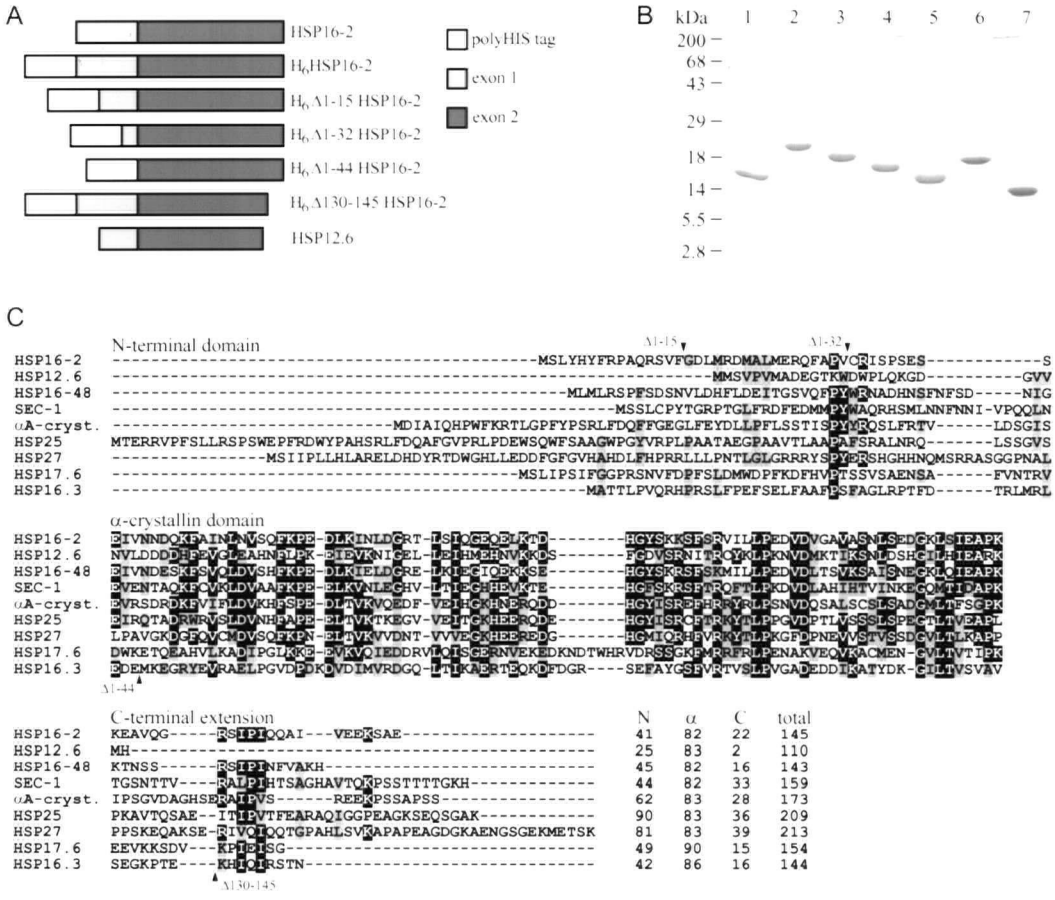

Figure 15. Summary of smHSP constructs, purified proteins, and alignment. **A.** Schematic of all smHSPs used in this study, drawn approximately to scale. The two-exon structure (exon 1, light grey and exon 2, dark grey) applies to *hsp16-2* and *hsp12.6*, as both have a single intron in the same relative position. The polyhistidine-containing pRSET tag is shown in white. **B.** Purified smHSPs separated on a 15% SDS-gel. Lanes 1-7 represent the constructs shown in (B) from top to bottom, respectively. **C.** Amino acid sequence alignment of smHSPs (with Genbank accession numbers): *C. elegans* HSP16-2 (M14334), HSP12.6 (also identified as F38E11.2; Z68342 and U92044), HSP16-48 (K03273), SEC-1 (Z35640); bovine αA-crystallin (M26142); murine HSP25 (L07577); *Drosophila* HSP27 (J01101); Soybean HSP17.6 (M11317); *M. tuberculosis* HSP16.3 (M76712). The first block of aligned sequences corresponds to the N-terminal domain, the second block corresponds to the α-crystallin domain, and the third block shows the C-terminal extension. Identical amino acids present in at least 4 of the 9 sequences are highlighted in black, and structurally similar amino acids (at least 4 of 9) are shaded.

In collaboration with Ronald Melki and Gérard Batelier (Laboratoire d' Enzymologie et Biochimie Structurales, CNRS, France), such studies were carried out on HSP16-2, $H_6\Delta$130-145, $H_6\Delta$1-44, and HSP12.6 (summarized in **Appendix VIII**). Sedimentation data confirmed that HSP16-2 forms large oligomeric complexes. The data fitted relatively well to a two-component system involving 10.5 S and 14.7 S species with proportions of about 58% and 42%, respectively (**Appendix VIII**). These correspond to apparent molecular masses of 239 and 395 kDa for the two species, consistent with the behaviour of wild-type HSP16-2 as an oligomer of approximately 14 and 24 subunits, respectively. Interestingly, the frictional ratio values (f / f_0) suggest that HSP16-2 is somewhat asymmetrical.

Waldmann *et al.* (1995c) previously reported difficulty in purifying an archaebacterial chaperonin complex carrying a polyhistidine extension fused to its C-terminus, due to poor accessibility of this region to the Ni^{2+}-chelate affinity resin. Since H_6HSP16-2 also forms an aggregate, a test to determine whether its polyhistidine-containing tag was exposed or not was carried out. Aliquots of native or urea-denatured H_6HSP16-2 were incubated with nickel-chelate affinity resin, and after washing the resin to remove non-specifically adsorbed proteins, specifically bound protein was eluted with 100 mM EDTA. No detectable binding of the native H_6HSP16-2 complex to the nickel resin was seen, whereas the unfolded H_6HSP16-2, with its exposed H_6 tag, bound efficiently (**Figure 17**). It is therefore likely that the N-terminal region of wild-type HSP16-2 is sequestered within the interior of the native complex.

3.1.3 HSP16-2 interacts with unfolded CS and prevents its aggregation

The various methods employed to assay for molecular chaperone activity all make use of the affinity of chaperones for unfolded proteins. The three assays used in this study to measure the interaction of smHSPs with unfolded proteins are summarized in **Figure 18**. The first method involves the protection of a given protein from aggregating at an elevated temperature. Similarly, the second assay measures the protection of a substrate from aggregation after dilution from a chemical denaturant. The third assay involves the detection of binary complexes formed between the chaperone and a denatured protein by native gel electrophoresis.

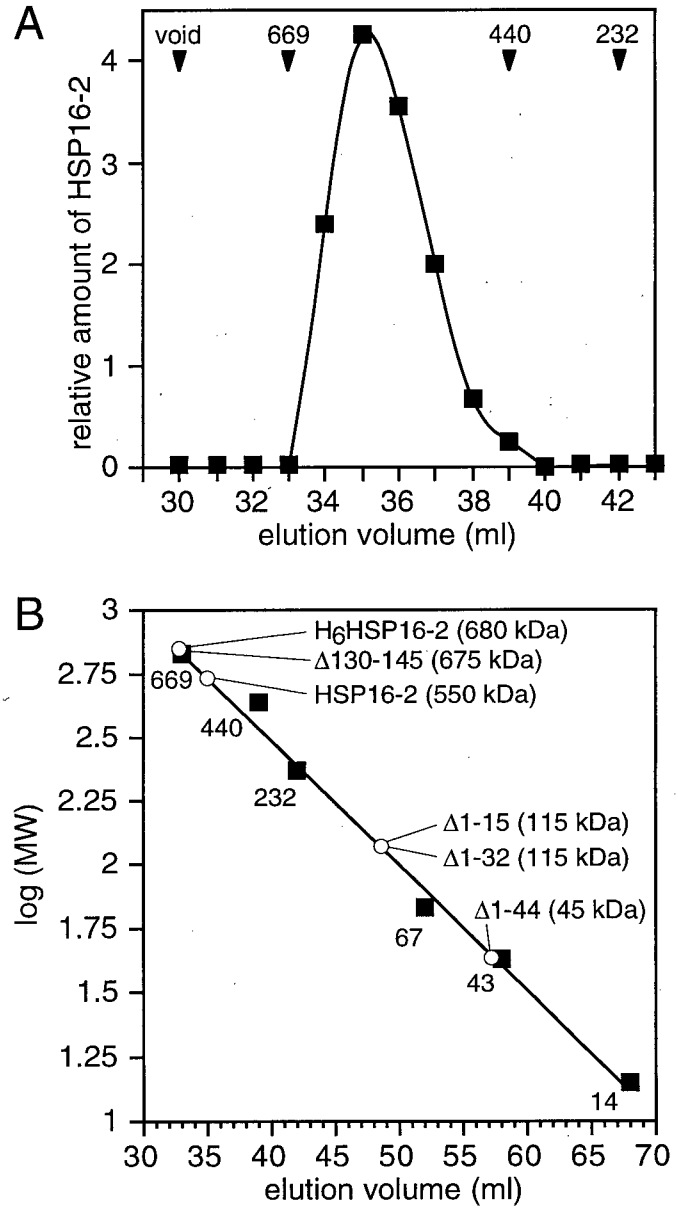

Figure 16. Elution profile of HSP16-2 and derivatives from a Sephacryl S-300HR size exclusion column. **A.** HSP16-2 elutes as a single peak corresponding to a species of approximately 550 kDa. **B.** Peak elution volumes of the smHSPs (O) relative to a series of molecular weight protein standards (■), thyroglobulin (669 kDa), ferritin (440 kDa), catalase (232 kDa), BSA (67 kDa), ovalbumin (43 kDa), and RNAse A (14 kDa). The estimated sizes of the eluting species, shown in parentheses, were derived from the log(MW) *versus* elution volume (ml) standard curve.

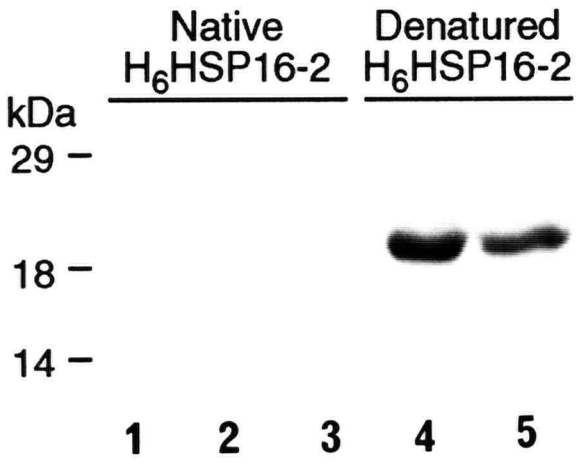

Figure 17. Affinity of native and denatured H_6HSP16-2 for nickel affinity resin. Native HSP16-2 complex and 6 M-urea denatured complex were incubated with separate aliquots of Ni^{2+}-chelate affinity resin equilibrated in buffer without or with 6 M urea, respectively. The resins were then washed multiple times with a pH 6.3 buffer without or with 6 M urea, respectively, and the first two washes without urea were combined and analyzed on a 12% SDS-gel (lane 1). Following the washes, any protein bound to the resin was eluted with 100 mM EDTA buffer. The EDTA washes without urea are shown in lanes 2 and 3, and the washes with urea are shown in lanes 4 and 5. Note that only the denatured HSP16-2 bound to the resin and therefore was eluted in the EDTA washes.

The molecular chaperone activity of HSP16-2 was investigated using citrate synthase (CS), a dimer of two identical 49-kDa subunits. The denaturation and renaturation of CS has been well studied (Zhi *et al.*, 1992), and CS has been used in chaperone studies with HSP90 and associated proteins (Wiech *et al.*, 1992; Jacob *et al.*, 1995; Bose *et al.*, 1996), GroEL (Buchner *et al.*, 1991), and smHSPs (Jakob *et al.*, 1993; Lee *et al.*, 1995; Chang *et al.*, 1996). When CS is incubated alone at 40-45°C it aggregates irreversibly, as detected by light scattering at 320nm, and loses activity. However, when CS is incubated together with increasing amounts of HSP16-2, there is a concomitant decrease in CS aggregation (**Figure 19A**). IgG has no effect on CS aggregation under these conditions, demonstrating the specificity of the chaperone-mediated inhibition of aggregation. The ability of HSP16-2 to prevent CS aggregation over a range of concentrations is summarized in **Figure 19B**. At molar ratios of HSP16-2 complex to CS monomer of 1:1 or higher, aggregation of CS is almost completely inhibited. The H_6HSP16-2 variant is also equally effective in preventing CS aggregation (see **Figure 29**).

To determine if HSP16-2 can re-solubilize protein aggregates, a 3.5-fold molar excess of HSP16-2 was added to a solution of CS which had aggregated for 15 minutes (**Figure 19C**). The addition of HSP16-2 prevented further aggregation, but did not reduce the light scattering caused by the preformed CS aggregates. This behavior of HSP16-2 parallels that of bovine α-crystallin and *M. tuberculosis* HSP16.3 (Wang and Spector, 1994; Chang *et al.*, 1996).

The aggregation of proteins at high temperatures may involve unfolded intermediates which are different from those generated when the proteins are diluted into buffer from chaotropes such as urea or guanidine hydrochloride. We therefore examined whether HSP16-2 can prevent the aggregation of 6 M guanidine hydrochloride-denatured CS which occurs after 100-fold dilution of the chaotrope. HSP16-2 interacts with and stabilizes CS diluted from denaturant essentially as efficiently as it prevents the thermally-induced aggregation of CS (**Figure 19D**).

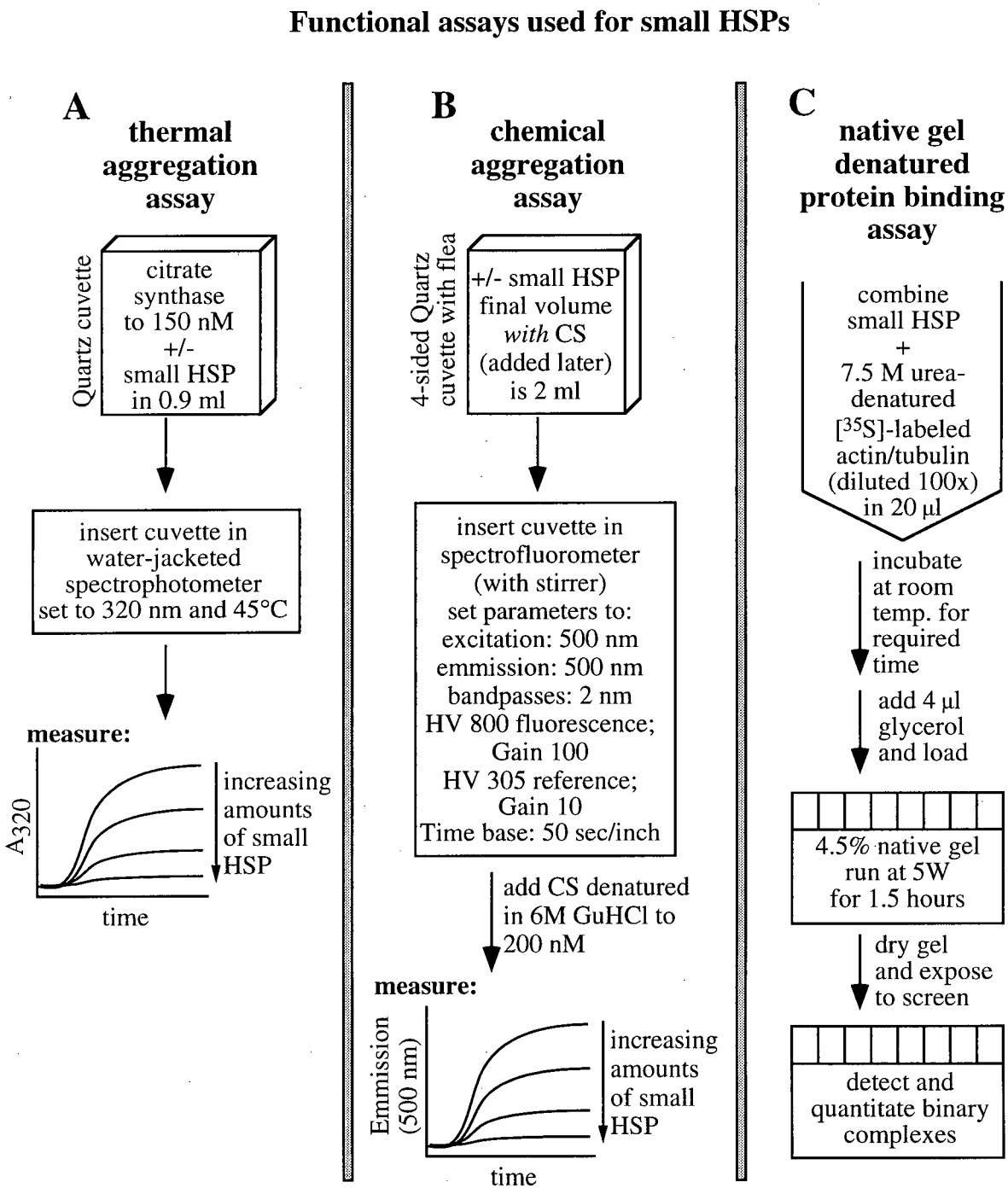

Figure 18. Three techniques for measuring the chaperone activity of smHSPs. **A.** Thermal aggregation assay using citrate synthase as substrate. **B.** Chemical aggregation assay using citrate synthase as substrate. **C.** Measuring binary complexes between smHSPs and labeled, denatured actin or tubulin on a native polyacrylamide gel.

3.1.4 Complex formation between HSP16-2 and denatured actin and tubulin

Although smHSPs have been shown to bind to and stabilize actin filaments (Bennardini *et al.*, 1992; Lavoie *et al.*, 1993b; Wang and Spector, 1996), detailed studies on the nature of the interaction between smHSPs and actin have not been reported. To further explore this property of smHSPs, we first investigated the formation of binary complexes between HSP16-2 and unfolded β-actin using a gel mobility assay. **Figure 20A** shows reactions in which urea-denatured [^{35}S]-labeled actin was diluted 100-fold into a solution with (lanes 1-4) or without (lanes 5 and 6) HSP16-2, or with HSP16-2 and a 2-fold molar excess of native BSA (lane 7), and separated on a non-denaturing gel. The denatured actin in reaction 4 was first incubated for 150 minutes before it was mixed with HSP16-2. The top panel of **Figure 20A** shows the Coomassie Blue-stained native gel (with the positions of the HSP16-2 complex and BSA indicated), and the bottom panel represents an autoradiogram of the same gel. In lanes 1-3, the binary (HSP16-2-actin) complex is visible, whereas if the actin is allowed to aggregate for 150 minutes before HSP16-2 is added, essentially no binary complex is detectable (lane 4). Reactions in which actin was incubated in the absence of HSP16-2 show only a trace of actin aggregates (lanes 5 and 6). The presence of a two-fold molar excess of BSA has no effect on binary complex formation between HSP16-2 and denatured actin (lane 7), indicating that HSP16-2 shows selective binding to unfolded polypeptide but not to native proteins.

The time course of binary complex formation between HSP16-2 and unfolded actin (**Figure 20B**) reveals that approximately 70% of the binary complexes are formed within the first minute of incubation. Interestingly, identical kinetic experiments performed with HSP16-2 and labeled, denatured β-tubulin gave very similar results (**Figure 20C**). This demonstrates that HSP16-2 has similar affinities for unfolded actin and tubulin, despite the fact that these proteins share no sequence homology. Melki and Cowan (1994) also showed that binary complexes between denatured actin and GroEL or HSP60 also formed very quickly (within 15 seconds). Although the binding of HSP16-2 to denatured actin is initially very rapid, it then proceeds with observable kinetics until a plateau is reached after about 20 minutes. The slower phase of binary

complex formation may indicate that the actin intermediates formed at later times are less well recognized by the smHSP or that the available binding sites become progressively saturated.

In light of the above results, the ability of HSP16-2 to interact with actin intermediates formed along the aggregation pathway was investigated. A constant amount of HSP16-2 was added to a reaction mixture containing actin which had been incubated alone in buffer for varying lengths of time. The binding reactions were allowed to proceed for 20 minutes, and then analyzed by native PAGE (**Figure 20D**). Under these conditions, the yield of binary complex formed decreased to almost zero over time. After a brief 2-minute pre-incubation of the actin alone, a significant proportion (about 25%) of the actin fails to form a complex with HSP16-2, and after a 5-minute pre-incubation, only approximately 50% of the actin is found in a binary complex, relative to the amount of actin bound to HSP16-2 in the absence of a pre-incubation. The same experiment with HSP16-2 and β-tubulin gave almost identical results (**Figure 20E**). It is noteworthy that the chaperonins HSP60 and CCT also have a decreasing ability to recognize actin intermediates which form during aggregation over the same time period (Melki and Cowan, 1994). Overall, the actin and tubulin binding studies suggest that HSP16-2 has a distinctly greater affinity for early refolding or aggregating intermediates but displays little protein specificity.

To complement the HSP16-2 actin and tubulin binding studies performed above, the affinity of HSP16-2 for actin and tubulin was further examined using fluorescently-labeled derivatives. These studies, presented in **Figure 21**, were carried out by Ronald Melki. Addition of increasing amounts of HSP16-2 to denatured pyrenyl-actin and DTAF-tubulin resulted in a quenching of the fluorescence of these proteins (**Figure 21A** and **B**). These data show that HSP16-2 binds to labeled, denatured actin and tubulin with a single association constant of 2.8×10^{-6} M^{-1}. The stoichiometry of binding appears to be 1:1. In contrast, addition of up to a 5-fold molar excess of HSP16-2 to the native pyrenyl- or NBD-labeled actin and DTAF-tubulin did not result in a quenching of the fluorescence of the labeled proteins. This demonstrates that HSP16-2 has an equally high affinity for unfolded actin and tubulin, but not for the native proteins.

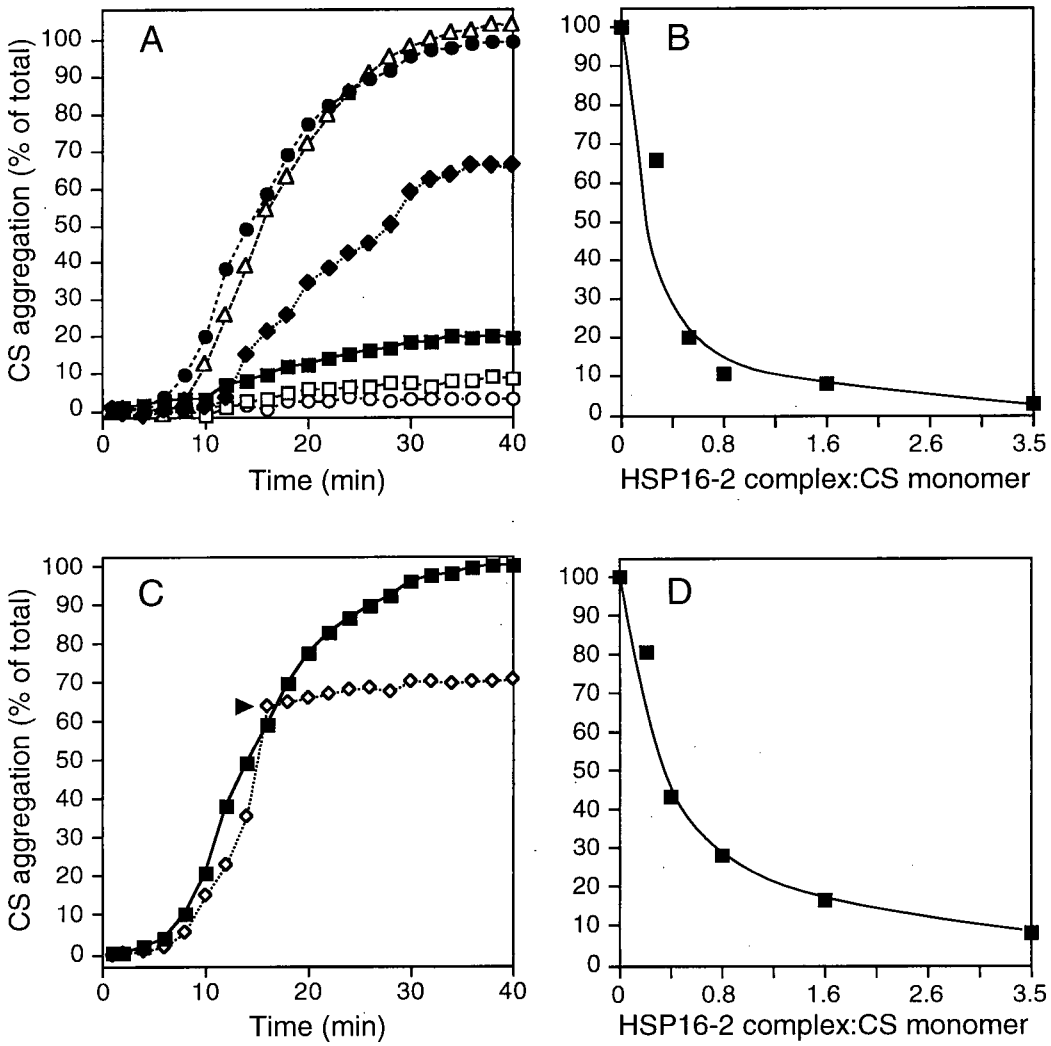

Figure 19. HSP16-2 prevents thermally- and chemically-unfolded CS from aggregating. **A.** Influence of various concentrations of the HSP16-2 oligomeric complex (O, 260 nM; □, 130 nM; ■, 85 nM; ◆, 44 nM; ●, 0 nM) and IgG (Δ, 300 nM) on the thermally-induced aggregation of CS (monomer concentration of 150 nM) at 45°C. **B.** Summary of data from the first panel, showing the ratio of HSP16-2 complex to CS monomers versus the % of CS aggregated after 40 min. **C.** Effect of no additions (■) or addition of HSP16-2 (to a final concentration of 525 nM, ◊) to a solution of CS (150 nM) which had aggregated for 15 minutes at 45°C (denoted by arrow). **D.** summary of the ability of various concentrations of HSP16-2 to prevent guanidine hydrochloride-denatured CS (200 nM) from aggregating when diluted into buffer at room temperature.

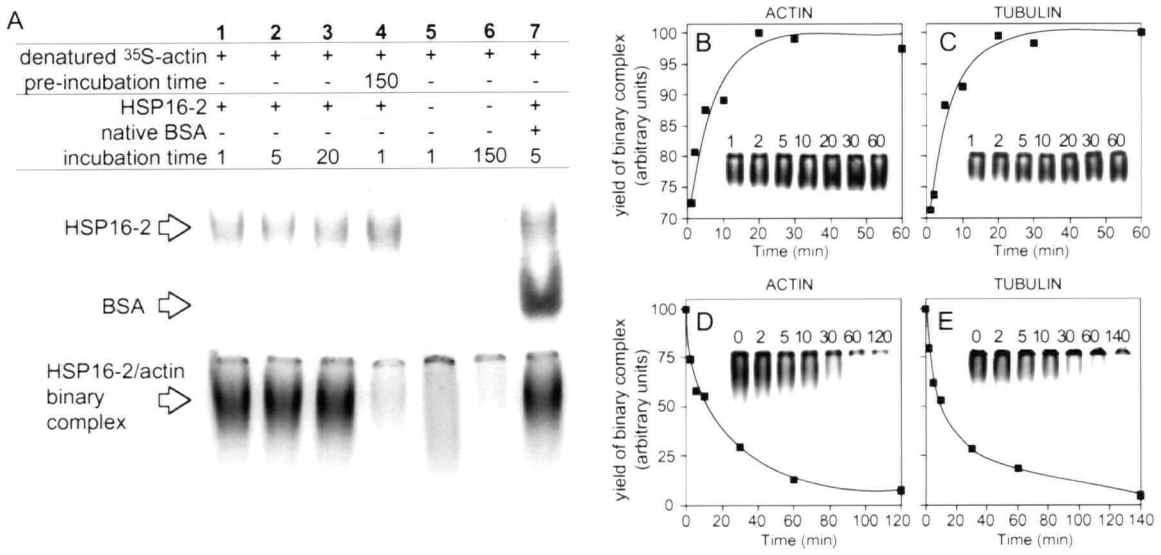

Figure 20. Binary complex formation between HSP16-2 and β-actin and β-tubulin. **A.** [^{35}S]-labelled, chemically-unfolded β-actin was diluted 100-fold into reactions containing HSP16-2 (lanes 1-3), no smHSP (lanes 5 and 6), or HSP16-2 and a two-fold molar excess of BSA (lane 7). Reactions were incubated for the times shown, and analyzed on a native gel. The upper panel shows the Coomassie-stained gel and the bottom panel is an autoradiogram of the same gel. Lane 4 shows the result of pre-incubating the unfolded actin before the addition of HSP16-2. The native HSP16-2 oligomeric species is indicated, as is native BSA. Binary complexes are shown in the autoradiogram. The kinetics of binary complex formation between HSP16-2 and β-actin (**B**) or β-tubulin (**C**) were measured by diluting the labelled, unfolded target proteins into reactions containing a fixed amount of HSP16-2, incubating for the times shown, and analyzing the reactions on native gels as in (A). The relative yields of binary complexes were quantified by phosphorimager. The binding of HSP16-2 to β-actin (**D**) or β-tubulin (**E**) intermediates formed on the aggregation pathway was measured by diluting the labelled, unfolded target protein into buffer alone, incubating for the times shown, and then adding a fixed amount of HSP16-2. Binding reactions were allowed to proceed for 20 minutes before analysis on native gels as before.

3.1.5 Chaperone assembly and activity is not affected by C-terminal deletion

The C-terminal extensions of smHSPs are variable in size and sequence, but often contain a region of limited similarity having the motif [R/K]-X-[I/V]-X-[I/V] (see **Figure 14** and **15C**). It was therefore of interest to determine whether the C-terminal extension of HSP16-2 (including the conserved motif RSIPI) plays a structural or functional role by studying the C-terminally-truncated $H_6\Delta$130-145 HSP16-2. Gel permeation chromatography of $H_6\Delta$130-145 HSP16-2 reveals that like H_6HSP16-2, the N-terminally-tagged variant forms a somewhat larger aggregate than wild-type HSP16-2, with an estimated M_r of 675 000 (**Figure 16B**).

Sedimentation velocity measurements of $H_6\Delta$130-145 HSP16-2 were also carried out (by R. Melki and G. Batelier), and the data agree with this smHSP variant having a large oligomeric size. The best theoretical fit of the sedimentation data was obtained assuming a two-component system involving a 12.8 S and a 17.6 S species with proportions of about 49% and 51%, respectively. The apparent molecular masses obtained for the two species are 322 and 520 kDa, which is consistent with oligomeric complexes consisting of approximately 17 and 28 subunits (**Appendix VIII**).

The ability of $H_6\Delta$130-145 HSP16-2 to protect CS from aggregation at an elevated temperature was then tested (**Figure 22**). Surprisingly, removal of the C-terminal extension has little or no influence on the chaperone function of HSP16-2: $H_6\Delta$130-145 is as effective as the wild-type smHSP in suppressing CS aggregation (compare with **Figure 19B**). In light of this data, it was expected that $H_6\Delta$130-145 HSP16-2 would have an affinity for denatured actin or tubulin. Indeed, results similar to those with wild-type HSP16-2 were obtained when $H_6\Delta$130-145 was added to pyrenyl-labeled actin (**Figure 21C**), demonstrating that the C-terminally-truncated smHSP interacts with unfolded polypeptides.

3.1.6 Correlation between multimerization and chaperone activity

Perhaps the most conspicuous feature of smHSPs is the presence of a nonconserved N-terminal domain which is highly variable in size. Three N-terminal truncations of HSP16-2, Δ1-15, Δ1-32, and Δ1-44 were used to probe the function of this domain.

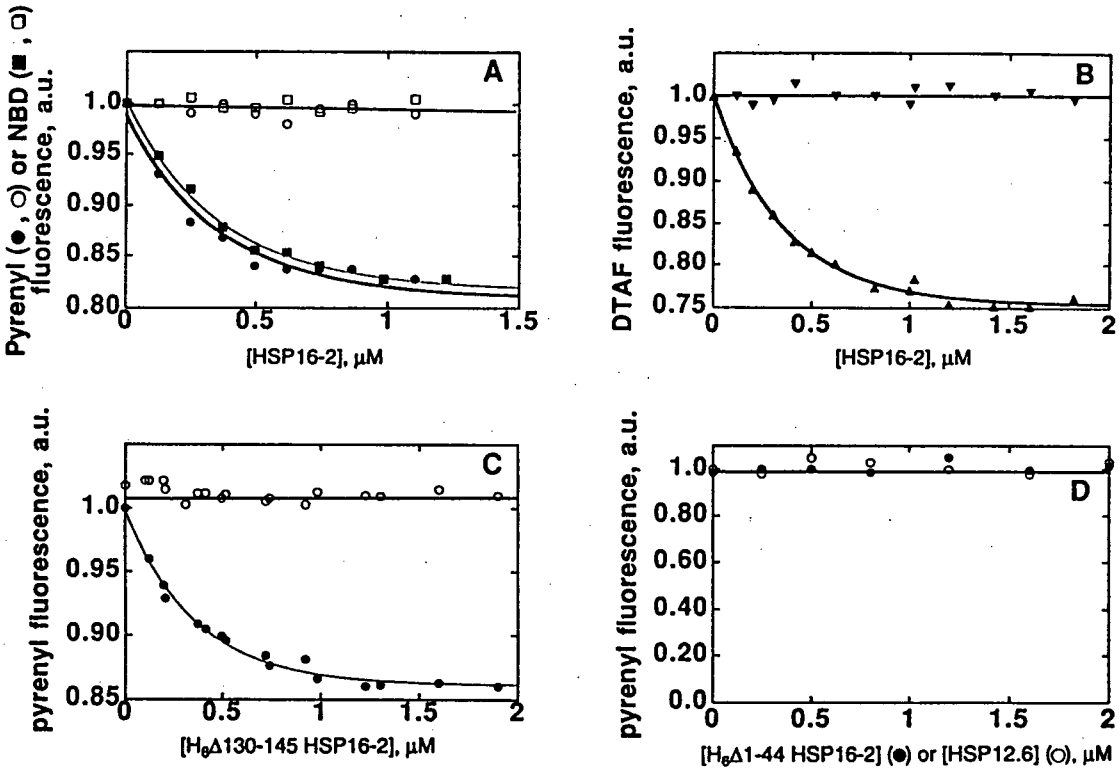

Figure 21. Fluorescence quenching studies. The quenching of pyrenyl, NBD and DTAF fluorescence upon binding of HSP16-2, $H_6\Delta$130-145 HSP16-2, $H_6\Delta$1-44 HSP16-2 and HSP12.6 to actin and tubulin in their native or denatured states was measured. **A.** increasing amounts of HSP16-2 were added to solutions of native (O) or urea-denatured (●) pyrenyl-actin and native (□) or denatured (■) NBD-actin in 5 mM Tris-HCl, pH 7.8, 0.2 mM DTT, 0.2 mM ATP, 0.1 mM $CaCl_2$. **B.** increasing amounts of HSP16-2 were added to solutions of native (▼) or urea-denatured (▲) DTAF-tubulin in 0.1 M PIPES, pH 6.9, 1 mM EGTA, 0.5 mM $MgCl_2$ and 1 mM GTP. **C.** increasing amounts of $H_6\Delta$130-145 HSP16-2 were added to a solution of native (O) or urea-denatured (●) pyrenyl-actin. (**D**) increasing amounts of $H_6\Delta$1-44HSP16-2 (●) or HSP12.6 (O) were added to a solution of urea-denatured pyrenyl-actin. The concentration of actin and tubulin solutions was 1 μM. The fluorescence was recorded after each addition as described in *Materials and Methods.* (Figure kindly provided by Ronald Melki).

To examine the quaternary structure of these N-terminal truncations as well as of other HSP16-2 derivatives, the purified proteins were subjected to chemical cross-linking using the homobifunctional cross-linker bis (sulfosuccinimidyl) suberate (BS^3) (Staros, 1982). To minimize nonspecific intermolecular cross-linking of non-oligomerized smHSP subunits, cross-linking reactions were carried out in the presence of low protein (1.5 μM monomer) and BS^3 (2 mM) concentrations, and a 10-fold molar excess of BSA (15 μM). Reactions were analyzed by Western blotting with an anti-HSP16-2 polyclonal antibody (**Figure 23**). All of the proteins yielded discernible monomeric, dimeric, and trimeric species. From the large number of products present in the high-MW range (above 100 kDa and at the origin of the separating gel), it can be concluded that the HSP16-2, H_6HSP16-2, and $H_6\Delta$130-145 proteins also form higher-order oligomeric structures which are too large to be well resolved on the 12% SDS-gel. These finding are consistent with the behaviour of these proteins as high-MW oligomers as judged by size exclusion chromatography and sedimentation velocity measurements. In contrast, the $H_6\Delta$1-15, $H_6\Delta$1-32, and $H_6\Delta$1-44 HSP16-2 proteins yielded essentially no high-MW cross-linked products but could be cross-linked to trimers (and possibly tetramers), suggesting that they exist as small aggregates. The presence of the N-terminal H_6 tag in each of these truncated proteins is unlikely to have resulted in disruption of the multimers since both H_6HSP16-2 and $H_6\Delta$130-145 HSP16-2 are able to form large oligomeric complexes.

The sizes of the N-terminally-truncated smHSPs were estimated by gel permeation chromatography on a Sephacryl S-300HR column. These smHSP derivatives elute as particles of 45-115 kDa (**Figure 16B**), and therefore appear to form small aggregates of trimers-heptamers. These results resemble those obtained on the C-terminal domains of αA-, αB-crystallin, and HSP25 . Removal of the N-terminal domains of these smHSPs resulted in dimers, tetramers, and higher-order multimers, based on size exclusion and cross-linking data (Merck *et al.*, 1992, 1993b).

In order to determine the true subunit stoichiometry of one of the truncated smHSPs, $H_6\Delta$1-44 HSP16-2, sedimentation velocity measurements were performed (by R. Melki and

G. Batelier). The sedimentation velocity data are best fitted by a two-component system involving 1.66 S and 4.0 S species. The apparent molecular masses obtained from the data are 15 and 56 kDa, consistent with the behaviour of $H_6\Delta$1-44 HSP16-2 as a monomer (95%) with a small proportion (5%) of tetramers (**Appendix VIII**)

Since the N-terminally-truncated smHSPs did not form wild-type-like oligomeric complexes, it was of interest to determine whether they still possessed molecular chaperone activity. The three derivatives were therefore tested for the ability to prevent thermally- or chemically-induced aggregation of CS. None of these smHSPs was effective in suppressing CS aggregation, even at a molar excess of 65 molecules of smHSP to 1 CS monomer (not shown). Furthermore, $H_6\Delta$1-44 HSP16-2 did not quench the fluorescence of denatured forms of pyrenyl-actin (**Figure 21D**).

3.2 Structure, function and expression of HSP12.6

3.2.1 A novel class of small HSPs from *C. elegans*

The advent of whole genome sequencing projects has resulted in a tremendous amount of information becoming rapidly available, which facilitates comparative studies of large multigene families. Caspers *et al.* (Caspers *et al.*, 1995) first reported the existence of an unusually diminutive smHSP which was uncovered by the *C. elegans* genome sequencing consortium (Wilson *et al.*, 1994). More recently, three additional closely related members in the genome sequence were identified.

These four smHSP genes encode proteins of 12.2-12.6 kDa (109 and 110 amino acids) which are highly similar to each other throughout their entire length (42-67% amino acid sequence identity), as shown in **Figure 24A**. The alignment also outlines the similarity between the α-crystallin domain of the *C. elegans* HSP12s and several other smHSPs. Compared with all other known smHSPs, the HSP12 proteins have the shortest N- and C-terminal regions, and represent a novel class of smHSPs. Previously, the smallest known member of the smHSP family was *E. coli* IbpA, at 15.8 kDa.

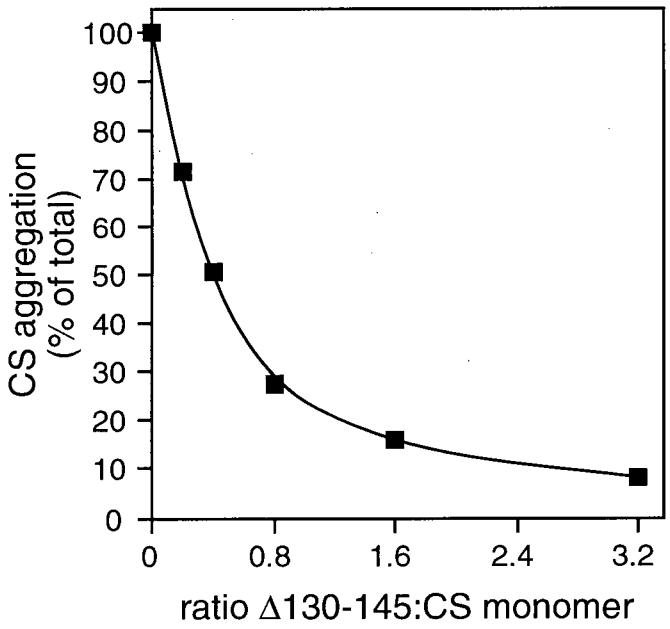

Figure 22. HSP16-2 lacking most of its C-terminal extension has chaperone activity. Summary of the $H_6\Delta$130-145 HSP16-2 concentration-dependent suppression of aggregation of a 150 nM (monomer) CS solution incubated at 45°C. Aggregation assays were carried out for 40 minutes, and are normalized with respect to a control incubation with CS alone (100% of total CS aggregation).

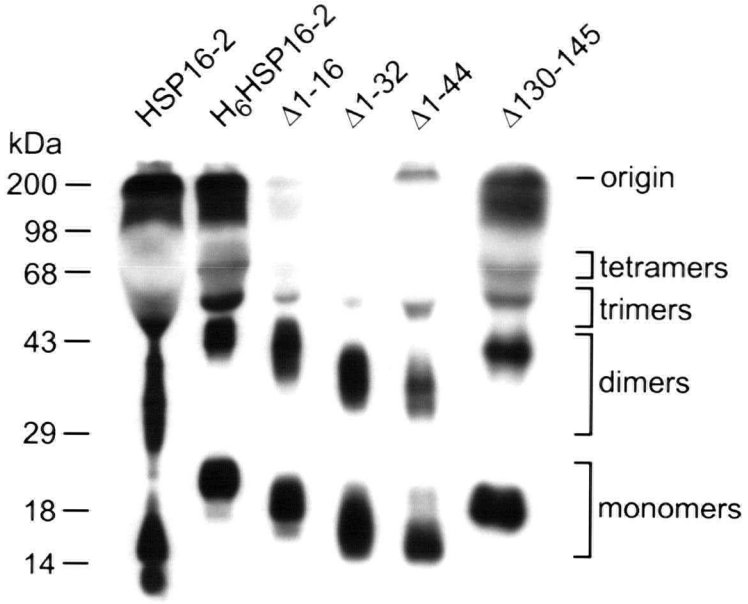

Figure 23. Chemical cross-linking of smHSPs. Samples of HSP16-2 and five derivatives were cross-linked with the cross-linking agent BS^3, electrophoresed on a 12% SDS-gel, transferred to a PVDF membrane, and probed with an anti-HSP16-2 antibody. Monomers and cross-linked products corresponding to dimers, trimers, and tetramers are indicated. The separating gel origin is also shown.

The predicted secondary structures of the α-crystallin domain of the *C. elegans* HSP12 and HSP16-2 smHSPs, and murine αB-crystallin are nearly identical, consisting almost exclusively of β-sheets (**Figure 24B**); this observation is consistent with the >90% β-sheet structure predicted for various smHSPs by circular dichroism studies (Merck *et al.*, 1993a, 1993b). The notion that the HSP12 proteins are evolutionarily related to other smHSPs is further supported by the presence of introns at conserved positions (**Figure 24C**). In particular, the intron which delineates the N-terminal region from the α-crystallin domain is found in three of the HSP12 genes, as well as in murine αB-crystallin, and many other *C. elegans* smHSPs, including HSP16-2 (**Figure 24C**). The *hsp12* multigene family can be inferred to have arisen by gene duplications and gains/losses of introns. For example, the genes encoding HSP12.6 and HSP12.3 are more similar to each other (67% amino acid sequence identity) than to either C14B9.1 or T22A3.2 (42-48% pairwise identity), and are found duplicated approximately 1000 bp apart in a head-to-tail orientation on chromosome IV. Similarly, the genes encoding T22A3.2 and C14B9.1, which are present on different chromosomes (I and III, respectively), are also more closely related to each other (63% identity), and share an intron near a location corresponding to the second intron of the murine αB-crystallin gene.

3.2.2 Cloning, expression, and purification of HSP12.6

To characterize the structural and functional properties of the HSP12 class of smHSPs from *C. elegans*, HSP12.6 was cloned from first-strand cDNA by PCR. Both wild-type and polyhistidine-tagged HSP12.6 (H_6HSP12.6) were overexpressed in *E. coli* from a T7 promoter, producing soluble protein in each case. HSP12.6 was purified by size exclusion and hydroxylapatite chromatography, and H_6HSP12.6 was purified by Ni^{2+}-chelate affinity chromatography (**Figure 25**). The gene encoding HSP12.3 (67% identity to HSP12.6) was also cloned by PCR (using the primers HSP13B.5 and HSP13B.3; see **Appendix II**), overexpressed in *E. coli*, and used to assess the specificity of the anti-HSP12.6 pAb; it was found that recombinant HSP12.6 and HSP12.3 are detected with similar efficiency in Western blots (see **Appendix VII**).

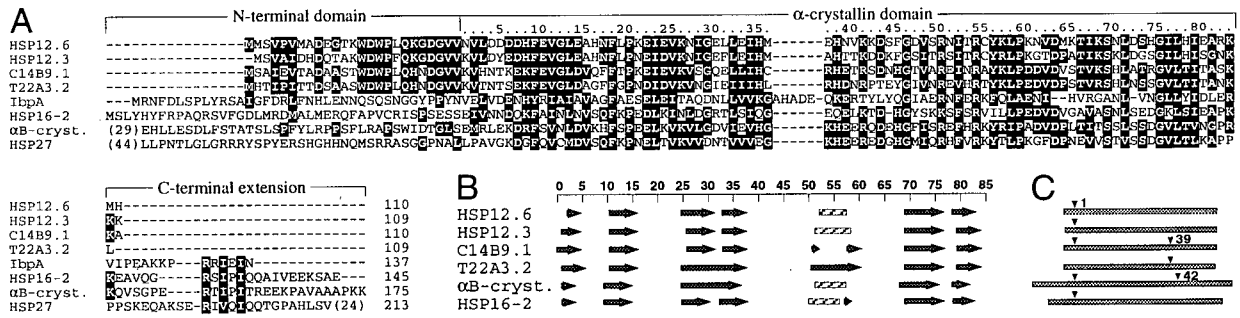

Figure 24. Comparison of the *C. elegans* HSP12 protein family with other smHSPs. **A.** an alignment of the four *C. elegans* HSP12 proteins and other selected smHSPs (Genbank accession numbers in parentheses): *C. elegans* HSP12.6, also referred to as F38E11.2 (Z68342 and U92044), HSP12.3, also referred to as F38E11.1 (Z68342), C14B9.1 (L15181), T22A3.2 (Z81125); *E. coli* IbpA (M94104); *C. elegans* HSP16-2 (M14334); murine αB-crystallin (M73741); *Drosophila* HSP27 (J01101). Conserved residues present in at least four of the smHSPs are highlighted. The α-crystallin domain residues are numbered for reference. The total number of amino acids in each smHSP is indicated at the end of the sequences, and numbers in parentheses represent smHSP residues not shown in the alignment. **B.** secondary structures of the four HSP12 proteins, αB-crystallin, and HSP16-2, as predicted by the program PHD; arrows represent β-sheets and striped bars α-helices. The scale parallels the α-crystallin domain numbering scheme. **C.** the intron positions of the genes shown in B are indicated by an arrow and follow the codon corresponding to the numbered α-crystallin domain amino acid residues.

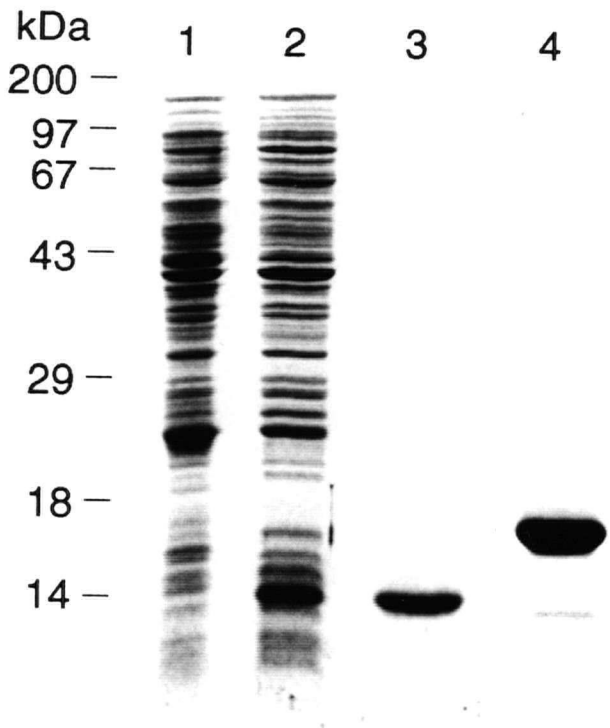

Figure 25. Overexpression in *E. coli* and purification of HSP12.6. **A.** Polyacrylamide gel electrophoresis of various protein samples on a 13.5% SDS-gel. Lane 1, uninduced BL21(DE3) soluble protein extract; lane 2, soluble fraction of BL21(DE3) expressing recombinant wild-type HSP12.6; lane 3, HSP12.6 purified by size exclusion and hydroxylapatite chromatography; lane 4, recombinant HSP12.6 containing N-terminal polyhistidine tag (H_6HSP12.6) purified by Ni^{2+}-chelate affinity chromatography, and used for antibody production.

3.2.3 The expression of HSP12.6 is developmentally regulated

The developmental expression pattern of *hsp12.6* in *C. elegans* was examined at the protein level using polyclonal antibodies raised against the purified H_6HSP12.6 protein. Western blots of total protein extracts from the major *C. elegans* developmental stages (embryo, larval, and adult stages) were probed with the anti-HSP12.6 pAb. Surprisingly, a cross-reacting polypeptide of approximately 13 kDa was detected only in the first larval (L1) stage (**Figure 26**). It is possible that the closely-related HSP12.3 smHSP is also recognized by the pAb and is likewise present only in the L1-stage, as a slightly smaller cross-reacting species of the same size as recombinant HSP12.3 is sometimes visible (see **Figure 28**).

Interestingly, the production of HSP12.6 is not appreciably augmented when *C. elegans* is exposed to a variety of stressors known to induce the expression of *hsp16* genes, including heat shock, heavy metals, and alcohols (Brian Ma, personal communication).

3.2.4 The quaternary structure of HSP12.6 differs from that of other smHSPs

As noted above, smHSPs thus far examined form large oligomeric assemblies. The native size of HSP12.6 was therefore examined by size exclusion chromatography. Interestingly, HSP12.6 eluted from a Sephacryl S-200HR column near chymotrypsinogen A (25 kDa), with an estimated MW of 23 kDa (**Figure 27A**). Given a calculated MW of 12.6 kDa, this experiment suggested that HSP12.6 exists as a dimer of ~25 kDa.

The oligomeric nature of HSP12.6 was further probed using the homobifunctional cross-linker BS^3, in the absence or presence of BSA competitor. At a relatively high concentration of HSP12.6 (1 μM) without competitor protein, a dimer and a few higher-MW cross-linked products were detected by Western blotting (**Figure 27B**, lane 1). In the presence of BSA (lane 2), however, a significally smaller amount of dimer product was formed, suggesting that non-specific cross-linking of HSP12.6 occurs at this concentration in the absence of competitor When a lower concentration of HSP12.6 was used (0.25 μM), little or no dimer product was seen with or without competitor (lanes 3 and 4), suggesting that HSP12.6 is monomeric, and that its behavior on the size exclusion matrix may be due to a non-globular conformation.

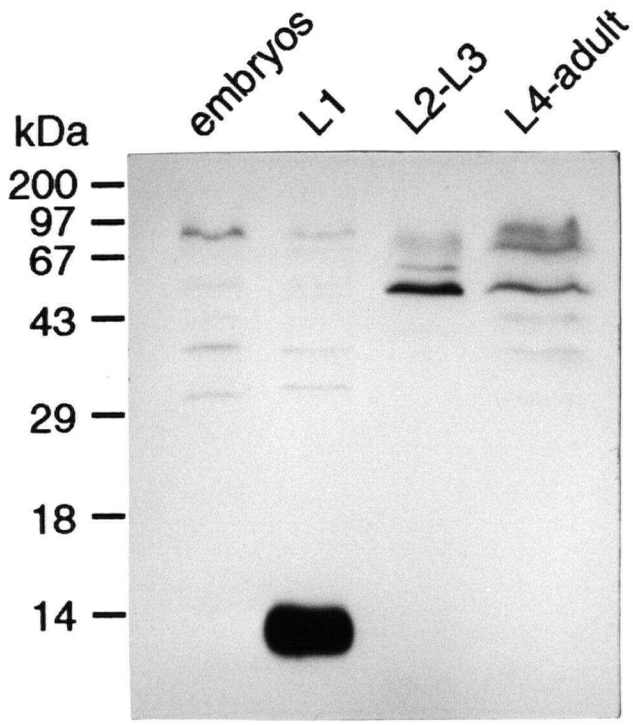

Figure 26. HSP12.6 is present in *C. elegans* L1 larvae. Total protein extracts (20 µg) from *C. elegans* embryos, first larval stage (L1), a mixture of second and third larval stages (L2-L3), and mixed fourth larval and adult stages (L4-adult) were separated on a 13.5% SDS-gel, transferred to a PVDF membrane, and probed with the antibody against HSP12.6. The antibody cross-reacts strongly with HSP12.6 in the L1 stage (prominent band near the 14 kDa marker).

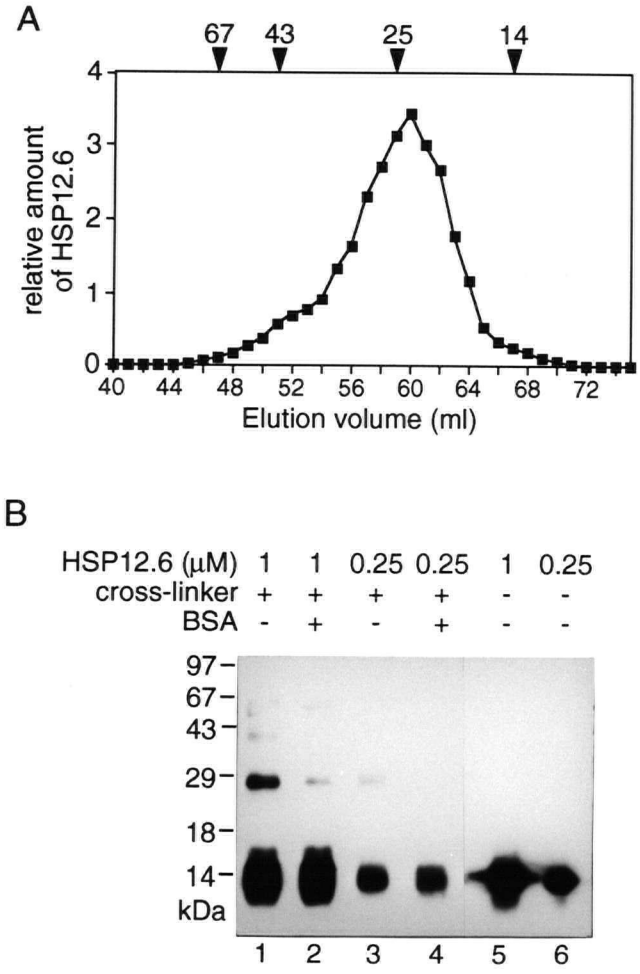

Figure 27. Size exclusion chromatography and cross-linking of HSP12.6. **A.** the native size of HSP12.6 was estimated by size exclusion chromatography on a Sephacryl S-200HR column. The elution volumes of the MW standards BSA (67 kDa), ovalbumin (43 kDa), chymotrypsinogen A (25 kDa), and ribonuclease A (14 kDa) are indicated above the graph. **B.** HSP12.6 was incubated with 2 mM BS^3 cross-linker for 30 minutes in the presence or absence of 15 μM BSA competitor (lanes 1-4). Control reactions without cross-linker were also carried out (lanes 5 and 6). All reactions were then analyzed by Western blotting with the antibody against HSP12.6.

To determine whether the elution behavior of HSP12.6 from a size exclusion column is due to dimerization or to an extended, non-globular conformation, sedimentation velocity experiments were carried out (by R. Melki and G. Batelier). The sedimentation data best fits a monomer model involving a 1.43 S species, which corresponds to a molecular mass of 12.2 kDa. The frictional ratio values (f/f_0) suggest that HSP12.6 is asymmetrical (**Appendix VIII**).

3.2.5 The *in vivo* M_r of HSP12.6 is identical to that of the recombinant protein

The size of HSP12.6 isolated from *C. elegans* L1 larvae was estimated by size exclusion chromatography of a protein extract on an S-200HR column under the same conditions used for recombinant HSP12.6. It was found that the endogenous HSP12.6 elutes as a single peak corresponding to a molecular mass of approximately 25 kDa (**Figure 28**). Based on the behavior of the recombinant protein on a sizing column, it is clear that the oligomeric structures of the natural and recombinant proteins are identical.

3.2.6 HSP12.6 may be functionally distinct from other smHSPs

Although the exact role of oligomeric assembly in the function of smHSPs is unclear, it is likely to be important given its ubiquitous nature. Since HSP12.6 is likely to be monomeric, it was of interest to determine whether it might still be functional as a molecular chaperone. HSP12.6 was therefore tested for the ability to prevent the aggregation of thermally-unfolded citrate synthase (CS). Contrary to other smHSPs and molecular chaperones in general, HSP12.6 has no significant effect on temperature-induced CS aggregation, even when present at a 225-fold molar excess over CS (**Figure 29**). However, the kinetics of CS aggregation were somewhat slowed in the presence of the large excess of HSP12.6, probably due to nonspecific stabilization of the denaturing CS by the additional protein, as shown by Zhi *et al.* (1992). To ensure that the assay conditions were optimal, a parallel experiment was performed using H_6HSP16-2. Addition of this protein effectively suppressed CS aggregation.

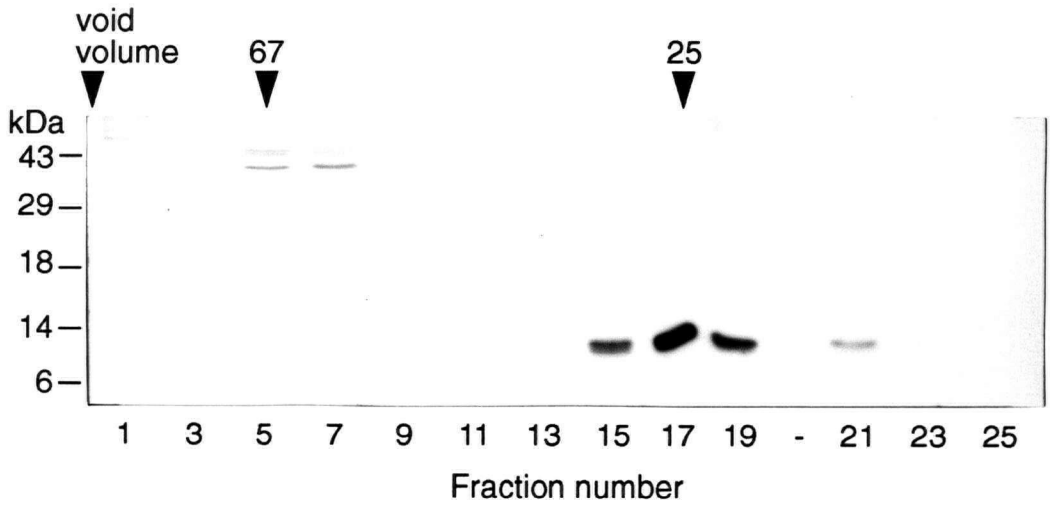

Figure 28. Size determination of HSP12.6 isolated from *C. elegans*. A protein extract from *C. elegans* first-stage larvae was prepared and chromatographed on a Sephacryl S-200HR column calibrated with the protein standards BSA (67 kDa) and chymotrypsinogen A (25 kDa). Fractions eluting after the void volume were Western-blotted using the anti-HSP12.6 pAb. Note the presence of two cross-reacting species which have slightly different elution profiles and therefore are partially resolved in certain fractions: the upper band is the same size as recombinant HSP12.6 and is visible in fraction 21; the lower band corresponds to the same size as recombinant HSP12.3 (see text) and is distinguishable as a single species in lane 13 (lane 15, in comparison, shows both upper and lower cross-reacting polypeptides). See **Appendix VII** for pAb specificity against HSP12.6 and HSP12.3.

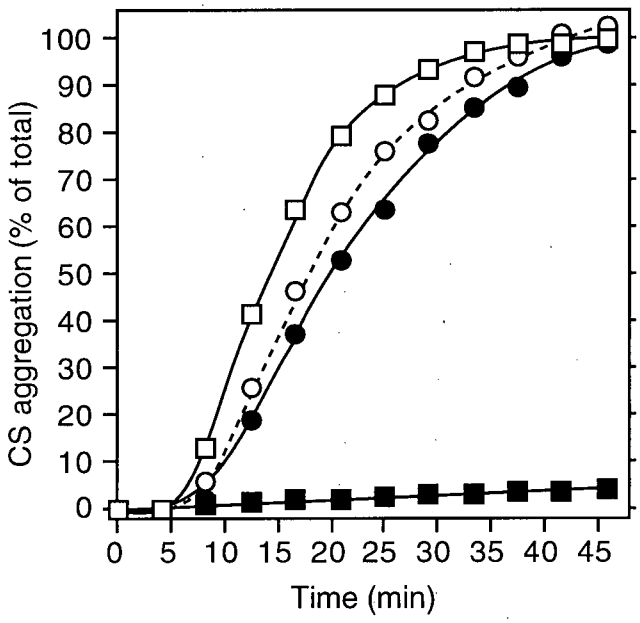

Figure 29. HSP12.6 lacks molecular chaperone activity. The effect of HSP12.6 and H_6HSP16-2 on the aggregation of a 150 nM solution of citrate synthase (CS) incubated at 45°C. The aggregation curves shown are of CS incubated alone (□), CS incubated with a 40-fold molar excess of HSP12.6 (O), CS incubated with a 225-fold molar excess of HSP12.6 (●), and CS incubated with a 60-fold molar excess of H_6HSP16-2 (■) as a positive control. HSP12.6, H_6HSP16-2, and CS concentrations refer to monomers. An experiment with a 1:1 ratio of CS to HSP12.6 gave results identical to that of CS incubated alone.

IV. DISCUSSION

The discovery by Ingolia and Craig in 1982 that four small *Drosophila* HSPs were related in sequence to the well-studied but poorly understood α-crystallins found in eye lenses hinted at the importance and ubiquitous nature of this class of proteins. Later studies (Caspers *et al.*, 1995) and recent whole-genome sequencing projects (Bult *et al.*, 1996) have identified smHSPs in the three Kingdoms of life, and have demonstrated their presence in a wide variety of tissues in multicellular eukaryotes in the presence and absence of stress (Stringham *et al.*, 1992; Arrigo and Landry, 1994; Groenen *et al.*, 1994; Caspers *et al.*, 1995; Waters *et al.*, 1996). The smHSPs are likely to play key roles during both normal development and particularly when organisms are subjected to environmental stressors.

The *C. elegans* HSP16s are among the smallest members of the α-crystallin family of HSPs, and it is reported here that they possess the multimeric structure and chaperone activities typical of these proteins. Very few mutational studies have been carried out on smHSPs, and these have concentrated mainly on mammalian α-crystallins (Merck *et al.*, 1992, 1993b; Smulders *et al.* 1995, 1996; Plater *et al.*, 1996). The present studies on HSP16-2 represent the most extensive structure-function analysis of a stress-inducible smHSP reported to date. The small size of the HSP16s is an advantage in such studies, and the combination of *in vitro* mutagenesis with the functional chaperone assays and substrate binding measurements reported here provide a number of important insights into the structure and function of smHSPs.

Structure of smHSPs

Many molecular chaperones are active as homo- or hetero-oligomers, requiring multiple subunit contacts with the unfolded polypeptide for activity. Chaperonins such as GroEL, HSP60, and CCT have characteristic bitoroidal structures containing 7-9 identical or related subunits per ring (reviewed in Hartl, 1996). The eukaryotic HSP104 and bacterial Clp homologues assemble into similar multimeric ring complexes (reviewed in Schirmer *et al.*, 1996). SmHSPs also form large oligomeric assemblies of one or two types of subunits, but their quaternary structures are remarkably variable. Thus, cardiac α-crystallin has been reported to exist as a torus resembling

that of chaperonins (Longoni *et al.*, 1990) whereas other vertebrate α-crystallins and smHSPs assemble into roughly globular particles of various sizes and shapes and contain 32-42 subunits (Behlke *et al.*, 1991; Groenen *et al.*, 1994); *M. tuberculosis* HSP16.3 forms a trimer of trimers particle (Chang *et al.*, 1996); lastly, two plant smHSPs were shown to form globular, or mixed globular and triangular structures of 12 subunits (Lee *et al.*, 1995). The analyses of wild-type HSP16-2 and various derivatives demonstrate that the N-terminal domain of smHSPs is required for subunit assembly and is buried within an aggregate which is highly accomodating for N-terminal regions of different sizes and compositions.

Recombinant wild-type HSP16-2 readily assembles into large oligomeric assemblies resembling those of the natural protein, and of ~550 kDa as estimated by size exclusion chromatography. Sedimentation velocity measurements reveal that HSP16-2 forms heterogeneous mixtures of two particles of 238 and 412 kDa, suggesting that the number of subunits per complex is approximately 14 and 24, respectively. The reason for the size discrepancy between the two techniques is unclear; it is possible that the HSP16-2 aggregates are loosely packed, or that they are non-globular. Interestingly, a similar apparent dichotomy exists for mammalian HSP27, which by size exclusion behaves as an ~800 kDa oligomer, whereas by native gel electrophoresis migrates as a doublet of approximately 200 and 250 kDa (Lavoie *et al.*, 1995). In sucrose gradients, HSP27 sediments as two distinct forms, one of 300-400 kDa and another of <70 kDa, depending on the phosphorylation state (Kato *et al.*, 1994). It is possible that the various smHSP species are in slow equilibrium with each other.

The H_6HSP16-2 variant, which forms active oligomeric complexes essentially indistinguishable from wild-type HSP16-2, was used to determine the orientation of the HSP16-2 monomers within the complex. It was found that the 4-kDa N-terminal H_6 tag was inaccessible for binding to a Ni^{2+}-chelate affinity matrix. Thus either the tag is collaterally positioned in the complex and masked by the HSP16-2 protein and neighbouring subunits (which would very likely have a detrimental effect on the assembly of the complex), or, more likely, the tag is accommodated within a central cavity in the complex. It is therefore very likely

that the N-terminal domain of HSP16-2 is oriented toward the interior of the complex. Also, the fact that HSP16-2 can accomodate an additional 4 kDa (36 residues) at its N-terminus, making this domain larger than those of α-crystallins and *Drosophila* HSP27, and only 8 residues shorter than that of murine HSP25 (refer to the alignment in **Figure 15C**), suggests that the arrangement of subunits within smHSP complexes provides considerable freedom for N-terminal regions of different lengths and amino acid sequence. Indeed, the alternatively-spliced αA^{ins}-crystallin variant which contains a 23-residue insertion near the N-terminal/α-crystallin domain boundary also has structural properties comparable to that of wild-type αA-crystallin, although its chaperone activity is somewhat reduced (Smulders *et al.*, 1995).

Merck *et al.* (1992) reported that the isolated N-terminal domain of α-crystallin formed large aggregates, while the removal of the entire N-terminal domain from α-crystallin largely abrogated multimerization, suggesting that this domain is important for subunit assembly. Interestingly, it was also shown that the C-terminal region (α-crystallin domain and C-terminal extension) of αA-, αB-crystallin, and HSP25 independently formed dimers, tetramers, or higher oligomers (Merck *et al.*, 1992, 1993b). The present work shows that deletion of only approximately one-third (15 residues) of the N-terminal domain of HSP16-2 results in a dramatic reduction in the size of the complex as judged by size exclusion chromatography and cross-linking analysis, suggesting that the region involved in multimerization may be distally located in the N-terminal domain. It is therefore conceivable that the HSP16-2 monomer has an extended conformation with the N-terminal region oriented toward the interior of the complex and provides the necessary contacts for subunit aggregation. In support of this hypothesis, HSP12.6, which has 16 fewer residues than HSP16-2 in the N-terminal region, is monomeric and predicted to be asymmetrical by sedimentation velocity analysis.

The studies by Merck *et al.* (1992, 1993b) suggest the existence of at least two major sites of interaction between smHSP monomers: one within the N-terminal domain, which permits the assembly of the complex, and the other in the C-terminal domain, which appears to have an inherent ability to form smaller oligomers. Chang *et al.* (1996) found that mycobacterial

HSP16.3 nonamers could be disassembled into trimers by treatment with 4 M urea or 1 M guanidine hydrochloride, also suggesting two different types of subunit interactions—one involved in trimer formation and another involved in trimer oligomerization. The data presented here lend further support to this notion, as removal of all or part of the HSP16-2 N-terminal domain prevents the formation of the native complex, but apparently permits the assembly of smaller oligomers: the estimated sizes of the truncated smHSPs are 45-115 kDa, and all cross-link to at least trimers. On the other hand, the sedimentation velocity measurements of $H_6\Delta$1-44 HSP16-2 and HSP12.6, which possess complete α-crystallin domains, reveal that these proteins are monomeric, with the exception that a small percentage of the $H_6\Delta$1-44 HSP16-2 (5%) assembles into tetramers. It is therefore possible that all N-terminally-truncated smHSPs are monomeric and are in equilibrium with higher-order oligomeric species. Sedimentation velocity and cross-linking analyses of HSP16-2 and other smHSP derivatives containing only the α-crystallin domain and C-terminal extension would help to determine whether this region has an intrinsic ability to oligomerize.

The removal of the last 16 residues of HSP16-2 has no effect on multimerization, but decreases the solubility of the complex significantly. Over 90% of $H_6\Delta$130-145 HSP16-2 precipitates from solution after freeze-thawing, while wild-type HSP16-2 and H_6HSP16-2 remain completely soluble following the same treatment (not shown). Similarly, a role for the C-terminal extension in the solubilization of α-crystallin particles has recently been documented (Smulders *et al.*, 1996). It has also been shown by ^{1}H NMR studies that the last 8-10 and 18 C-terminal residues of α-crystallins and HSP25, respectively, form flexible extensions (Carver *et al.*, 1992, 1995a). Accordingly, it seems likely that the C-terminal extension in HSP16-2 is on the surface of the complex and exposed to solvent, where it imparts increased solubility to the complex.

Augusteyn and Koretz (1987) proposed that α-crystallin forms micelle-like structures, with the hydrophobic N-terminal domain buried inside and providing the driving force for subunit aggregation. The structural studies presented here on HSP16-2 are entirely consistent with the

micellar-like aggregate model (Tardieu *et al.*, 1986; Wistow, 1993), and further demonstrate the inherent heterogeneity in the quaternary structures of many smHSPs.

Function of smHSPs

Under stress conditions, heat shock proteins such as HSP60, HSP70, HSP90, and smHSPs likely prevent partially unfolded proteins from aggregating and becoming insoluble (Martin *et al.*, 1992; Horwitz, 1992; Jakob *et al.*, 1993, 1995; Freeman and Morimoto, 1996). Whereas most HSPs perform necessary functions in non-stressed cells and are also induced following cellular insults (Gething and Sambrook, 1992; Parsell and Lindquist, 1994; Arrigo and Landry, 1994), the *C. elegans* HSP16-class smHSPs are produced exclusively when nematodes are exposed to a heat shock or to proteotoxic agents (Jones *et al.*, 1986, 1996). The present studies on HSP16-2 confirm the ability of this class of smHSPs to interact with and stabilize proteins which become unfolded following heat or chemical treatment. The HSP16s therefore likely constitute specialized smHSP chaperones that protect cells by stabilizing proteins which become structurally compromised during stress conditions.

It is noteworthy that in eukaryotes, cytoskeletal proteins are one of the most sensitive targets of cellular stresses, and there is increasing evidence that smHSPs specifically interact with cytoskeletal elements, modulating their dynamic nature, and protecting them during stress conditions (Welch and Suhan, 1985; Chiesi *et al.*, 1990; Bennardini *et al.*, 1992; Lavoie *et al.*, 1993a, 1993b, 1995; Nicholl and Quinlan, 1994). It was shown that the affinity of HSP16-2 for native actin and tubulin is negligible, whereas it is very high for the same thermally- or chemically-unfolded proteins. Similarly, the interaction of cardiac αB-crystallin with actin and desmin filaments was shown to be enhanced during ischemic conditions, where a decrease in the pH of the cytosol is known to affect the stability of cytoskeletal elements (Bennardini *et al.*, 1992). Interestingly, HSP16-2 has nearly identical affinities for actin and tubulin, and can also prevent the aggregation of citrate synthase, suggesting that this chaperone may have a general affinity for unfolded proteins *in vivo*. Other smHSPs also display little protein specificity,

preventing the aggregation of numerous proteins. Thus, whether smHSP chaperones have specialized roles in protecting the cellular cytoskeleton network during stresses remains to be seen.

Linder *et al.* (1996) reported on a novel 18-kDa *C. elegans* protein highly similar to the HSP16 smHSPs and named SEC-1 (for Small Embryonic Chaperone-1) (see **Figure 15C** alignment for sequence). SEC-1 is detectable only during early embryogenesis, where it performs an essential but unknown function. Interestingly, SEC-1 confers thermotolerance to *E. coli*, even though its expression is not augmented by environmental stresses. Therefore, although the physiological functions of this smHSP are not redundant with those of the stress-inducible HSP16s, it is likely that both possess similar structural and functional characteristics as molecular chaperones.

Recent data suggest that α-crystallin preferentially interacts with thermally-generated early unfolding intermediates which have exposed hydrophobic regions and are committed to the aggregation pathway (Carver *et al.*, 1995b; Das *et al.*, 1996; Rajaraman *et al.*, 1996). In agreement with this notion, α-crystallin does not interact with largely unfolded but stable proteins (*e.g.*, reduced and carboxymethylated α-lactalbumin and α-casein) (Carver *et al.*, 1995b), or prevent the aggregation of chemically-denatured rhodanese which occurs following dilution into buffer, even at a three-fold molar excess of oligomer over unfolded substrate (Das and Surewicz, 1995). This unusual characteristic of α-crystallin is intriguing, since other molecular chaperones (*e.g.*, HSP90, HSP70, HSP60, and HSP40) can interact with and stabilize such unfolded intermediates (Hartl, 1996; Wiech *et al.*, 1992). The present study demonstrates that HSP16-2 is equally capable of preventing the aggregation of thermally- and chemically-unfolded citrate synthase. Furthermore, it is shown that HSP16-2 has a substantially higher affinity for actin and tubulin unfolded intermediates with occur early on the renaturation or aggregation pathway, and is incapable of resolubilizing citrate synthase aggregates. Taken together, these data present strong evidence that HSP16-2 and perhaps other smHSPs can

interact with and stabilize proteins in the early stages of unfolding, or which are grossly unfolded, before the onset of extensive aggregation.

The mechanism by which smHSPs interact with and prevent unfolded polypeptides from aggregating is unknown. It is generally agreed that hydrophobic regions in smHSPs are important for polypeptide binding (Carver *et al.*, 1994b; Plater *et al.*, 1996), but hydrophilic interactions may be necessary as well (Farahbakhsh *et al.*, 1995; Smulders *et al.*, 1995). Although C-terminal extensions are likely to be flexible and exposed on the surface of smHSPs (Carver *et al.*, 1992, 1995a), there is some evidence that unfolded polypeptides are not necessarily involved in specific interactions with these structures (Carver *et al.*, 1994b, 1995b). In accord with these observations, it was found that deletion of the last 16 C-terminal residues has little effect on HSP16-2 structure or chaperone activity. The C-terminal extension seems to play a role in maintaining the solubility of the oligomeric complex (presumably by virtue of its exposure to solvent), and this may be the case with other smHSPs as well (Smulders *et al.*, 1996). In contrast, studies involving deletions or mutations of the αA-crystallin C-terminal extension suggest a role for this region in chaperone activity (Takemoto *et al.*, 1993; Andley, *et al.*, 1996; Smulders *et al.*, 1996). The reason for this discrepancy is unclear, and will require the characterization of C-terminal regions from other smHSPs for clarification.

Since the C-terminal extension of HSP16-2 appears to be largely dispensable for polypeptide binding and chaperone activity, the interaction between unfolded polypeptides and the smHSP may not take place at the surface, but instead may occur in a region between subunits, in contact with the α-crystallin domain. In agreement with this, studies with unstructured spin-labeled peptides have suggested that these were not bound on the surface or clustered in an interior cavity of the α-crystallin complex, but rather were strongly immobilized at least 25 Å apart in polar environments (Farahbakhsh *et al.*, 1995). A detailed computer-generated model of the interaction between partially unfolded γ-crystallin and α-crystallin which predicted the site of polypeptide interaction to be within clefts in the α-crystallin complex (Singh *et al.*, 1995) is also consistent with the results presented here.

Merck *et al.* (1992, 1993b) showed that the chaperone activity of α-crystallins and HSP25 lacking their entire N-terminal region was lost. The present studies on HSP16-2 show that removal of only one-third of the N-terminal domain disrupts multimerization and abrogates chaperone activity. Therefore, it seems unlikely that the N-terminal domain *per se* is required for chaperone activity—it is probably the assembly of subunits which is important for this function. In addition, smHSPs not present in a complex (*i.e.*, the Δ1-44 HSP16-2 and HSP12.6 proteins) are incapable of interacting with unfolded proteins. The structure-function studies on HSP16-2 and HSP12.6 strongly suggest that smHSP multimerization may depend on a limited region of the N-terminal domain, and is a prerequisite both for the interaction of the chaperone with unfolded protein and for chaperone activity.

In conclusion, it was demonstrated that HSP16-2 forms large oligomeric complexes which have a high affinity for unfolded actin and tubulin and prevent the thermally- or chemically-induced aggregation of citrate synthase. Despite considerable effort, conditions were not found under which HSP16-2 could refold denatured test proteins *in vitro*. The function of HSP16-2 *in vivo* may be to interact with and stabilize a large variety of unfolding proteins, effectively buffering the cell against the deleterious effects caused by misfolded and aggregated proteins. The fate(s) of the unfolded proteins bound to smHSPs is poorly understood. However, it is now established that many molecular chaperones cooperate in refolding denatured proteins (Langer *et al.*, 1992; Freeman and Morimoto, 1996; Freeman *et al.*, 1996; Melki *et al.*, 1996), and are involved in targeting proteins for degradation (Straus *et al.*, 1988; also reviewed in Hayes and Dice, 1996). Recently, HSP25 and HSP70 were shown to act in concert *in vitro* in the refolding of citrate synthase (Ehrnsperger *et al.*, 1997). It is therefore possible that *in vivo*, the smHSP-bound unfolded proteins are folded by molecular chaperones such as those involved in *de novo* protein folding (HSP40/HSP70, HSP60; Hartl *et al.*, 1996), or are degraded by the cellular proteolytic system.

The data on HSP12.6 complement the HSP16-2 studies

The studies on *C. elegans* HSP12.6, a member of a novel class of smHSP, provide new insights into the structure and function of smHSPs, and reinforce the notion that two distinct features of smHSPs, namely their assembly into variable quaternary structures and molecular chaperone activity, may be strictly dependent on sequences present in their structurally divergent N-terminal regions. Although HSP12.6 possesses only 16 and 17 fewer N-terminal residues than *C. elegans* HSP16-2 or *M. tuberculosis* HSP16.3, respectively, it does not form high-MW complexes. It is doubtful that this inability to multimerize could be attributed to the shorter C-terminal extension of HSP12.6 since this region in smHSPs appears unnecessary for aggregate formation (Siezen *et al.*, 1979, and the present work). Rather, it is likely that the N-terminal domains of smHSPs have strict minimum structural requirements for multimerization, and that any alteration in their size and perhaps composition can influence the assembly and overall quaternary structures of these proteins. The short N-terminus and monomeric nature of HSP12.6 suggest that the oligomerization domain of smHSPs may be located in the distal end of the N-terminal region. There is also evidence that smHSPs may assemble cooperatively from smaller aggregates such as dimers/tetramers or trimers (Chang *et al.*, 1996, Merck *et al.*, 1993b). However, the data on HSP12.6 provide evidence that beyond N-terminal-dependent multimerization, smHSPs have no intrinsic ability to self-associate. In support of these results, bifunctional cross-linking experiments have suggested that α-crystallin aggregates are not likely to be built up of smaller clusters such as trimers or tetramers (Bindels *et al.*, 1979; Siezen *et al.*, 1980a). Another recent study also suggests that the minimal cooperative unit of α-crystallin unit is the monomer (Gesierich and Pfeil, 1996).

Since HSP12.6 is clearly related to other smHSPs, it is both intriguing and informative that it is not functional as a molecular chaperone. While it is possible that HSP12.6 lacks chaperone activity because of its unusually short C-terminal extension, it should be noted that N-terminally-deleted αA-, αB-crystallin, and HSP25, which fail to form native-like complexes, are also ineffective in preventing thermally-induced protein aggregation (Merck *et al.*, 1993b). These results imply that the conserved α-crystallin domain of smHSPs, which is presumed to be the site

of interaction with unfolded protein, is insufficient in itself for molecular chaperone activity but is functional in the context of an oligomeric assembly. Computer-modeling studies indicate that the interaction between an unfolded polypeptide and α-crystallin takes place within clefts formed by adjoining subunits, implying that smHSP multimerization may be a prerequisite for chaperone activity (Singh *et al.*, 1995). Again, the work by Farahbakhsh *et al.* (1995) on spin-labeled lends further support to this observation.

Despite its apparent lack of chaperone activity *in vitro*, HSP12.6 presumably carries out specific function(s) *in vivo*, as it is one of a family of similar proteins found in *C. elegans*. One possible clue to the function of HSP12 proteins comes from the fact that there is a precedent for a monomeric smHSP *in vivo*. Murine HSP25 from Ehrlich ascites tumor cells can be recovered as two species, one mostly monomeric and the other multimeric (Benndorf *et al.*, 1994). The presence of HSP25 monomers is surprising given that recombinant HSP25 readily forms 730-kDa particles (Behlke *et al.*, 1991). Nevertheless, non-phosphorylated HSP25 monomers were shown to be effective in inhibiting actin polymerization, a property shared by other smHSPs (Miron *et al.*, 1991; Rahman *et al.*, 1995). Whether HSP12.6 is active in preventing actin polymerization remains to be tested experimentally; it will be interesting to see whether the chaperone activity of HSP12.6 has been lost and uncoupled from an ability to influence actin polymerization. It is noteworthy that a region thought to be involved in actin polymerization and binding to DNAse I, and suggested to be required for the inhibition of actin polymerization activity of smHSPs (Rahman *et al.*, 1995), is partly conserved in the HSP12 family. The motif, G-[V/I]-L-T-[X_3]-P, is present in full in C14B9.1 and T22A3.2 with the exception of the proline residue (see **Figure 14**; perhaps non-coincidentally, this residue is found in nearly all the *C. elegans* Class I and III smHSPs).

Alternatively, HSP12.6 may regulate the function of other smHSPs by preventing their oligomerization, or act as a co-chaperone with smHSPs or other molecular chaperones.

It is becoming increasingly apparent that some smHSPs perform necessary functions during specific stages of development, and are not necessarily induced under physiological stresses. For example, expression of the 20-kDa smHSP from the gastrointestinal nematode *Nippostrongylus*

brasiliensis is developmentally regulated, but is not increased by stress conditions (Tweedie *et al.*, 1993). In plants, specific subsets of smHSPs are produced during many developmental stages, although usually in response to heat stress (Waters *et al.*, 1996). The developmentally-regulated expression pattern of HSP12.6 is reminiscent of the expression of *C. elegans* SEC-1, an HSP16-like smHSP produced only during embryogenesis, where it serves an unknown but essential function (Linder *et al.*, 1996). Like HSP12.6, SEC-1 is not induced by stress conditions, which suggests that these smHSPs may have fundamentally different roles from other stress-inducible smHSPs. It has been suggested by Linder *et al.* (1996) that SEC-1 may be required to facilitate the folding of the large number of nascent polypeptides produced, or to regulate the assembly and disassembly of cytoskeletal structures during early embryonic development. HSP12.6 may play similar role(s) during the first larval stage, a period when a significant number of somatic cell divisions occur (Wood, 1988).

Although *hsp12* genes from other species have not been uncovered, the gene family is likely to be ubiquitous in nematodes. Numerous cDNAs homologous to *C. elegans* C14B9.1 from two other nematodes, *Brugia malayi* and *Onchocerca volvulus*, were recently isolated as part of a pilot project designed to identify genes expressed in these human filarial nematode parasites (Blaxter *et al.*, 1996). The *B. malayi* HSP12 cDNA encodes a protein of 113 amino acids which displays 60% identity to its *C. elegans* homolog over its entire length. Interestingly, the cDNAs were isolated from third- and fourth-stage infective larvae. It is possible that the difference in expression patterns of the *hsp12* genes in the free-living and parasitic nematodes may be due to different temporal requirements for the smHSP.

Models summarizing HSP16-2 structure and function

The present work on *C. elegans* HSP16-2 and HSP12.6 provides insights into the structure and function of HSP16-2 and other smHSPs in general. The functional data obtained on HSP16-2 are in agreement with an ability of this protein to interact with and stabilize proteins which become structurally compromised during cellular insults. Specifically, HSP16-2 recognizes protein conformers which are in the early stages of the aggregation pathway, and

prevents their aggregation (**Figure 30A**). It is likely that the mechanism of action of other smHSPs is very similar, although the HSP16s may have more specialized roles compared with some other smHSPs, since they are produced only during stress conditions.

Of all the structural models proposed to date for α-crystallin, the micellar-like aggregate and variations on this structure have received the most support (Tardieu *et al.*, 1986; Walsh *et al.*, 1991; Wistow, 1993; Groth-Vasselli *et al.*, 1995; Singh *et al.*, 1995), although much controversy remains. The structural studies presented here on two minimalist members of the smHSP family are entirely consistent with such a model. Although this model is presently rather crude, it is likely that its basic premises, including N-terminal-dependent oligomerization, the presence of a central cavity which can accomodate N-terminal domains of various sizes and sequences, an exposed C-terminal extension which imparts aggregate solubility, and the necessity for multiple subunit interactions for binding to the unfolded substrate, are all valid for smHSPs in general (**Figure 30B**).

Future studies

Major advances in our understanding of chaperone function have resulted from the structural determination of a limited number of chaperones, including bacterial GroEL/GroES (Braig *et al.*, 1994; Hunt *et al.*, 1996), HSP70 ATPase and DnaK polypeptide-binding domains (Flaherty *et al.*, 1990; Zhu *et al.*, 1996), and PapD (Holmgren and Bränden, 1989). In contrast, the multimeric and heterogeneous nature of smHSPs have represented major obstacles to determining their structure by crystallization or high-resolution 2D NMR techniques. Consequently, progress on determining the function of small HSPs has been hampered by a lack of structural information. The simple structure of HSP12.6 may make it amenable to structure determination, and such studies are now underway in collaboration with Andrzej Joachimiak, a crystallographer who was involved in solving the GroEL structure (Braig *et al.*, 1994).

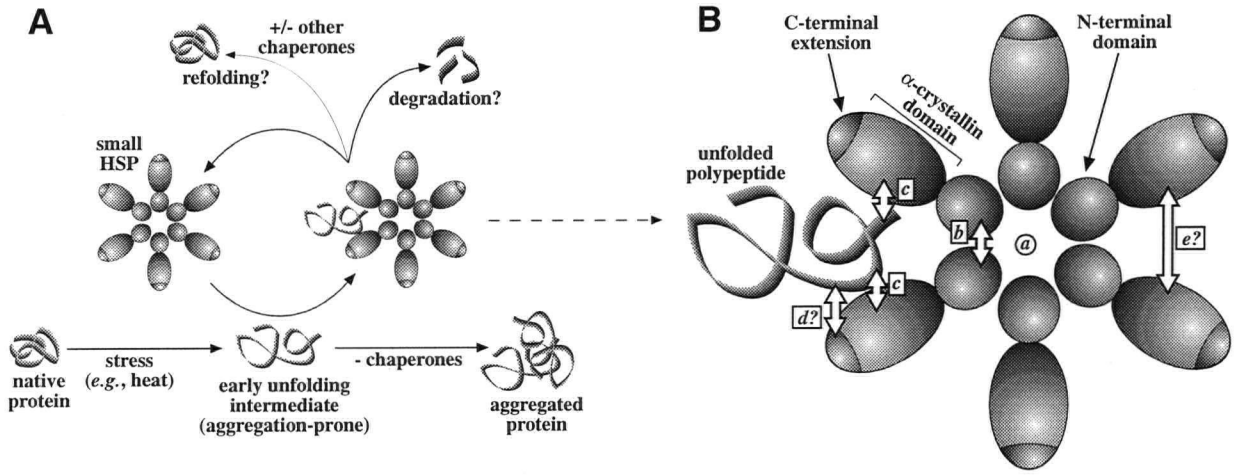

Figure 30. Model of *in vivo* function and oligomeric structure of smHSPs. **A.** Proposed model for the *in vivo* function of stress-inducible smHSPs. SmHSPs interact with structurally-compromised polypeptides which expose hydrophobic regions, and prevents them from forming insoluble aggregates. The smHSP therefore acts as a reservoir for unfolded proteins which may then be refolded in the presence or absence of other molecular chaperones, or may be degraded by the cellular proteolytic machinery. **B.** Model for small HSP oligomeric structure and interaction with unfolded polypeptides. This schematic depicts a hypothetical cross-section through a smHSP complex with an arbitrary number of subunits and quaternary structure. SmHSP monomers are shown as having a two-domain structure consisting of the N-terminal domain and C-terminal domain (which includes the α-crystallin domain and C-terminal extension). Double-headed arrows indicate possible sites of interaction between different smHSP monomers and between smHSP subunits and unfolded substrates. ***a.*** A proposed feature of smHSPs is their central cavity, which can accomodate N-terminal domains of varying lengths and sequences. ***b.*** N-terminal domain interactions are necessary for subunit assembly and are likely to modulate the arrangement of subunits within the smHSP quaternary structure. The multimerization domain may be restricted to a small section (*e.g.*, the distal end) of the N-terminal region. ***c.*** the chaperone activity of smHSPs relies on their ability to interact with and stabilize unfolded polypeptides; this interaction is likely to be mediated through multiple contacts with α-crystallin domains in clefts formed by neighboring subunits. ***d.*** although the role of the C-terminal extension in the interaction of the smHSP with unfolded polypeptides is unclear, it is probable that this region is largely responsible for maintaining the solubility of the smHSP complex. ***e.*** there is evidence that smHSPs assemble cooperatively from small oligomers, but the exact region of interaction between subunits, and whether this is a general feature of smHSPs, is unknown.

If successful, this project would constitute a significant breakthrough in the study of these proteins. Since HSP12.6 contains all of the core α-crystallin domain in addition to a significant amount of N-terminal domain region, insights into the assembly of subunits in complexes might be obtained by modeling studies. Furthermore, information regarding the mechanisms of polypeptide binding and chaperone activity could probably be inferred from the three-dimensional structure.

Additional studies on HSP16-2, which represents a good model system for studying smHSPs in general, could further our understanding of the oligomeric assembly and function of these chaperones. While the present study revealed a strict correlation between multimerization and chaperone activity, the amino acids required for multimerization were not precisely defined. Removal of fewer than 16 amino acids (one third of the N-terminal domain), and site directed mutagenesis of one or more residues may pinpoint more accurately the regions involved in the formation of oligomeric complexes. A domain-swapping experiment in which the N-terminal domains of HSP16-2 and HSP16-48 are interchanged could reveal whether the N- and C-terminal domains of smHSPs are relatively independent of each other in the native complex. This experiment would determine whether compensating changes between the two domains have evolved in the two closely-related smHSPs in order to maintain function. Also, further truncations of the C-terminal extension (beyond the Δ130-145 truncation) could provide additional insight with regard to which regions within the smHSP are required for chaperone activity in the context of a normal oligomeric assembly.

An intriguing question raised in this study concerns the function of HSP12.6 *in vivo*. First, the stage-specific expression of HSP12.6 during normal physiological conditions and the fact that it does not prevent thermally-induced protein aggregation *in vitro* may suggest a specialized function in the cell. It may, for example, be able to bind unfolded protein and stabilize it temporarily until it can be assisted by other molecular chaperones, much in the way that HSP40 requires the presence of HSP70 for assisting in the renaturation of unfolded polypeptides (Langer *et al.*, 1992; Rassow *et al.*, 1995). Alternatively, HSP12s may have an inhibitory effect on the function of other smHSPs. The presence of HSP12s under non-stress conditions could

serve to regulate the activity of various stress-inducible smHSPs by binding to and preventing the oligomeric assembly of the newly synthesized smHSPs. Such a possible role for HSP12.6 could be demonstrated by determining whether HSP16-2 complex formation is suppressed in the presence of a comparable or sub-stoichiometric amount of HSP12.6. The function of HSP12s might also be ascertained by testing to see whether they bind certain *C. elegans* proteins—even native proteins cannot be excluded. This could be accomplished by passing a total *C. elegans* first-stage larval extract over a column containing H_6HSP13 bound to Ni^{2+}-chelate affinity resin, eluting any bound proteins with a chaotropic agent, and separating them by SDS-PAGE. Proteins could be tentatively identified by their size alone, and if found to be of interest, by internal peptide sequencing.

REFERENCES

Ahnert, V., May, C., Gerke, R., and Kindl, H. (1996) Cucumber T-complex protein. Molecular cloning, bacterial expression and characterization within a 22-S cytosolic complex in cotyledons and hypocotyls. *Eur. J. Biochem.* **235**, 114-119.

Altschul, S. F., Gish, W., Miller, W., Myers, E. W., and Lipman, D. J. (1990) Basic local alignment search tool. *J. Molec. Biol.* **215,** 403-410.

Ananthan, J., Goldberg, A. L., and Voellmy, R. (1986) Abnormal proteins serve as eukaryotic stress signals and trigger the activation of heat shock genes. *Science* **232**, 522-524.

Andley, U. P., Mathur, S., Griest, T. A., Petrash, J. M. (1996) Cloning, expression, and chaperone-like activity of human αA-crystallin. *J. Biol. Chem.* **271**, 31973-31980.

Anfinsen, C. B. (1973) Principles that govern the folding of protein chains. *Science* **181**, 223-230.

Antonucci, T. K. (1985) Isolation of high MW RNA from mammalian tissues. *Recombinant DNA Techniques* (now called *DNA Prot. Eng. Tech.*) **6**, 22-24.

Arrigo, A.-P. and Landry, J. (1994) Expression and function of the low-molecular-weight heat shock proteins. In *The Biology of Heat Shock Proteins and Molecular Chaperones*. Morimoto, R. I., Tissières, A., and Georgopoulos, C., eds. Cold Spring Harbor Laboratory Press, Cold Spring Harbor, NY., 335-373.

Arrigo, A.-P. and Tanguay, R. M. (1991) Expression of heat shock proteins during development in *Drosophila*. In Heat shock and development. Hightower, L. and Nover, L., eds. Springer-Verlag, Berlin, 106-119.

Augusteyn, R. C. and Koretz, J. F. (1987) A possible structure for α-crystallin. *FEBS Lett.* **222**, 1-5.

Barraclough, R. and Ellis, R. J. (1980) Assembly of newly-synthesized large subunits into ribulose bisphosphate carboxylase in isolated intact pea chloroplasts. *Biochim. Biophys. Acta* **608**, 19-31.

Beckmann, R. P., Mizzen, L. A., and Welch, W. J. (1990) Interaction of Hsp70 with newly synthesized proteins: implications for protein folding and assembly. *Science* **248**, 850-854.

Behlke, J., Lutsch, G., Gaestel, M., and Bielka, H. (1991) Supramolecular structure of the recombinant murine small heat shock protein hsp25. *FEBS* **288**, 119-122.

Bennardini, F., Wrzosek, A., and Chiesi, M. (1992) αB-crystallin in cardiac tissue. Association with actin and desmin filaments. *Circ. Res.* **71**, 288-294.

Benndorf, R., Haye, K., Ryazantsev, S., Wieske, M., Behlke, J., and Lutsch, G. (1994) Phosphorylation and Supramolecular organization of murine small heat shock protein HSP25 abolish its actin polymerization-inhibiting activity. *J. Biol. Chem.* **269**, 20768-20784.

Bentley, N. J., Fitch, I. T., and Tuite, M. F. (1992) The small heat-shock protein Hsp26 of *Saccharomyces cerevisiae* assembles into a high molecular weight aggregate. *Yeast* **8**, 95-106.

Bhat, S. P., Nagineni, C. N. (1989) αB subunit of lens-specific protein α-crystallin is present in other ocular and non-ocular tissues. *Biochem. Biophys. Res. Commun.* **158**, 319-325.

Bindels, J. G., Siezen, R. J., and Hoenders, H. J. (1979) A model for the architecture of α-crystallin. *Ophthalmic Res.* **11**, 441-452.

Blaxter, M. L., Raghavan, N., Ghosh, I., Guiliano, D., Lu, W., Williams, S. A., Slatko, B., and Scott, A. L. (1996) Genes expressed in *Brugia malayi* infective third stage larvae. *Mol. Biochem. Parasitol.* **77**, 77-93.

Blumenthal, T. (1995) *Trans*-splicing and polycistronic transcription in *Caenorhabditis elegans*. *Trends Genet.* **11**, 132-136.

Boisvert, D. C., Wang, J., Otwinowski, Z., Horwich, A. L., Sigler, P. B. (1996) The 2.4 Å crystal structure of the bacterial chaperonin GroEL complexed with ATP-γS. *Nature Struct. Biol.* **3**, 170-177.

Bose, S., Weikl, T., Bügl, H., and Buchner, J. (1996) Chaperone functions of Hsp90-associated proteins. *Science* **274**, 1715-1717.

Bossier, P., Fitch, I. T., Boucherie, H., and Tuite, M. F. (1989) Structure and expression of a yeast gene encoding the small heat-shock protein Hsp26. *Gene* **78**, 71-94.

Bouchard, R. A. (1990) Characterization of expressed meiotic prophase repeat transcript clones of *Lilium*: meiosis-specific expression, relatedness, and affinities to small heat shock protein genes. *Genome* **33**, 68-79.

Braig, K., Otwinowski, Z., Hegde, R., Boisvert, D. C., Joachimiak, A., Horwich, A. L., and Sigler, P. B. (1994) The crystal structure of the bacterial chaperonin GroEL at 2.8 Å. *Nature* **371**, 578-586.

Brenner, S. (1974) The genetics of *Caenorhabditis elegans*. *Genetics* **77**, 71-94.

Brown, C. R., Doxsey, S. J., Hong-Brown, L. Q., Martin, R. L., and Welch, W. J. (1996) Molecular chaperones and the centrosome. *J. Biol. Chem.* **271**, 824-832.

Buchner, J. (1996) Supervising the fold: functional principles of molecular chaperones. *FASEB J.* **10**, 10-19.

Buchner, J., Schmidt, M., Fuchs, M., Jaenicke, R., Rudolph, R., Schmid, F. X., and Kiefhaber, T. (1991) GroE facilitates refolding of citrate synthase by suppressing aggregation. *Biochemistry* **30**, 1586-1591.

Bult, C. J., White, O., Olsen, G. J., Zhou, L., Fleischmann, R. D., Sutton, G. G., Blake, J. A., FitzGerald, L. M., Clayton, R. A., Gocayne, J. D., Kerlavage, A. R., Dougherty, B. A., Tomb, J.-F., Adams, M. D., Reich, C. I., Overbeek, R., Kirkness, E. F., Weinstock, K. G., Merrick, J. M., Glodek, A., Scott, J. L., Geoghagen, N. S. M., Weidman, J. F., Fuhrmann, J. L., Nguyen, D., Utterback, T. R., Kelley, J. M., Peterson, J. D., Sadow, P. W., Hanna, M. C., Cotton, M. D., Roberts, K. M., Hurst, M. A., Kaine, B. P., Borodovsky, M., Klenk, H.-P., Fraser, C. M., Smith, H. O., Woese, C. R., and Venter, J. C. (1996) Complete genome sequence of the methanogenic archeon, *Methanococcus jannaschii*. *Science* **273**, 1058-1073.

Burston, S. G., Weissman, J. S., Farr, G. W., Fenton, W. A., and Horwich, A. L. (1996) Release of both native and non-native proteins from a *cis*-only GroEL ternary complex. *Nature* **383**, 96-99.

Candido, E. P. M., Jones, D., Dixon, D. K., Graham, R. W., Russnak, R. H., and Kay, R. J. (1989) Structure, organization, and expression of the 16-kDa heat shock gene family of *Caenorhabditis elegans*. *Genome* **31**, 690-697.

Carver, J. A., Aquilina, J. A., and Truscott, R. J. (1993) An investigation into the stability of α-crystallin by NMR spectroscopy; evidence for a two-domain structure. *Biochim. Biophys. Acta* **1164**, 22-28.

Carver, J. A., Aquilina, J. A., and Truscott, R. J. W. (1994a) A possible chaperone-like quaternary structure for α-crystallin. *Exp. Eye Res.***59**, 231-234.

Carver, J. A., Aquilina, J. A., Cooper, P. G., Williams, G. A., and Truscott, R. J. W. (1994b) α-crystallin: molecular chaperone and protein surfactant. *Biochim. Biophys. Acta* **1204**, 195-206.

Carver, J. A., Aquilina, J. A., Truscott, R. J., and Ralston, G. B. (1992) Identification by ^{1}H NMR spectroscopy of flexible C-terminal extensions in bovine lens α-crystallin. *FEBS Lett.*, **311**, 143-149.

Carver, J. A., Esposito, G., Schwedersky, G., and Gaestel, M. (1995a) ^{1}H NMR spectroscopy reveals that mouse Hsp25 has a flexible C-terminal extension of 18 amino acids. *FEBS Lett.*, **369**, 305-310.

Carver, J. A., Guerreiro, N., Nicholls, K. A., and Truscott, R. J. W. (1995b) On the interaction of α-crystallin with unfolded protein. *Biochim. Biophys. Acta*, **1252**, 251-260.

Caspers, G.-J., Leunissen, J. A. M., and De Jong, W. W. (1995) The expanding small heat-shock protein family, and structure predictions of the conserved "α-crystallin domain". *J. Mol. Evol.* **40**, 238-248.

Chang, Z., Primm, T. P., Joanita J., Lee, I. H., Serysheva, I., Chiu, W., Gilbert, H. F., Quiocho, F. A. (1996) *Mycobacterium tuberculosis* 16-kDa antigen (Hsp16.3) functions as an oligomeric structure *in vitro* to suppress thermal aggregation. *J. Biol. Chem.* **271**, 7218-7223.

Chen, Q., Lauzon, L. M., DeRocher, A. E., and Vierling, E. (1990) Accumulation, stability, and localization of a major chloroplast heat-shock protein. *J. Cell Biol.* **110**, 1873-1883.

Chen, X., Sullivan, D. S., and Huffaker, T. C. (1994) Two yeast genes with similarity to TCP-1 are required for microtubule and actin function *in vivo*. *Proc. Natl. Acad. Sci. USA* **91**, 9111-9115.

Cheng, M. Y., Hartl, F.-U., Horwich, A. L. (1990) The mitochondrial chaperonin hsp60 is required for its own assembly. *Nature* **348**, 455-458.

Cheng, M. Y., Hartl, F.-U., Martin, J., Pollock, R. A., Kalousek, R., Neupert, W., Hallberg, E. M., Hallberg, R. L., and Horwich, A. L. (1989) Mitochondrial heat-shock protein Hsp60 is essential for assembly of proteins imported into yeast mitochondria. *Nature* **337**, 620-625.

Chiesi, M., Longoni, S., and Limbruno, U. (1990) Cardiac α-crystallin. Involvement during heart ischemia. *Mol. Cell. Biochem.* **97**, 129-136.

Coca, M. A., Almoguera, C., and Jordano, J. (1994) Expression of sunflower low-molecular-weight heat-shock proteins during embryogenesis and persistence after germination: localization and possible functional implications. *Plant Mol. Biol.* **25**, 479-492.

Conway de Macario, E. and Macario, A. J. L. (1994) Heat-shock response in Archaea. *Trends Biotech.* **12**, 512-518.

Cooper, J. A. (1992) Actin filament assembly and organization *in vitro*. In *The cytoskeleton.* Carraway, K. L. and Carraway, G. A. C., eds. Oxford University Press, NY., 47-72.

Creutz, C. E., Liou, A., Snyder, S. L., Brownawell, A., and Willison, K. (1994) Identification of the major chromaffin granule-binding protein, chromobindin A, as the cytosolic chaperonin CCT (Chaperonin Containing TCP-1). *J. Biol. Chem.* **269**, 32035-32038.

Das, K. P. and Surewicz, W. K. (1995) Temperature-induced exposure of hydrophobic surfaces and its effect on the chaperone activity of α-crystallin. *FEBS Lett.* **369**, 321-325.

Das, K. P., Petrash, J. M., and Surewicz, W. K. (1996) Conformational properties of substrate proteins bound to a molecular chaperone α-crystallin. *J. Biol. Chem.* **271**, 10449-10452.

DeRocher, A. E., Helm, K. W., Lauzon, L. M., Vierling, E. (1991) Expression of a conserved family of cytoplasmic low molecular weight heat shock proteins during heat stress and recovery. *Plant Physiol.* **96**, 1038-1047.

Detmers, P., Weber, A., Elzinga, M., and Stephens, R. E. (1981) 7-Chloro-4-nitrobenzeno-2-oxa-1,3-diazole actin as a probe for actin polymerization. *J. Biol. Chem.* **256**, 99-105.

Dixon, D. K., Jones, D., and Candido, E. P. M. (1990) The differentially expressed 16-kD heat shock genes of *Caenorhabditis elegans* exhibit differential changes in chromatin structure during heat shock. *DNA Cell Biol.* **9**, 177-191.

Dobrzynski, J. K., Sternlicht, M. L., Farr, G. W., Sternlicht, H. (1996) Newly-synthesized β-tubulin demonstrates domain-specific interactions with the cytosolic chaperonin. *Biochemistry* **35**, 15870-15882.

Dudich, I. V., Zav'yalov, V. P., Pfeil, W., Gaestel, M., Zav'yalov, G. A., Denesyuk, A. I., Korpela, T. (1995) Dimer stucture as a minimum cooperative subunit of small heat-shock proteins. *Biochim. Biophys. Acta* **1253**, 163-168.

Dunn, M. K. and Mercola, M. (1996) Cloning and expression of Xenopus CCTγ, a chaperonin subunit developmentally regulated in neural-derived and myogenic lineages. *Devel. Dynamics.* **205**, 387-394.

Ehmann, B., Krenz, M., Mummert, E., Schafer, E. (1993) Two Tcp-1-related but highly divergent gene families exist in oat encoding proteins of assumed chaperone function. *FEBS Lett.* **336**, 313-316.

Ehrnsperger, M., Graber, S., Gaestel, M., and Buchner, J. (1997) Binding of non-native protein to Hsp25 during heat shock creates a reservoir of folding intermediates for reactivation. *EMBO J.* **16**, 221-229.

Eisenberg, E. and Kielley, W. W. (1974) Troponin-tropomyosin complex. Column chromatographic separation and activity of the three, active troponin components with and without tropomyosin present. *J. Biol. Chem.* **249**, 4742-4748.

Ellis, R. J. (1987) Proteins as molecular chaperones. *Nature* **328**, 378-379.

Ellis, R. J. (1990) Molecular chaperones: the plant connection. *Science* **250**, 954-959.

Ellis, R. J. (1992) Cytosolic chaperonin confirmed. *Nature* **358**, 191-192.

Ellis, R. J. and Hartl, F.-U. (1996) Protein folding in the cell: competing models of chaperonin function. *FASEB J.* 10, 20-26.

Emmons, S. W., Klass, M. R., and Hirsh, D. (1979) Analysis of the consistancy of DNA sequences during development and evolution of the nematode *Caenorhabditis elegans. Proc. Natl. Acad. Sci. USA* **76**, 1333-1337.

Farahbakhsh, Z. T., Huang, Q.-L., Ding, L.-L., Altenbach, C., Steinhoff, H.-J., Horwitz, J., and Hubbell, W. L. (1995) Interaction of α-crystallin with spin-labeled peptides. *Biochemistry* **34**, 509-516.

Feder, M. E., Cartano, N. V., Milos, L., Krebs, R. A., and Lindquist, S. L. (1996) Effect of engineering Hsp70 copy number on Hsp70 expression and tolerance of ecologically relevant heat shock in larvae in larvae and pupae of *Drosophila. J. Exp. Biol.* **199**, 1837-1844.

Feinberg, A. P. and Vogelstein, B. (1983) A technique for radiolabeling DNA restriction endonuclease fragments to high specific activity. *Anal. Biochem.* **132,** 6-13.

Fenton, W. A., Kashi, Y., Furtak, K., and Horwich, A. L. (1994) Residues in chaperonin GroEL required for polypeptide binding and release. *Nature* **371**, 614-619.

Findly, R. C., Gillies, R. J., and Shulman, R. G. (1983) *In vivo* ^{31}P nuclear magnetic resonance reveals lowered ATP during heat shock of *Tetrahymena*. *Science* **219**, 1223-1225.

Fire, A. (1992) Histochemical techniques for locating *E. coli* β-galactosidase activity in transgenic organisms. *Genetic Analysis, Techniques & Applications* **9**, 151-158.

Fire, A., Harrison, S. W., Dixon, D. (1990) A modular set of *lacZ* fusion vectors for studying gene expression in *Caenorhabditis elegans*. *Gene* **93**, 189-198.

Flaherty, K. M., DeLuca-Flaherty, C., and McKay, D. B. (1990) Three-dimensional structure of the ATPase fragment of a 70K heat-shock cognate protein. *Nature* **346**, 623-628.

Fleischmann, R. D., Adams, M. D., White, O., Clayton, R. A., Kirkness, E. F., Kerlavage, A. R., Bult, C. J., Tomb, J.-F., Dougherty, B. A., Merrick, J. M., McKenney, K., Sutton, G., FitzHugh, W., Fields, C., Gocayne, J. D., Scott, J., Shirley, R., Liu, L.-I., Glodek, A., Kelley, J. M., Weidman, J. F., Phillips, C. A., Spriggs, T., Hedblom, E., Cotton, M. D., Utterback, T. R., Hanna, M. C., Nguyen, D. T., Saudek, D. M., Brandon, R. C., Fine, L. D., Fritchman, J. L., Fuhrmann, J. L., Geoghagen, N. S. M., Gnehm, C. L., McDonald, L. A., Small, K. V., Fraser, C. M., Smith, H. O., Venter, J. C. (1995) Whole-gemome random sequencing and assembly of *Haemophilus influenzae* Rd. *Science* **269**, 496-512.

Fraser, C. M., Gocayne, J. D., White, O., Adams, M. D., Clayton, R. A., Fleischmann, R. D., Bult, C. J., Kerlavage, A. R., Sutton, G., Kelley, J. M., Fritchman, J. L., Weidman, J. F., Small, K. V., Sandusky, M., Fuhrmann, J., Nguyen, D., Utterback, T. R., Saudek, D. M., Phillips, C. A., Merrick, J. M., Tomb, J.-F., Dougherty, B. A., Bott, K. F., Hu, P.-C., Lucier, T. S., Peterson, S. N., Smith, H. O., Hutchison III, C. A., and Venter, J. C. (1995) The minimal gene complement of *Mycoplasma genitalium*. *Science* **270**, 397-403.

Fray, R. G., Lycett, G. W., and Grierson, D. (1990) Nucleotide sequence of a heat-shock and ripening-related cDNA from tomato. *Nucleic Acids Res.* **18**, 7148.

Freeman, B. C. and Morimoto, R. I. (1996) The human cytosolic molecular chaperones hsp90, hsp70 (hsc70) and hdj-1 have distinct roles in recognition of a non-native protein and protein refolding. *EMBO J.* **15**, 2969-2979.

Freeman, B. C., Toft, D. O., and Morimoto, R. I. (1996) Molecular chaperone machines: chaperone activities of the cyclophilin Cyp-40 and the steroid aporeceptor-associated protein p23. *Science* **274**, 1718-1720.

Frydman, J. and Hartl, F. U. (1996) Principles of chaperone-assisted protein folding: differences between *in vitro* and *in vivo* mechanisms. *Science* **272**, 1497-1502.

Frydman, J., Nimmesgern, E., Erdjument-Bromage, H., Wall, J. S., Tempst, P., and Hartl, F.-U. (1992) Function in protein folding of TRiC, a cytosolic ring complex containing TCP-1 and structurally related subunits. *EMBO J.* **11**, 4767-4778.

Frydman, J., Nimmesgern, E., Ohtsuka, K., and Hartl, F.-U. (1994a) Folding of nascent polypeptide chains in a high molecular mass assembly with molecular chaperones. *Nature* **370**, 111-117.

Frydman, J., Nimmesgern, E., Ohtsuka, K., and Hartl, F.-U. (1994b) Function in protein folding of TRiC, a cytosolic ring complex containing TCP-1 and structurally related subunits. *EMBO J.* **11**, 4767-4778.

Fukushige, T., Yasuda, H., and Siddiqui, S. S. (1993) Molecular cloning and developmental expression of the alpha-2 tubulin gene of *Caenorhabditis elegans*. *J. Mol. Biol* **234**, 1290-1300.

Gao, Y., Thomas, J. O., Chow, R. L., Lee, G.-H., and Cowan, N. J. (1992) A cytoplasmic chaperonin that catalyzes β-actin folding. *Cell* **69**, 1043-1050.

Gao, Y., Vainberg, I. E., Chow, R. L., and Cowan, N. J. (1993) Two cofactors and cytoplasmic chaperonin are required for the folding of α- and β-tubulin. *Mol. Cell Biol.* **13**, 2478-2485.

Georgopoulos, C. and Welch, W. J. (1993) Role of the major heat shock proteins as molecular chaperones. *Annu. Rev. Cell Biol.* **9**, 601-634.

Georgopoulos, C. P., Hendrix, R. W., Casjens, S. R., and Kaiser, A. D. (1973) Host participation in bacteriophage lamda head assembly. *J. Molec. Biol.* **76**, 45-60.

Gesierich, U. and Pfeil, W. (1996) The conformational stability of α-crystallin is rather low—calorimetric results. *FEBS Lett.* **393**, 151-154.

Gething, M.-J. and Sambrook, J. (1992) Protein folding in the cell. *Nature* **355**, 33-45.

Gopalakrishnan, S. and Takemoto, L. (1992) Binding of actin to lens α-crystallins. *Curr. Eye Res.* **11**, 929-933.

Gray, M. W. (1992) The endosymbiont hypothesis revisited. *Int. Rev. Cytol.* **141**, 233-357.

Gray, T. E. and Fersht, A. R. (1991) Cooperativity in ATP hydrolysis by GroEL is increased by GroES. *FEBS Lett.* **292**, 254-258.

Groenen, P. J. T. A., Merck, K. B., De Jong, W. W., Bloemendal, H. (1994) Structure and modifications of the junior chaperone α-crystallin. *Eur. J. Biochem.* **225**, 1-19.

Groth-Vasselli, B., Kumosinski, T. F., and Farnsworth, P. N. (1995) Computer-generated model of the quaternary structure of alpha crystallin in the lens. *Exp. Eye Res.* **61**, 249-253.

Guagliardi, A., Cerchia, L., and Rossi, M. (1995) Prevention of *in vitro* protein thermal aggregation by the *Sulfolobus solfataricus* chaperonin. *J. Biol. Chem.* **270**, 28126-28132.

Guagliardi, A., Cerchia, L., Bartolucci, S., and Rossi, M. (1994) The chaperonin from the archeon *Sulfolobus solfataricus* promotes correct refolding and prevents thermal denaturation *in vitro*. *Protein Sci.* **3**, 1436-1443.

Gupta, R. S. (1990) Sequence and structural homology between a mouse t-complex protein TCP-1 and the chaperonin family of bacterial (GroEL 65kDa heat-shock antigen) and eukaryotic proteins. *Biochem Int.* **20**, 833-841.

Gupta, R. S. (1995) Evolution of the chaperonin families (Hsp60, Hsp10 and Tcp-1) of proteins and the origin of eukaryotic cells. *Mol. Microbiol.* **15**, 1-11.

Gupta, R. S. and Singh, B. (1994). Phylogenetic analysis of 70 kD heat shock protein sequences suggests a chimeric origin for the eukaryotic cell nucleus. *Curr. Biol.* **4**, 1104-1114.

Gurley, W. B. and Key, J. L. (1991) Transcriptional regulation of the heat-shock response: A plant perspective. *Biochemistry* **30**, 1-12.

Hanahan, D. (1983) Studies on transformation of *Escherichia coli* with plasmids. *J. Mol. Biol.* **166,** 557-580.

Hartl, F.-U. (1996) Molecular chaperones in cellular protein folding. *Nature* **381**, 571-580.

Hartl, F.-U., Hlodan, R., and Langer, T. (1994) Molecular chaperones in protein folding: the art of avoiding sticky situations. *Trends Biochem. Sci.* **19**, 20-25.

Hayer-Hartl, M. K., Martin, J., and Hartl, F.-U. (1995) Asymmetrical interaction of GroEL and GroES in the ATPase cycle of assisted protein folding. *Science* **269**, 836-841.

Hemmingsen, S. M., Woolford, C., Van Der Vies, S. M., Tilly, K., Dennis, D. T., Georgopoulos, C. P., Hendrix, R. W., and Ellis, R. J. (1988) Homologous plant and bacterial proteins chaperone oligomeric protein assembly. *Nature* **333**, 330-334.

Hendrick, J. P. and Hartl, F.-U. (1993) Molecular chaperone functions of heat-shock proteins. *Annu. Rev. Biochem.* **62**, 349-384.

Hendrick, J. P., Langer, T., Davis, T. A., Hartl, F. U., Wiedmann, M. (1993) Control of folding and membrane translocation by binding of the chaperone DnaJ to nascent polypeptides. *Proc. Natl. Acad. Sci. USA* **90**, 10216-10220.

Herrin, D. L. and G. W. Schmidt. (1988) Rapid, reversible staining of Northern blots prior to hybridization. *BioTechniques* **6,** 196-200.

Hightower, L. E. (1980) Cultured animal cells exposed to amino acid analogues or puromycin rapidly synthesize several polypeptides. *J. Cell. Physiol.* **102**, 407-427.

Hockertz, M. K., Clark-Lewis, I., and Candido, E. P. M. (1991) *FEBS Lett.* **280**, 375-378.

Hodgkin, J. (1995) Genetic nomenclature guide. *Caenorhabditis elegans. TIG* **11**, 24-25.

Höhfeld, J. and Hartl, F.-U. (1994) Post-translational protein import and folding. *Curr. Opin. Cell Biol.* **6**, 499-509.

Höhfeld, J., Minami, Y., Hartl, F.-U. (1995) Hip, a novel cochaperone involved in the eukaryotic Hsc70/Hsp40 reaction cycle. *Cell* **83**, 589-598.

Holmgren, A., and Bränden, C.-I. (1989) Crystal structure of chaperone protein PapD reveals an immunoglobulin fold. *Nature* **342**, 248-251

Horowitz, P. M., Hua, S., and Gibbons, D. L. (1995) Hydrophobic surfaces that are hidden in chaperonin Cpn60 can be exposed by formation of assembly-competent monomers or by ionic perturbation of the oligomer. *J. Biol. Chem.* **270**, 1535-1542.

Horwich, A. L. and Willison, K. R. (1993) Protein folding in the cell: functions of two families of molecular chaperone, hsp60 and TF55-TCP1. *Phil. Trans. R. Soc. Lond. B* **339**, 313-326.

Horwich, A. L., Caplan, S., Wall, J. S., and Hartl, F.-U. (1992) Chaperonin-mediated protein folding. In *Membrane biogenesis and protein targeting*. Neupert, W. and Lill, R., eds. Elsevier Science Publishers.

Horwich, A. L., Low, K. B., Fenton, W. A., Hirshfield, I. N., Furtak, K. Folding *in vivo* of bacterial cytoplasmic proteins: role of GroEL. *Cell* **74**, 909-917.

Horwitz, J. (1992) α-crystallin can function as a molecular chaperone. *Proc. Natl. Acad. Sci. USA*, **89**, 10449-10453.

Hunt, J. F., Weaver, A. J., Landry, S. J., Gierasch, L., Deisenhofer, J. (1996) The crystal structure of the GroES co-chaperonin at 2.8 Å resolution. *Nature* **379**, 37-45.

Huot, J., Houle, F., Spitz, D. R., and Landry, J. (1996) HSP27 phosphorylation-mediated resistance against actin fragmentation and cell death induced by oxidative stress. *Cancer Res.* **56**, 273-279.

Hynes, G., Kubota, H., Willison, K. R. (1995) Antibody characterisation of two distinct conformations of the chaperonin-containing TCP-1 from mouse testis. *FEBS Lett.* **358**, 129-132.

Ingolia, T. D. and Craig, E. A. (1982) Four small *Drosophila* heat shock proteins are related to each other and to mammalian α-crystallin. *Proc. Natl. Acad. Sci. USA* **79**, 2360-2364.

Irwin, D. M. (1994). Who are the parents of eukaryotes? *Curr. Biol.* **4**, 1115-1117.

Iwabe, N., Kuma, K., Hasegawa, M., Osawa, S., And Miyata, T. (1989). Evolutionary relationships of archaebacteria, eubacteria and eukaryotes inferred from phylogenetic trees of duplicated genes. *Proc. Natl. Acad. Sci. USA* **86**, 6661-6665.

Jakob, U., Gaestel, M., Engel, K. and Buchner, J. (1993) Small heat shock proteins are molecular chaperones. *J. Biol. Chem.*, **268**, 1517-1520.

Jakob, U., Hauke, L., Meyer, I., and Buchner, J. (1995) Transient interaction of Hsp90 with early unfolding intermediates of citrate synthase. *J. Biol. Chem.* **270**, 7288-7294.

Jecock, R. M. and Devaney, E. (1992) Expression of small heat shock proteins by the third-stage larvae of Brugia pahangi. *Mol. Biochem. Parasitol.* **56**, 219-226.

Joly, E. C., Tremblay, E., Tanguay, R. M., Wu, Y., and Bibor-Hardy, V. (1994) TRiC-P5, a novel TCP1-related protein, is localized in the cytoplasm and in the nuclear matrix. *J. Cell Sci.* **107**, 2851-2859.

Jones, D. and Candido, E. P. M. (1993) Novel ubiquitin-like ribosomal fusion genes from the nematodes *Caenorhabditis elegans* and *Caenorhabditis briggsae. J. Biol. Chem.* **268**, 19545-19551.

Jones, D., Dixon, D. K., Graham, R. W., and Candido, E. P. M. (1989) Differential regulation of closely related members of the *hsp16* gene family in *Caenorhabditis elegans. DNA* **8**, 481-490.

Jones, D., Russnak, R. H., Kay, R. J., and Candido, E. P. M. (1986) Structure, expression, and evolution of a heat shock gene locus in *Caenorbaditis elegans* that is flanked by repetitive elements. *J. Biol. Chem.* **261**, 12006-12015.

Jones, D., Stringham, E. G., Babich, S. L., and Candido, E. P. M. (1996) Transgenic strains of the nematode *C. elegans* in biomonitoring and toxicology: Effects of captan and related compounds on the stress response. *Toxicol.* **109**, 199-127.

Jones, K. A., Kadonaga, J. T., Rosenfeld, P. J., Kelly, T. J., and Tjian, R. (1987) A cellular DNA-binding protein that activates eukaryotic transcription and DNA replication. *Cell* **48**, 79-89.

Kato, K., Hasgawa, K., Goto, S., and Inaguma, Y. (1994) Dissociation as a result of phosphorylation of an aggregated form of the small stress protein, hsp27. *J. Biol. Chem.* **269**, 11274-11278.

Kato, K., Shinohara, H., Kurobe, N., Goto, S., Inaguma, Y., Ohshima, K. (1991) Immunoreactive αA-crystallin in rat non-lenticular tissues detected with a sensitive immunoassay method. *Biochim. Biophys. Acta* **1080**, 173-180.

Kim, S., Willison, K. R., and Horwich, A. L. (1994) Cytosolic chaperonin subunits have a conserved ATPase domain but diverged polypeptide-binding domains. *Trends Biochem. Sci.* **19**, 543-548.

King, C. R. and Piatigorsky (1983) Alternative RNA splicing of the murine αA-crystallin gene: protein-coding information within an intron. *Cell* **32**, 707-712.

Knapp, S., Schmidt-Krey, I., Hebert, H., Bergman, T., Jornvall, H., and Ladenstein, R. (1994) The molecular chaperonin TF55 from archaeon *Sulfolobus solfataricus. J. Mol. Biol.* **242**, 397-407.

Kouyama, T. and Mihashi, K. (1981) Fluorimetry study of N-(1-pyrenyl)iodoacetamide-labelled F-actin. Local structural change of actin protomer both on polymerization and on binding of heavy meromyosin. *Eur. J. Biochem.* **114**, 33-38.

Krause, M. and Hirsh, D. (1986) The actin genes in *Caenorhabditis elegans*. In *Cell and Molecular Biology of the Cytoskeleton*. Shay, J. W., ed. Plenum Publishing Corporation, NY., 151-178.

Krause, M. and Hirsh, D. (1987) A *trans*-spliced leader sequence on actin mRNA in *C. elegans*. *Cell* **49**, 753-761.

Kubota, H., Hynes, G. M., Kerr, S. M., and Willison, K. R. (1997) Tissue-specific subunit of the mouse cytosolic chaperonin-containing TCP-1. *FEBS Lett.* **402**, 53-56.

Kubota, H., Hynes, G., and Willison, K. (1995a) The eighth *Cct* gene, *Cctq*, encoding the theta subunit of the cytosolic chaperonin containing TCP-1. *Gene* **154**, 231-236.

Kubota, H., Hynes, G., and Willison, K. (1995b) The chaperonin containing *t*-complex polypeptide 1 (TCP-1). Multisubunit machinery assisting in protein folding and assembly in the eukaryotic cytosol. *Eur. J. Biochem.* **230**, 3-16.

Kubota, H., Hynes, G., Carne, A., Ashworth, A., and Willison, K. (1994) Identification of six *Tcp-1*-related genes encoding divergent subunits of the TCP-1-containing chaperonin. *Curr. Biol.* **4**, 89-99.

Kubota, H., Willison, K., Ashworth, A., Nozaki, M., Miyamoto, H., Yamamoto, H., Matsushiro, A., and Morita, T. (1992) Structure and expression of the gene encoding mouse *t*-complex polypeptide-1 (*Tcp-1*). *Gene* **120**, 207-215.

Kuntz, I. D. (1971) Hydration of macromolecules. IV. Polypeptide conformation in frozen solutions. *J. Am. Chem. Soc.* **93**, 514-516.

Laemmli, U. D. (1970) Cleavage of structural proteins during the assembly of the head of bacteriophage T4. *Nature* **277**, 680-685.

Landry, J. and Huot, J. (1995) Modulation of actin dynamics during stress and physiological stimulation by a signaling pathway involving p38 MAP kinase and heat-shock protein 27. *Biochem. Cell Biol.* **73**, 703-707.

Landry, J., Chretien, P., Lambert, H., Hickey, E., and Weber, L. A. (1989) Heat shock resistance conferred by expression of the human HSP27 gene in rodent cells. *J. Cell Biol.* **109**, 7-15.

Langer, T., Lu, C., Echols, H., Flanagan, J., Hayer, M. K., and Hartl, F.-U. (1992) Successive action of DnaK, DnaJ and GroEL along the pathway of chaperone-mediated protein folding. *Nature* **356**, 683-689.

Laskey, R. A., Honda, B. M., Mills, A. D., and Finch, J. T. (1978) Nucleosomes are assembled by an acidic protein which binds histones and transfers them to DNA. *Nature* **275**, 416-420.

Laue, T. M., Shah, B. D., Ridgeway, T. M. and Pelletier, S. L. (1992) In *Analytical ultracentrifugation in Biochemistry and polymer Sciences*. Harding, S. E., Rowe, A. J. and Horton, J. C., eds. The Royal Society of Chemistry, Cambridge, UK., 90-125.

Lavoie, J. N., Gingras-Breton, G., Tanguay, R. M., and Landry, J. (1993a) Induction of chinese hamster HSP27 gene expression in mouse cells confers resistance to heat shock. HSP27 stabilization of the microfilament organization. *J. Biol. Chem.* **268**, 3420-3429.

Lavoie, J. N., Hickey, E., Weber, L. A., and Landry, J. (1993b) Modulation of actin microfilament dynamics and fluid phase pinocytosis by phosphorylation of heat shock protein 27. *J. Biol. Chem.* **268**, 24210-24214.

Lavoie, J. N., Lambert, H., Hickey, E., Weber, L. A., and Landry, J. (1995) Modulation of cellular thermoresistance and actin filament stability accompanies phosphorylation-induced changes in the oligomeric structure of heat shock protein 27. *Mol. Cell Biol.* **15**, 505-516.

Lee, G. J., Pokala, N., and Vierling, E. (1995) Structure and *in vitro* molecular chaperone activity of cytosolic small heat shock proteins from pea. *J. Biol. Chem.* **270**, 10432-10438.

Lee, G. J., Roseman, A. M., Saibil, H. R., and Vierling, E. (1997) A small heat shock protein stably binds heat-denatured model substrates and can maintain a substrate in a folding-competent state. *EMBO J.* **16**, 659-671.

Lewis, J. A. and Fleming, J. T. (1995) *Caenorhabditis elegans*: modern biological analysis of an organism. In *Methods in Cell Biology*. Epstein, H. F. and Shakes, D. C., ed. Academic Press, Inc. **38**, 14-15.

Lewis, S. A., Tian, G., Vainberg, I. E., and Cowan, N. J. (1996) Chaperonin-mediated folding of actin and tubulin. *J. Cell Biol.* **132**, 1-4.

Lewis, S. A., Wang, D., and Cowan, A. J. (1988) Microtubule-associated protein MAP2 shares a microtubule binding motif with tau protein. *Science* **242**, 936-939.

Lewis, V. A., Hynes, G. M., Zheng, D., Saibil, H., and Willison, K. (1992) T-complex polypeptide-1 is a subunit of a heteromeric particle in the eukaryotic cytosol. *Nature* **358**, 249-252.

Lillibridge, C. D., Rudin, W., and Philipp, M. T. (1996) Utrastructural localization, molecular characterization, and analysis of the expression of p27, a small heat shock protein homolog of nematodes. *Exp. parasititol.* **83**, 30-45.

Lin, T.-H., Quinn, T., Walsh, M., Grandgenett, D. and Lee, J. C. (1991) Avian myeloblastosis virus reverse transcriptase. Effect of glycerol on its hydrodynamic properties. *J. Biol. Chem.* **266**, 1635-1640.

Linder, B., Jin, Z., Freedman, J. H., and Rubin, C. (1996) Molecular characterization of a novel, developmentally regulated small embryonic chaperone from *Caenorhabditis elegans. J. Biol. Chem.* 271, 30158-30166.

Lindquist, S. and Craig, E. A. (1988) The heat shock proteins. *Annu. Rev. Genet.* **22**, 631-677.

Lingappa, J. R., Martin, R. L., Wong, M. L., Ganem, D., Welch, W. J., and Lingappa, V. R. (1994) A eukaryotic cytosolic chaperonin is associated with a high molecular weight intermediate in the assembly of Hepatitis B virus capsid, a multimeric particle. *J. Cell. Biol.* **125**, 99-111.

Longoni, S., Lattonen, S., Bullock, G., and Chiesi, M. (1990) Cardiac alpha-crystallin. II. Intracellular location. *Mol. Cell. Biochem.* **97**, 121-128.

Lorimer, G. H. (1995) GroEL structure: a new chapter on assisted folding. *Structure* **2**, 1125-1128.

Lubben, T. H., Donaldson, G. K., Viitanen, P. V., Gatenby, A. A. (1989) Several proteins imported into chloroplasts form stable complexes with the GroEL-related molecular chaperone. *Plant Cell* **1**, 1223-1230.

Lubben, T. H., Gatenby, A. A., Donaldson, G. K., Lorimer, G. H., and Viitanen, P. V. (1990) Identification of a GroES-like chaperonin in mitochondria that facilitates protein folding. *Proc. Natl. Acad. Sci. USA* **87**, 7683-7687.

Maercker, C. and Lipps, H. J. (1994) A macronuclear DNA molecule from the hypotrichous ciliate *Stylonychia lemnae* encoding a *t*-complex polypeptide 1-like protein. *Gene* **141**, 147-148.

Mande, S. C., Mehra, V., Bloom, B. R., Hol, W. G. (1996) Structure of the heat shock protein chaperonin-10 of Mycobacterium leprae. *Science* **271**, 203-207.

Marco, S., Carrascossa, J. L., Valpuesta, J. M. (1994) Reversible interaction of β-actin along the channel of the TCP-1 cytoplasmic chaperonin. *Biophys. J.* **67**, 364-368.

Martin, J. and Hartl, F.-U. (1997) Chaperone-assisted protein folding. *Curr. Opin. Struct. Biol.* **7**, 41-52.

Martin, J., Horwich, A. L., and Hartl, F. U. (1992) Prevention of protein denaturation under heat stress by the chaperonin Hsp60. *Science* **258**, 995-998.

Martin, J., Mayhew, M., Langer, T., and Hartl, F.-U. (1993) The reaction cycle of GroEL and GroES in chaperonin-assisted protein folding. *Nature* **366**, 228-233.

Mayhew, M., da Silva, A. C. R., Martin, J., Erdjument-Bromage, H., Tempst, P., and Hartl, F.-U. (1996) Protein folding in the central cavity of the GroEL-GroES chaperonin complex. *Nature* **379**, 420-426.

McLean-Fletcher, S. and Pollard, T. D. (1980) Identification of a factor in conventional muscle actin preparations which inhibits actin filament self-association. *Biochem. Biophys. Res. Commun.* **96**, 18-27.

Mejillano, M. R. and Himes, R. H. (1989) Tubulin dimer dissociation detected by fluoresence anisotropy. *Biochemistry* **28**, 6518-6524.

Melki, R. and Cowan, N. J. (1994) Facilitated folding of actins and tubulins occurs via a nucleotide-dependent interaction between cytoplasmic chaperonin and distinctive folding intermediates. *Mol. Cell. Biol.* **14**, 2895-2904.

Melki, R., Rommelaere, H., Leguy, R., Vandekerckhove, J., and Ampe, C. (1996) Cofactor A is a molecular chaperone required for β-tubulin folding—functional and structural characterization. *Biochem.* **35**, 10422-10435.

Melki, R., Vainberg, I. E., Chow, R. L., and Cowan, N. J. (1993) Chaperonin-mediated folding of vertebrate actin-related protein and γ-tubulin. *J. Cell Biol.* **122**, 1301-1310.

Mello, C. C., Kramer, J. M., Stinchcomb, D., and Ambros, V. (1991) Efficient gene transfer in *C. elegans*: extrachromosomal maintenance and integration of transforming sequences. *EMBO J.* **10**, 3959-3970.

Mello, C. C., Schubert, C., Draper, B., Zhang, W., Lobel, R., Priess, J. R. (1996) The PIE-1 protein and germline specification in C. elegans embryos. *Nature* **382**, 710-712.

Merck, K. B., de Haard-Hoekman, W. A., Oude Essink, B. B., Bloemendal, H., and De Jong, W. W. (1992) Expression and aggregation of recombinant αA-crystallin and its two domains. *Biochim. Biophys. Acta* **1130**, 267-276.

Merck, K. B., Groenen, P. J. T. A., Voorter, C. E. M., de Haard-Hoekman, W. A., Horwitz, J., Bloemendal, H., and De Jong, W. W. (1993a) Structural and functional similarities of bovine α-crystallin and mouse small heat-shock proteins. *J. Biol. Chem.* **268**, 1046-1052.

Merck, K. B., Horwitz, J., Kersten, M., Overkamp, P., Gaestel, M., Bloemendal, H., and De Jong, W. W. (1993b) Comparison of the homologous carboxy-terminal domain and tail of α-crystallin and small heat shock protein. *Mol. Biol. Rep.* **18**, 209-215.

Messing, J. (1983) New M13 vectors for cloning. *Meth. Enzymol.* **101,** 20-78.

Miklos, D., Caplan, S., Mertens, D., Hynes, G., Pitluk, Z., Kashi, Y., Harrison-Lavoie, K., Stevenson, S., Brown, C., Barrell, B., Horwich, A. L., and Willison, K. (1994) Primary structure and function of a second essential member of the heterooligomeric TCP1 chaperonin complex of yeast, TCP1*β*. *Proc. Natl. Acad. Sci. USA* **91**, 2743-2747.

Miron, T., Vancompernolle, K., Vandekerckhove, J., Wilchek, M., and Geiger, B. (1991) A 25-kD inhibitor of actin polymerization is a low molecular mass heat shock protein. *J. Cell Biol.* **114**, 255-261.

Morelle, G. (1989) A plasmid extraction procedure on a miniprep scale. *Focus* **11,** 7-8.

Morimoto, R. I., Tissières, A., and Georgopoulos, C. (1990) The stress response, function of the proteins, and perspectives. In *Stress proteins in biology and medicine.* Morimoto, R. I., ed. Cold Spring Harbor Laboratory Press, NY., 1-36.

Nicholl, I. D. and Quinlan, R. A. (1994) Chaperone activity of α-crystallins modulates intermediate filament assembly. *EMBO J.* **13**, 945-953.

Nimmesgern, E. and Hartl, F.-U. (1993) ATP-dependent protein refolding activity in reticulocyte lysate. Evidence for the participation of different chaperone components. *FEBS Lett.* **331**, 25-30.

Ostermann, J., Horwich, A. L., Neupert, W., and Hartl, F.-U. (1989) Protein folding in mitochondria requires complex formation with hsp 60 and ATP hydrolysis. *Nature* **341**, 125-130.

Palazzolo, M. J., Hamilton, B. A., Ding, D., Martin, C. H., Mead, D. A., Mierendorf, R. C., Raghavan, K. V., Meyerowitz, E. M., and Lipshitz, H. D. (1990) Phage lambda cDNA cloning vectors for subtractive hybridization, fusion-protein synthesis and Cre-*loxP* automatic plasmid subcloning. *Gene* **88,** 25-36.

Parsell, D. A. and Lindquist, S. (1994) Heat shock proteins and stress tolerance. In *The Biology of Heat Shock Proteins and Molecular Chaperones.* Morimoto, R. I., Tissières, A. and Georgopoulos, C., eds. Cold Spring Harbor Laboratory Press, Cold Spring Harbor, NY., 457-494.

Philo, J. S. (1994) In *Modern Analytical Ultracentrifugation: acquisition and interpretation of data for biological and synthetic polymer systems.* Schuster, T. M. and Laue, T. M., eds. Birkhauser, Boston, 156-170.

Phipps, B. M., Hoffmann, A., Stetter, K. O., and Baumeister, W. (1991) A novel ATPase complex selectively accumulated upon heat shock is a major cellular component of thermophilic archaebacteria. *EMBO J.* **10**, 1711-1722.

Phipps, B. M., Typke, D., Hegerl, R., Volker, S., Hoffmann, A., Stetter, K. O., and Baumeister, W. (1993) Structure of a molecular chaperone from a thermophilic archaebacterium. *Nature* **361**, 475-477.

Plasterk, R. H. A. and Groenen, J. T. M. (1992) Targeted alterations of the *Caenorhabditis elegans* genome by transgene instructed DNA double strand break repair following Tc1 excision. *EMBO J.* **11**, 287-290.

Plater, M. L., Goode, D., and Crabbe, M. J. C. (1996) Effects of site-directed mutations on the chaperone-like activity of αB-crystallin. *J. Biol. Chem.* **272**, 28558-28566.

Rahman, D. R. J., Bentley, N. J., and Tuite, M. F. (1995) The *Saccharomyces cerevisiae* small heat shock protein Hsp26 inhibits actin polymerization. *Bioch. Soc. Trans.* **23**, 77S.

Rajaraman, K., Raman, B., and Rao, Ch. M. (1996) Molten-globule state of carbonic anhydrase binds to the chaperone-like α-crystallin. *J. Biol. Chem.* **271**, 27595-27600.

Raman, B. and Rao, C. M. (1994) Chaperone-like activity and quaternary structure of α-crystallin. *J. Biol. Chem.* **269**, 27264-27268.

Rassow, J., Voos, W., and Pfanner, N. (1995) Partner proteins determine multiple functions of Hsp70. *Trends Cell Biol.* **5**, 207-212.

Reading, D.S., Hallberg, R.L., and Myers, A.M. (1989). Characterization of the yeast HSP60 gene coding for a mitochondrial assembly factor. *Nature* **337**, 655-659.

Rivera, M. C., and Lake, J. A. (1992). Evidence that eukaryotes and eocyte prokaryotes are immediate relatives. *Science* **257**, 74-76.

Rommelaere, H., Van Troys, M., Gao, Y., Melki, R., Cowan, N. J., Vandekerckhove, J., and Ampe, C. (1993) Eukaryotic cytosolic chaperonin contains *t*-complex polypeptide 1 and seven related subunits. *Proc. Natl. Acad. Sci. USA* **90**, 11979-11979.

Roobol, A. and Carden, M. J. (1993) Identification of chaperonin particles in mammalian brain cytosol and *t*-complex polypeptide 1 as one of their components. *J. Neurochem.* **60**, 2327-2330.

Roobol, A., Holmes, F. E., Hayes, N. V. L., Baines, A. J., and Carden, M. (1995) Cytoplasmic chaperonin complexes enter neurites developing *in vitro* and differ in subunit composition within single cells. *J. Cell Sci.* **108**, 1477-1488.

Rost, B. and Sander, C. (1993) Prediction of protein secondary structure at better than 70% accuracy. *J. Mol. Biol* **232**, 584-599.

Rost, B. and Sander, C. (1994) Combining evolutionary information and neural networks to predict protein secondary structure. *Proteins* **19**, 55-72.

Russnak, R. H. and Candido, E. P. M. (1985) Locus encoding a family of small heat shock genes in the *Caenorhabditis elegans*: two genes duplicated to form a 3.8-kilobase inverted repeat. *Mol. Cell. Biol.* **5**, 1268-1278.

Russnak, R. H., Jones, D., and Candido, E. P. M. (1983) Cloning and analysis of cDNA sequences coding for two 16 kilodalton heat shock proteins (hsps) in *Caenorhabditis elegans*: homology with the small hsps of *Drosophila*. *Nucleic Acids Res.* **11**, 3187-3205.

Saibil, H. (1996) The lid that shapes the pot—structure and function of the chaperonin GroES. *Structure* **4**, 1-4.

Saiki, R. K., Gelfand, D. H., Stoffel, S. Scharf, S. J., Higuchi, R., Horn, G. T., Mullis, K. B., Erlich, H. A. (1988) Primer-directed enzymatic amplification of DNA with a thermostable DNA polymerase. *Science* **239,** 487-491.

Sambrook, J., Fritsch, E. F., and Maniatis, T. (1989) *Molecular cloning: a laboratory manual,* Cold Spring Harbor Laboratory, NY.

Sanchez, Y. and Lindquist, S. L. (1990) HSP104 required for induced thermotolerance. *Science* **248**, 1112-1115.

Sanchez, Y., Taulien, J., Borkovich, K. A., and Lindquist, S. (1992) Hsp104 is required for tolerance to many forms of stress. *EMBO J.* **11**, 2357-2364.

Sanger, F., Nicklen, S., and Coulson, A. R. (1977) DNA sequencing with chain terminating inhibitors. *Proc. Natl. Acad. Sci. USA* **74**, 5463-5467.

Schirmer, E. C., Glover, J. R., Singer, M. A., and Lindquist, S. (1996) HSP100/Clp proteins: a common mechanism explains diverse functions. *Trends Biochem. Sci.* **21**, 289-296.

Schmidt, A., Kunz, J., and Hall, M. N. (1996) TOR2 is required for organization of the actin cytoskeleton in yeast. *Proc. Natl. Acad. Sci. USA* **93**, 13780-13785.

Sévigny, G., Joly, E. C., Bibor-Hardy, V., and Lemieux, N. (1994) Assignment of the human homologue of the mTRiC-P5 gene (TRIC5) to band 1q23 by fluorescence *in situ* hybridization. *Genomics* **22**, 634-636.

Sévigny, G., Kothary, R., Tremblay, E., De Repentigny, Y., Joly, E. C., and Bibor-Hardy, V. (1995) The cytosolic chaperonin subunit TRIC-P5 begins to be expressed at the two-cell stage in mouse embryos. *Biochem. Biophys. Res. Commun.* **216**, 279-283.

Seydoux, G., Mello, C. C., Pettitt, J., Wood, W. B., Priess, J. R., and Fire, A. (1996) Repression of gene expression in the embryonic germ lineage of *C. elegans*. *Nature* **382**, 713-716.

Shelanski, M. L., Gaskin, F., and Cantor, C. R. (1973) Microtubule assembly in the absence of added nucleotides. *Proc. Natl. Acad. Sci. USA* **70**, 765-768.

Short, J. M., Fernandez, J. M., Sorge, J. A., and Huse, W. D. (1988) λ ZAP: a bacteriophage λ expression vector with *in vivo* excision properties. *Nucleic Acids Res.* **16,** 7583-7600.

Siezen, R. J. and Argos, P. (1983) Structural homology of lens crystallins. III. Secondary structure estimation from circular dichroism and prediction from amino acid sequences. *Biochim. Biophys. Acta* **748**, 55-67.

Siezen, R. J., Bindels, J. G., and Hoenders, H. J. (1980a) The quaternary structure of bovine α-crystallin. Chemical cross-linking with bifunctional imido esters. *Eur. J. Biochem.* **107**, 243-249.

Siezen, R. J., Bindels, J. G., and Hoenders, H. J. (1980b) The quaternary structure of bovine α-crystallin. Effects of variation in alkaline pH, ionic strength, temperature and calcium ion concentration. *Eur. J. Biochem.* **111**, 435-444.

Siezen, R., Bindels, J. G., and Hoenders, H. J. (1979) The interrelationship between monomeric, oligomeric and polymeric α-crystallin in the calf lens nucleus. *Exp. Eye Res.* **28**, 551-567.

Singh, K., Groth-Vasselli, B., Farnsworth, P. N. (1996) Electrostatic parameters of the theoretical quaternary structure of bovine α-crystallin. *Int. J. Bio. Macromol.* **18**, 205-209.

Singh, M., Brooks, G. C., and Srere, P. A. (1970) Subunit structure and chemical characteristics of pig heart citrate synthase. *J. Biol. Chem.* **245**, 4636-4640.

Smulders, R. H. P. H., Carver, J. A., Lindner, R. A., van Boekel, M. A. M., Bloemendal, H., and De Jong, W. W. (1996) Immobilization of the C-terminal extension of bovine αA-crystallin reduces chaperone-like activity. *J. Biol. Chem.* **271**, 29060-29066.

Smulders, R. H. P. H., Merck, K. B., Aendekerk, J., Horwitz, J., Takemoto, L., Slingsby, C., Bloemendal, H., and De Jong, W. W. (1995) The mutation Asp69→Ser affects the chaperone-like activity of αA-crystallin. *Eur. J. Biochem.* **232**, 834-838.

Soares, H., Penque, D., Mouta, C., and Rodrigues-Pousada, C. (1994) A *Tetrahymena* orthologue of the mouse chaperonin subunit CCTγ and its coexpression with tubulin during cilia recovery. *J. Biol. Chem.* **269**, 29299-29307.

Sorger, P. (1991) Heat shock factor and the heat shock response. *Cell* **65**, 363-366.

Spudich, J. A. and Watt, S. (1971) The regulation of rabbit skeletal muscle contraction. I. Biochemical studies of the interaction of the tropomyosin-troponin complex with actin and the proteolytic fragments of myosin. *J. Biol. Chem.*, **246** 4866-4871.

Stafford, W. F., III (1992) Boundary analysis in sedimentation transport experiments: a procedure for obtaining sedimentation coefficient distributions using the time derivative of the concentration profile. *Analyt. Biochem.* **203**, 295-301.

Staros, J. V. (1982) N-hydroxysulfosuccinimide active esters: *Bis*(N-hydroxysuccinimide) esters of two dicarboxylic acids are hydrophilic, membrane impermeant, protein cross-linkers. *Biochem.* **21**, 3950-3955.

Sternberg, N. (1973) Properties of a mutant of Escherichia coli defective in bacteriophage λ head formation (groE). II. The propagation of phage λ. *J. Molec. Biol.* **76**, 25-44.

Sternlicht, H., Farr, G. W., Sternlicht, M. L., Driscoll, J. K., Willison, K., and Yaffe, M. B. (1993) The T-complex polypeptide 1 complex is a chaperonin for tubulin and actin *in vivo*. *Proc. Natl. Acad. Sci. USA* **90**, 9422-9426.

Stoldt, V., Rademacher, F., Kehren, V., Ernst, J. F., Pearce, D. A., and Sherman, F. (1996) Review: the Cct eukaryotic chaperonin subunits of *Saccharomyces cerevisiae* and other yeasts. *Yeast* **12**, 523-529.

Straus, D. B., Walter, W. A., and Gross, C. A. (1988) *Escherichia coli* heat shock gene mutants are defective in proteolysis. *Genes Dev.* **2**, 1851-1858.

Stringham, E. G., Dixon, D. K., Jones, D., and Candido, E. P. M. (1992) Temporal and spatial expression patterns of the small heat shock (*hsp16*) genes in transgenic *Caenorhabditis elegans Molec. Biol. Cell* **3**, 221-233.

Studier, F. W. and Moffatt, B. A. (1986) Use of bacteriophage T7 RNA polymerase to direct selective high-level expression of cloned genes. *J. Mol. Biol.* **189**, 113-130.

Studier, F. W., Rosenberg, A. H., Dunn, J. J., and Dubendorff, J. W. (1990) Use of T7 RNA polymerase to direct expression of cloned genes. *Methods Enzymol.* **185**, 60-89.

Sulston, J. E. and Brenner, S. (1974) The DNA of *Caenorhabditis elegans. Genetics* **77**, 95-104.

Sulston, J. E. and Horvitz, H. R. (1977) Post-embryonic cell lineages of the nematode, *Caenorhabditis elegans. Dev. Biol.* **56**, 110-156.

Sulston, J. E., Schierenberg, E., White, J. G., and Thomson, J. N. (1983) The embryonic cell lineage of the nematode *Caenorhabditis elegans. Dev. Biol.* **100**, 64-119.

Sulston, J., Du, Z., Thomas, K., Wilson, R., Hillier, L., Staden, R., Halloran, N., Green, P., Thierry-Mieg, J., Qiu, L., Dear, S., Coulson, A., Craxton, M., Durbin, R., Berks, M., Metzstein, M., Hawkins, T., Ainscough, R., and Waterston, R. (1992). The *C. elegans* genome sequencing project: a beginning. *Nature* **356,** 37-41.

Sun, H. B., Neff, A. W., Mescher, A. L., and Malacinski, G. M. (1995) Expression of the axolotl homologue of mouse chaperonin *t*-complex protein-1 during early development. *Biochim. Biophys. Acta* **1260**, 157-166.

Takemoto, L., Emmons, T., and Horwitz, J. (1993) The C-terminal region of α-crystallin: involvement in protection against heat-induced aggregation. *Biochem. J.* **294**, 435-438.

Tardieu, A., Laporte, D., Licinio, P., Krop, B., and Delaye, M. (1986) Calf lens α-crystallin quaternary structure: a three-layer tetrahedral model. *J. Mol. Biol.* **192**, 711-724.

Tian, G., Huang, Y., Rommelaere, H., Vandekerckhove, J., Ampe, C., and Cowan, N. J. (1996) Pathway leading to correctly folded beta-tubulin. *Cell* **86**, 287-296.

Tian, G., Vainberg, I. E., Tap, W. D., Lewis, S. A., and Cowan, N. J. (1995) Specificity in chaperonin-mediated protein folding. *Nature* **375**, 250-253.

Trent, J. D., Nimmesgern, E., Wall, J. S., Hartl, F.-U., and Horwich, A. L. (1991) A molecular chaperone from a thermophilic archaebacterium is related to the eukaryotic protein t-complex polypeptide-1. *Nature* **354**, 490-493.

Tweedie, S., Grigg, M. E., Ingram, L., and Selkirk, M. E. (1993) The expression of a small heat shock protein homologue is developmentally regulated in *Nippostrongylus braziliensis*. *Mol. Biochem. Parasitol.* **61**, 149-154.

Ursic, D. and Culbertson, M. R. (1991) The yeast homolog to mouse TCP-1 affects microtubule-mediated processes. *Mol. Cell Biol.* **11**, 2629-2640.

Ursic, D. and Culbertson, M. R. (1992) Is yeast TCP1 a chaperonin? *Nature* **356**, 392.

Ursic, D. and Ganetzky, B. (1988) A *Drosophila melanogaster* gene encodes a protein homologous to the mouse *t* complex polypeptide 1. *Gene* **68**, 267-274.

Ursic, D., Sedbrook, J. C., Himmel, K. L., and Culbertson, M. R. (1994) The essential yeast TCP-1 protein affects actin and microtubules. *Mol. Biol. Cell* **5**, 1065-1080.

Van Berkel, J., Salamini, F., and Gebhardt, C. (1994) Transcripts accumulating during cold storage of potato (*Solanum tuberosum L.*) tubers are sequence related to stress-responsive genes. *Plant Physiology* **104**, 445-452.

Van den Oetelaar, P. J. and Hoender, H. J. (1989) Folding-unfolding and aggregation-dissociation of bovine alpha-crystallin subunits; evidence for unfolding intermediates of the αA subunits. *Biochim. Biophys. Acta* **995**, 91-96.

Vandekerckhove, J. (1990) Actin-binding proteins. *Curr. Opin. Cell Biol.* **2**, 41-50.

Vandenbergh, D. J., James-Pederson, M., and Hardison, R. C. (1991) An apparent pause site in the transcription unit of the rabbit α-globin gene. *J. Mol. Biol.* **220**, 255-270.

Viale, A. M. and Arakaki, A. K. (1994) The chaperone connection to the origins of the eukaryotic organelles. *FEBS Lett.* **341**, 146-151.

Vierling, E. and Sun, A. (1989) Developmental expression of heat shock proteins in higher plants. In *Environmental stress in plants*. Cherry, J., ed. Springer-Verlag, Berlin, 343-354.

Viitanen, P., Gatenby, A. A., and Lorimer, G. H. (1992) Purified chaperonin 60 (groEL) interacts with the nonnative states of a multitude of *Escherichia coli* proteins. *Protein Sci.* **1**, 363-369.

Vinh, D. B.-N. and Drubin, D. G. (1994) A yeast TCP-1-like protein is required for actin function *in vivo*. *Proc. Natl. Acad. Sci. USA* **91**, 9116-9120.

Waldmann, T., Lupas, A., Kellermann, J., Peters, J., and Baumeister, W. (1995a) Primary structure of the Thermosome from *Thermoplasma acidophilum*. *Biol. Chem. Hoppe-Seyler* **376**, 119-126.

Waldmann, T., Nimmesgern, E., Nitsch, M., Peters, J., Pfeifer, G., Müller, S., Kellermann, Engel, A., Hartl, F.-U., and Baumeister, W. (1995b) The thermosome of *Thermoplasma acidophilum* and its relationship to the eukaryotic chaperonin TRiC. *Eur. J. Biochem.* **227**, 848-856.

Waldmann, T., Nitsch, M., Klumpp, M., and Baumeister, W. (1995c) Expression of an archaeal chaperonin in *E. coli*: formation of homo-(α, β) and hetero-oligomeric (α+β) thermosome complexes. *FEBS Lett.* **376**, 67-73.

Walkley, N. A., Page, R. A., and Malik, A. N. (1996) Molecular characterisation of the *Xenopus laevis* chaperonin gene *Cctg*. *Biochim. Biophys. Acta* **1309**, 25-30.

Walsh, M. T., Sen, A. C., and Chakrabarti, B. (1991) Micellar subunit assembly in a three-layer model of oligomeric α-crystallin. *J. Biol. Chem.* **266**, 20079-20084.

Wang, K. and Spector, A. (1994) The chaperone activity of bovine α crystallin. *J. Biol. Chem.* **269**, 13601-13608.

Wang, K. and Spector, A. (1996) α-crystallin stabilizes actin filaments and prevents cytochalasin-induced depolymerization in a phosphorylation-dependent manner. *Eur. J. Biochem.* **242**, 56-66.

Wang, S., Sakai, H., Wiedmann, M. (1995) NAC covers ribosome-associated nascent chains thereby forming a protective environment for regions of nascent chains just emerging from the peptidyl transferase center. *J. Cell Biol.* **130**, 519-528.

Waters, E. R., Lee, G. J. and Vierling, E. (1996) Evolution, structure and function of the small heat shock proteins in plants. *J. Exp. Bot.* **47**, 325-338.

Waterston, R., Martin, C., Craxton, M., Huynh, C., Coulson, A., Hillier, L., Durbin, R., Green, P., Shownkeen, R., Halloran, N., Metzstein, M., Hawkins, T., Wilson, R., Berks, M., Du, Z., Thomas, K., Thierry-Mieg, J., and Sulston, J. (1992) A survey of expressed genes in *Caenorhabditis elegans*. *Nature Genet.* **1,** 114-123.

Weingarten, M. D., Lockwood, A. H., Hwo, S. Y., and Kirschner, M. W. (1975) A protein factor essential for microtubule assembly. *Proc. Natl. Acad. Sci. USA* **72**, 1858-1862.

Weissman, J. S., Hohl, C. M., Kovalenko, O., Kashi, Y., Chen, S., Braig, K., Saibil, H. R., Fenton, W. A., and Horwich, A. L. (1995) Mechanism of GroEL action: productive release of polypeptide from a sequestered position under GroES. *Cell* **83**, 577-587.

Weissman, J. S., Rye, H. S., Fenton, W. A., Beechem, J. M., and Horwich, A. L. (1996) Characterization of the active intermediate of a GroEL-GroES-mediated protein folding reaction. *Cell* **84**, 481-490.

Welch, W. J. (1993) Heat shock proteins functioning as molecular chaperones: their roles in normal and stressed cells. *Philos. Trans. R. Soc. Lond. B Biol. Sci.* **339**, 327-333.

Welch, W. J. and Suhan, J. P. (1985) Morphological study of the mammalian stress response: characterization of changes in cytoplasmic organelles, cytoskeleton, and nucleoli, and appearance of intranuclear actin filaments in rat fibroblasts after heat-shock treatment. *J. Cell Biol.* **101**, 1198-1211.

White, J. G., Southgate, E., Thomson, J. N., and Brenner, S. (1986) The structure of the nervous system of *Caenorhabditis elegans*. *Philos. Trans. R. Soc. Lond. B Biol. Sci.* **314**, 1-340.

Wiech, H., Buchner, J., Zimmermann, R. and Jakob, U. (1992) Hsp90 chaperones protein folding *in vitro*. *Nature*, **358**, 169-170.

Wiedmann, B., Sakai, H., Davis, T. A., and Wiedmann, M. (1994) A protein complex required for signal-sequence-specific sorting and translocation. *Nature* **370**, 434-440.

Willison, K. R. and Kubota, H. (1994) The structure, function, and genetics of the chaperonin containing TCP-1 (CCT) in eukaryotic cytosol. In *The Biology of Heat Shock Proteins and Molecular Chaperones*. R. I. Morimoto, A. Tissières, and C. Georgopoulos, eds. Cold Spring Harbor Laboratory Press, Cold Spring Harbor, NY., 299-312.

Willison, K. R., Dudley, K., and Potter, J. (1986) Molecular cloning and sequence analysis of a haploid gene expressed encoding *t* complex polypeptide 1. *Cell* **44**, 727-738.

Willison, K. R., Hynes, G., Davies, P., Goldsborough, A., and Lewis, V. A. (1990) Expression of three *t*-complex genes, *Tcp-1*, *D17Leh117c3*, and *D17Leh66*, in purified murine spermatogenic cell populations. *Gen. Res.* **56**, 193-201.

Willison, K., Lewis, V. A., Zuckerman, K. S., Cordell, J., Dean, C., Miller, K., Lyon, M. F., and Marsh, M. (1989) The *t* complex polypeptide 1 (TCP-1) is associated with the cytoplasmic aspect of Golgi membranes. *Cell* **57**, 621-632.

Wilson, R., Ainscough, R., Anderson, K., Baynes, C., Berks, M., Bonfield, J., Burton, J., Connell, M., Copsey, T., Cooper, J., Coulson, A., Craxton, M., Dear, S., Du, Z., Durbin, R., Favello, A., Fraser, A., Fulton, L., Gardner, A., Green, P., Hawkins, T., Hillier, L., Jier, M., Johnston, L., Jones, M., Kershaw, J., Kirsten, J., Laisster, N., Latreille, P., Lightning, J., Lloyd, C., Mortimore, B., O'callaghan, M., Parsons, J., Percy, C., Rifken, L., Roopra, A., Saunders, D., Shownkeen, R., Sims, M., Smaldon, N., Smith, A., Smith, M., Sonnhammer, E., Staden, R., Sulston, J., Thierry-Mieg, J., Thomas, K., Vaudin, M., Vaughan, K., Waterston, R., Watson, A., Weinstock, L., Wilkinson-Sproat, J., And Wohldman, P. (1994) 2.2 Mb of contiguous nucleotide sequence from chromosome III of *C. elegans*. *Nature* **368**, 32-38.

Wistow, G. (1985) Domain structure and evolution in α-crystallins and small heat-shock proteins. *FIBS Lett.* **181**, 1-6.

Wistow, G. (1993) Possible tetramer-based quaternary structures for α-crystallin and small heat shock proteins. *Exp. Eye Res.* **56**, 729-732.

Wood, W. B. (1988) Introduction to *C. elegans* biology. In *The nematode Caenorhabditis elegans*. W. B. Wood, and the community of *C. elegans* researchers, eds. Cold Spring Harbor Laboratory Press, Cold Spring Harbor, NY., 1-16.

Wotton, D., Freeman, K., and Shore, D. (1996) Multimerization of Hsp42p, a novel heat shock protein of *Saccharomyces cerevisiae*, is dependent on a conserved carboxyl-terminal sequence. *J. Biol. Chem.* **271**, 2717-2723.

Yaffe, M. B., Farr, G. W., Miklos, D., Horwich, A. L., Sternlicht, M. L., and Sternlicht, H. (1992) TCP1 complex is a molecular chaperone in tubulin biogenesis. *Nature* **358**, 245-248.

Yanisch-Perron, C., Vieira, J., and Messing, J. (1985) Improved M13 phage cloning vectors and host strains: Nucleotide sequences of the M13mp18 and pUC19 vectors. *Gene* **33,** 103-119.

Yeh, K. W., Jinn, T. L., Yeh, C. H., Chen, Y. M., and Lin, C. Y. (1994) Plant low-molecular-mass heat-shock proteins: their relationship to the acquisition of thermotolerance in plants. *Biotech. and Appl. Biochem.*, **19**, 41-49.

Zav'yalov, V. P., Zav'yalova, G. A., Denesyuk, A. I., Gaestel, M., and Korpela, T. (1995) Structural and functional homology between periplasmic bacterial molecular chaperones and small heat shock proteins. *FEMS Immunol. Med. Microbiol.* **11**, 265-272.

Zhen, M. (1995) Cloning, characterization and functional analysis of *ubc-2*, a gene encoding a ubiquiting-conjugating enzyme in the nematode, *Caenorhabditis elegans*. Ph.D. thesis, University of British Columbia, Vancouver, B. C., Canada.

Zhi, W., Landry, S. J., Gierasch, L. M., and Srere, P. A. (1992) Renaturation of citrate synthase: influence of denaturant and folding assistants. *Protein Sci.* **1**, 522-529.

Zhu, X., Zhao, X., Burkholder, W. F., Gragerov, A., Ogata, C. M., Gottesman, M. E., and Hendrickson, W. A. (1996) Structural analysis of substrate binding by the molecular chaperone DnaK. *Science* **272**, 1606-1614.

APPENDIX

I. Bacterial strains used in this study

Table 1. *E. coli* strains used for plasmid propagation and protein expression.

Strain	Genotype	Use
DH5α[a]	*supE*44 Δ*lac* U169 (ϕ80 *lacZ*ΔM15) *hsdR*17 *recA*1 *endA*1 *gyrA*96 *thi*-1 *relA*1	Propagation of plasmids for subcloning and sequencing
JM109[b]	*recA1 supE*44 *endA*1 *hsdR*17 *gyrA*96 *relA*1 *thi* Δ(*lac-proAB*) F'[*t r a D*36 *p r o A B*+ lacI *lacZ*ΔM15]	Electrotransformation with plasmid DNA
BM25.8[c]	*recA*+ F' Tc^S λ*imm*434*kan* P1CmRr$^-$m$^-$	Conversion of λSHLX2 clones to pRatII plasmids
BL21(DE3)[d]	*hsdS gal* (λcI*ts*857 *ind*1 *S*am7 *nin*5 *lac*UV5-T7 gene *1*	Propagation of bacterial expression vectors

a. Hanahan, 1983.
b. Yanisch-Perron *et al.*, 1985.
c. Palazollo *et al.*, 1990.
d. Studier and Moffatt, 1986.

II. List of oligonucleotides used in this study

Table 2. Oligodeoxyribonucleotides used for sequencing, PCR, and/or subcloning.

Name	Sequence (5'→3')[a]	Position spanned
	primers for CCT studies	
MIC1	AGTCTGATGTGCATGGCGGCTC	462→-441 (*cct-1* gene)[b]
MIC2	GCATCAGCTGGAGATTC	4→20 (*cct-1* gene)
MIC3	CAGAATTGTGGCTCCG	242→227 (*cct-1* gene)
MIC4	ACGGATCGAATTGCAGCACCAG	2530→2508 (*cct-1* gene)
MIC5	GCAGTCGACGCGATCGCAACTGCCGCGGT *Sal*I	142→123 (*cct-1* gene)
MIC6	CTTGCTCAATTGCCAAC	1308→1325 (*cct-2* cDNA)
MIC7	TGGACACTGACAAAGTG	713→729 (*cct-2* cDNA)
MIC8	ACTTCACATTGTAAGAC	1483→1467 (*cct-2* cDNA)
MIC9	CCAGAAATGATCGTCTG	377→361 (*cct-2* cDNA)
MIC10	TGAGGATCCATGCGCGAGATCGTTC *Bam*HI	1→16 (*mec-7* cDNA)
MIC11	TAATACGGTTGTGTTTCAGG	-23→-3 (*cct-1* gene)
MIC12	TATTACCAAACGCCGCATTG	949→968 (*cct-1* gene)
MIC13	AGAACAACGTTGGCTCCGGC	1002→983 (*cct-1* gene)
MIC14	ATATAAACGGGGTAAACGGG	1974→1955 (*cct-1* gene)
OZM12	TCACAAGCTGATCGACTCGATGCCACGTCG	binds Tc1 sequence
OZM13	GATTTTGTGAACACTGTGGTGAAG	binds Tc1 sequence
SL1	GGTTTAATTACCCAAGTTTGAG	binds splice leader 1
SL2	GTTTTAACCCAGTTACTCAA	binds splice leader 2
oligodT	CGAGCATGCGTCGACAGGCA$(T)_{17}$	binds polyA
	primers for small HSP studies	
OH2-A	GACTCGAGGTGATCTTATGAG *Xho*I	46→59 (*hsp16-2* cDNA)
OH2-C	GCTGAATTCTTATCCTTGAACCGCTTCTTTC *Eco*RI	387→369 (*hsp16-2* cDNA)
OBM1	GCGTGGATCCATGTCACTTTACCACTATTTC *Bam*HI	1→21 (*hsp16-2* cDNA)
OBM2	CGATGAATTCGTTATTCAGCAGATTTCTCTTCGAC *Eco*RI	438→415 (*hsp16-2* cDNA)

Table 2 cont'd. Oligodeoxyribonucleotides used for sequencing, PCR, and/or subcloning.

Name	Sequence (5'→3')[a]	Position spanned
OH48-A	CTACATATGCTCATGCTCCGTTC *Nde*I	1→17 (*hsp16-48* cDNA)
OH48-B	CTAGGATCCAAGATTAATGTTTTGCAAC *Bam*HI	432→414 (*hsp16-48* cDNA)
F38A	ATGGGATCCATGATGAGCGTTCCAGTG *Bam*HI	1→18 (*hsp12.6* cDNA)
F38B	ATGAAGCTTTTAATGCATTTTTCTTGCTTC *Hin*dIII	333→313 (*hsp12.6* cDNA)
HSP13B.5	AGTCATATGTCTGTTGCTATTGATCAC *Nde*I	1→21 (*hsp12.3* cDNA)
HSP13B.3	GCTGGATCCTTACTTTTTCTTGTTTCCGGAGATGTG *Bam*HI	330→304 (*hsp12.3* cDNA)
	Vector-specific primers	
RG02	GTGTGGAATTGTGAGCGGAT	860→841 (pBSII KS, MCS)[c]
RG05	AGGGTTTTCCCAGTCACGAC	577→596 (pBSII KS, MCS)
KS	CGAGGTCGACGGTATCG	743→727 (pBSII KS, MCS)
SK	TCTAGAACTAGTGGATC	677→693 (pBSIIKS, MCS)
T3	ATTAACCCTCACTAAAG	790→774 (pBSII KS, MCS)
T7	AATACGACTCACTATAG	627→643 (pBSII KS, MCS)
SP6-5'	ATAGAATATGCATCAAGCTGAG	pRAT II MCS (5' of cDNA)
T7-3'	ACTATAGGGAGCTAAGCTTGG	pRAT II MCS (3' of cDNA)

a. Some PCR primers contain engineered restriction sites at their 5'-ends (underlined). These sites are for subcloning purposes only and are not complementary to the target sequence.

b. Numbering for the *cct* genes follows the convention of increasingly positive numbers beginning with the first nucleotide in the start codon (ATG, where A is +1), and increasingly negative numbers 5' of the start codon (-1, -2, etc.). Numbering for cDNAs begins from the start codon (ATG, where A is +1).

c. The numbering used here parallels that of the pBluescript plasmid restriction map in the Stratagene® catalogue. MCS, Multiple Cloning Site.

III. Conditions used for polymerase chain reactions

Table 3. Summary of PCR conditions used for amplifying DNA from various sources.

Sample	Plasmid DNA	cDNA	Genomic DNA	Cosmid DNA
Concentration	1 ng/µl	~300 ng/µl	500 ng/µl	~5 ng/µl
Sample DNA	1.0 µl	2.0	1.0	1.0
Oligo 1 (50 pmol/µl)	1.0 µl	1.0	1.0	1.0
Oligo 2 (50 pmol/µl)	1.0 µl	1.0	1.0	1.0
10X PCR buffer[a]	5.0 µl	5.0	5.0	5.0
$MgCl_2$ (25 mM)[b]	3.0 µl	3.0	3.0	3.0
dNTPs[c]	1.0 µl	1.0	1.0	1.0
dH_2O	37.75 µl	36.75	37.75	37.75
Taq DNA pol. (5 U/µl)[d]	0.25 µl	0.25	0.25	0.25
total volume	50 µl	50 µl	50 µl	50 µl

a. Promega 10X PCR buffer: 500 mM KCl, 100 mM Tris-HCl (pH 9.0), 1.0% Triton X-100

b. The final $MgCl_2$ concentration used (1.5 mM) was sometimes adjusted to 0.5 or 1.0 mM.

c. 5 mM of each deoxyribonucleotide (dATP, dCTP, dGTP, and dTTP) in 20 mM $MgCl_2$

d. Taq DNA polymerase enzyme was purchased from Promega or Pharmacia; *Pfu* DNA polymerase (Stratagene) was sometimes used because of its proof-reading function.

IV. Large-scale culturing of *C. elegans* and isolation of embryos

4.1 Maintenance of *C. elegans* on plates and in liquid media

The *C. elegans* Bristol (N2) strain was maintained on NG plates (0.3% NaCl, 0.25% tryptone, 1 mM $CaCl_2$, 1 mM $MgSO_4$, 10 µg/ml cholesterol, 25 mM KH_2PO_4, and 1.7% agarose) spread with a lawn of *E. coli* OP50 (Brenner, 1974). Nematodes were grown in a vigorously aerated liquid growth medium consisting of 50 mM KH_2PO_4/K_2HPO_4 buffer (pH 6.0), 2 mM potassium citrate (pH 6.0), 100 mM NaCl, 0.3 mM $CaCl_2$, 0.3 mM $MgSO_4$, and trace metals (0.5 ml of a 2.5 mM $FeSO_4$, 1 mM $MnCl_2$, 1 mM $ZnSO_4$, and 0.1 mM $CuSO_4$ solution per litre). Frozen *E. coli* (K12, log phase, from U. of Alabama Fermentation Facility) was added periodically as a food source. Synchronous nematode populations were obtained by isolating embryos from gravid adults and allowing the embryos to hatch completely in the absense of food, thereby causing them to arrest at the L1 stage.

4.2 Preparatory culture used for inoculating 20 litre culture

Two 250-ml cultures were grown and the embryos harvested and floated on a sucrose cushion essentially according to Sulston and Brenner (1974). Following this, two one-litre cultures were each inoculated with approximately 6 million of the embryos. The embryos were allowed to hatch in the absence of food for 15 hours at 15°C, and 15 g of frozen *E. coli* was then added to each culture. Over the course of 6 days, an additional 35-40 g of frozen *E. coli* was added to each culture. The embryos were then harvested and floated. This gave 7.5 g of packed, live embryos (*i.e.*, embryos not staining blue upon incubation with a methylene blue solution). These were placed in 200 ml of liquid medium without food and allowed to hatch completely overnight at 15°C.

4.3 First 20-litre culture

18.5 litres of water and one litre of 20X Basal S (117 g NaCl in 1 M potassium phosphate pH 6.0) were autoclaved *in situ* in a 35-litre fermenter. The following solutions were filter-

sterilized into the medium after cooling to room temperature: 12 ml $CaCl_2$ (1 M), 12 ml $MgSO_4$ (1 M), 40 ml potassium citrate pH 5.75 (1 M), 10 ml trace metals, 40 ml cholesterol (5 mg/ml in EtOH), and 25 ml antifoam C (Sigma).

The L1 larvae were then added via an ethanol-rinsed funnel, as was 500 g of frozen *E. coli* (thawed completely in 300 ml of Basal S at 50°C for about 3 hours). The air flow was adjusted from the beginning to 20 litres/min, and the stirring rate was set to 250 rpm to maintain proper aeration. The rpm was increased to 300, then 420 after the first and second days following inoculation. Antifoam C was added periodically to keep frothing to a minimum; about 40-50 ml of the antifoam was added in total. 45 hours after inoculation, an extra 250 g of thawed *E. coli* in 150 ml of Basal S was added to the culture (concomitantly with 10 ml of antifoam). The temperature of the culture was maintained at 20°C except for the final 15 hours, where it was increased to 20.7°C to allow the adults to become fully gravid (*i.e.*, contain at least 10 embryos per nematode).

After 72 hours, the nematodes were harvested. The 20-litre culture was subdivided equally into five-10 litre buckets, which were placed on a large tray filled with ice. The buckets were stored in a cold room at 4°C for 3 hours, allowing the nematodes to settle completely. Approximately 4.2 litres of the top layer from the 5-litre cultures were removed. This left a total of four litres of culture, which was centrifuged in 50 ml Falcon tubes (2000 x *g* for 2 minutes), and divided such that each tube had between 5-6 ml of packed nematodes. These were kept on ice.

Isolation of embryos was carried out using an alkaline hypochlorite treatment as described previously (Emmons *et al.*, 1979). This was done most efficiently using these guidelines:

1. pack 5-6 ml of nematodes and remove all supernatant
2. add 50 ml of bleaching solution (88 ml dH_2O, 12 ml bleach, 2 g NaOH per 100 ml)
3. shake vigorously for 2 min and then centrifuge at 2000 rpm in a benchtop centrifuge
4. remove supernatant completely, and add 45-50 ml of fresh bleaching solution
5. shake vigorously until the total elapsed time from the first addition of bleach is 9 min
6. centrifuge, remove supernatant, then wash twice with 0.14 M NaCl
7. remove supernatant, combine embryos into one 50-ml tube, and add NaCl to 50 ml
8. keep on ice until ready–check for viability and presence of undissolved nematodes

The yield for the 20-litre culture was 73 g of unfloated embryos, although 18 g were accidentally lost during the procedure. The preparation was sufficiently clean to avoid sucrose flotation, and viability of the embryos, as judged by methylene blue exclusion was greater than 90%. 50 g of embryos was made into a 50% slurry by adding 50 ml of homogenization buffer (250 mM sucrose, 10 mM Tris pH 8.0, 10 mM $MgCl_2$). The slurry was frozen dropwise in liquid nitrogen, and stored in 4 separate vials. The remaining 15 g of unfloated embryos were added to 200 ml liquid medium and allowed to starve-hatch overnight at 15°C, and then for about 8 hours at room temperature to ensure complete hatching.

4.4 Second 20-litre culture

The starve-hatched nematodes were used to inoculate a 20-litre culture identical to the first. 500 g of thawed *E. coli* (in 250 ml of Basal S) was added to the embryos, as well as 25 ml of Antifoam C. The rpm level was kept at 215 initially, raised to 275 after 15 hours of inoculation, and was maintained at approximately 420 after about 36 hours. After 48 hours, an additional 250 g of thawed *E. coli* were added (in 150 ml Basal S). The rpm was increased to a final value of 490. During this run, the pH of the culture increased above the optimal 6.0, so to keep the pH below this level, glacial acetic acid, diluted three-fold in distilled water, was added periodically.

After growing for 3 days at 20°C and overnight at 14°C, the nematodes were harvested as before. These were packed to approximately 5 ml and bleached as before except that the spin after the second bleach was initiated after only 7.5 min, and not 9 min as before. The reason for this is that the nematodes were harvested at a slightly later stage than in the first isolation, and less bacteria was present. This resulted in more efficient bleaching. The eggs were floated on a sucrose cushion as there was a greater amount of undissolved debris compared to the first isolation. Flotation was performed by packing eggs to a volume of about 8 ml, resuspending in 0.14 M NaCl to a volume of 20 ml, adding 20 ml of 60% (w/v) sucrose, briefly mixing, and centrifuging at 2000 rpm. The floated eggs were then washed twice in the salt solution, centrifuged, and frozen in liquid nitrogen as a 50% slurry. The final yield of floated eggs was 61 g, so 111 g were frozen and stored in 6 separate vials.

V. Transgenic lines generated and used in this study

The following *C. elegans* transient or integrated transgenic line stocks are available frozen in liquid nitrogen in the containers shown:

Strain	Integrated?	Can#	Cane#	Description
NL708/PK58	No	OR#5	M1	*cct-1*::*Tc1* insertion strain
PC146 UbEx132 (#8)	Maybe	OR#5	P100	*cct-1* promoter-*lacZ* (pPD16.43.5'.3')
PC147 UbEx133 (#9)	No	OR#5	P101	*cct-1* promoter-*lacZ*
PC148 UbEx134 (#11)	No	OR#5	P102	*cct-1* promoter-*lacZ*
PC149 UbEx135 (#16)	No	OR#5	P103	*cct-1* promoter-*lacZ*

Note: all strains except the first are in an N2 background contain the pRF4 selection marker.

VI. *C. elegans* strain containing a Tc1 insertion in *cct-1* gene

The *C. elegans* strain NL708/PK58 (*cct-1*::Tc1) contains a Tc1 insertion between the stop codon and polyadenylation signal (**Figure 31**). This location corresponds to nt 2145 in the *cct* genomic sequence. The strain has not been outcrossed to wild-type N2s to remove other possible disruptions caused by multiple Tc1 insertions.

```
C  H  A  *
TGCCACGCTTAAattttcccgtttaccccgtttatatatccctgttttccgcgtgcttctcacata<Tc1>attccg
atctgctgctccttatcccaaattctcatgttcagcttttgttttcttcttttgatgatactttattgaacgaaatg
ttgtaagttttaatgttttgatttcaaagttgtttgtattcgtttttcattattcaaacaatgaagaagctttgcca
```

Figure 31. *C. elegans* strain NL708/PK58 contains a Tc1 insertion near *cct-1*. Two sets of nested PCR primers (MIC1/MIC2 at the 5'-end and MIC3/MIC4 at the 3'-end) flanking *cct-1* were designed and used to isolate a strain from a Tc1-insertion bank containing a Tc1 insertion near *cct-1* (this strain was isolated by Ronald Plasterk). The region containing the Tc1 insertion site was then amplified by nested PCR using MIC1/OZM12 and then MIC2/OZM13 (which yields an ~2 kb frament). This fragment was then subcloned into pBS and sequenced. Shown here are the last three codons of *cct-1* (including amino acid above), the location of the Tc1 insertion (labeled **<Tc1>**), and the polyadenylation signal (shown in bold).

VII. Antibodies used in this study

Various polyclonal antibodies were produced and used for detection of specific proteins in Western blots. The specificity of each antibody for one or more proteins is shown in **Figure 32**.

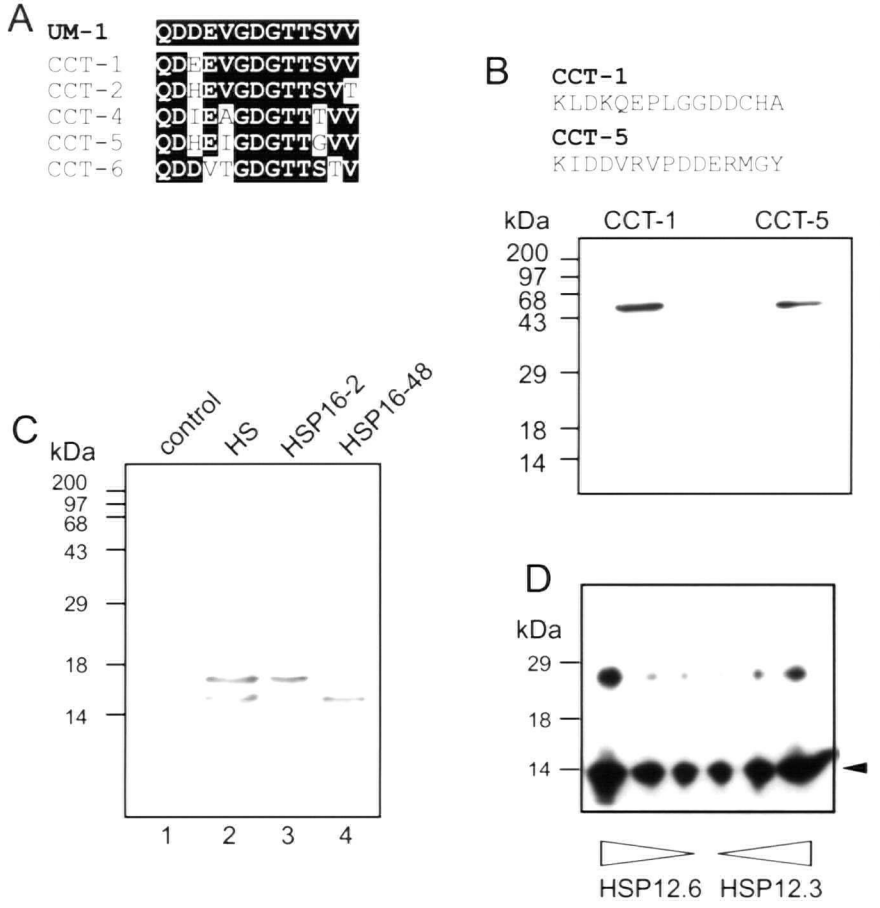

Figure 32. Specificities of the polyclonal antibodies against CCT and HSP16-2. **A.** A peptide with the sequence shown (UM-1) was used to generate polyclonal antibodies against a conserved region in all CCT subunits (provided by Keith Willison; Hynes *et al.*, 1995). An alignment with the five known *C. elegans* CCT subunits is shown for comparison. **B.** Peptides corresponding to the last 15 amino acids of *C. elegans* CCT-1 and CCT-5 were used to produce polyclonal antibodies against the respective CCT subunits. The antibodies (anti-CCT-1 and anti-CCT-5) cross-react specifically with approximately 59 kDa proteins in a total *C. elegans* extract. **C.** Polyclonal antibodies raised against H_6HSP16-2 (Jones *et al.*, 1996) do not cross-react with any protein in a control, total *C. elegans* extract (lane 1), but recognize two proteins of approximately 16.5 and 15.5 kDa in a heat-shocked nematode extract (lane 2). The sizes of these two proteins on the 18% SDS-gel correspond precisely to the sizes of the bacterially-produced wild-type HSP16-2 (lane 3) and HSP16-48 (lane 4), which were separated on the same gel and Western blotted with the same antibody. **D.** Polyclonal antibodies raised against H_6HSP12.6 cross-react with recombinant HSP12.6 and HSP12.3 from bacterial extracts with similar efficiency (black arrow); three different amounts of each recombinant protein were Western blotted with a 1:500 dilution of the anti-HSP12.6 pAb.

VIII. Sedimentation velocity analyses of smHSPs

Sedimentation velocity measurements on smHSPs were performed by Ronald Melki and Gérard Batelier. The sedimentation data were fitted by nonlinear least-squares procedures as described by Philo (1994) (see *Material and Methods*). Results are presented in **Table 4** below.

Table 4. Hydrodynamic parameters of HSP16-2, two derivatives, and HSP12.6[a]

	molecular mass (Da)	$\bar{v}$ ($cm^3\ g^{-1}$)	$s°_{20,w}$ (S)	f/f_0	R_S (m)	n-mer	relative abundance (%)
theoretical							
HSP16-2	16232	0.735	-	-	-	-	-
experimental							
HSP16-2							
form 1	239470	0.735	10.48	1.10	4.82×10^{-9}	14-15	58
form 2	394920	0.735	14.47	1.08	5.65×10^{-9}	24-25	42
theoretical							
Δ130-145	18580	0.723	-	-	-	-	-
experimental							
Δ130-145							
form 1	322395	0.723	12.8	1.16	5.29×10^{-9}	17-18	49
form 2	520385	0.723	17.6	1.16	6.20×10^{-9}	28	51
theoretical							
Δ1-44	15227	0.723	-	-	-	-	-
experimental							
Δ1-44							
form 1	14990	0.723	1.66	1.14	1.92×10^{-9}	1	95
form 2	56235	0.723	4.0	1.15	2.99×10^{-9}	3-4	5
theoretical							
HSP12.6	12612	0.737	-	-	-	-	-
experimental							
HSP12.6	12231	0.737	1.43	1.12	1.81×10^{-9}	1	100

[a]The conformational parameters were calculated as described in *Materials and Methods*, using the molecular mass and the partial specific volume ($\bar{v}$) values determined from the amino acid composition. Experimental points representing the distribution of each molecular form were decomposed into Gaussian curves. The area of each Gaussian is proportional to the concentration of the oligomer. Numerical values for the n-mer of each species were obtained by dividing the experimental molecular mass of each species by the corresponding theoretical molecular mass. $s°_{20,w}$ is the sedimentation coefficient; f and f_0 are the frictional coefficients and R_S the Stokes radius. (Data kindly provided by R. Melki and G. Batelier).